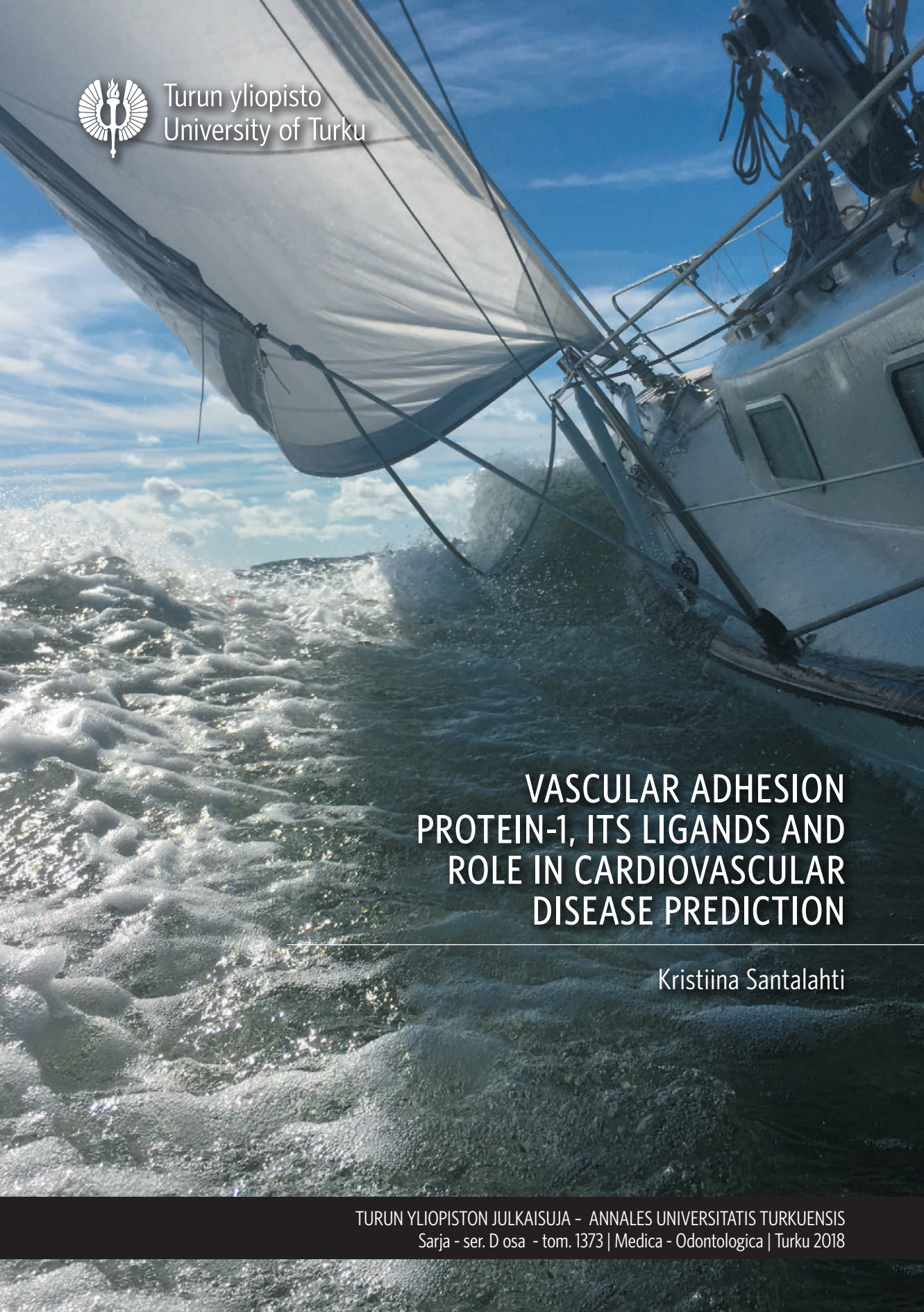

Turun yliopisto
University of Turku

VASCULAR ADHESION PROTEIN-1, ITS LIGANDS AND ROLE IN CARDIOVASCULAR DISEASE PREDICTION

Kristiina Santalahti

TURUN YLIOPISTON JULKAISUJA – ANNALES UNIVERSITATIS TURKUENSIS
Sarja - ser. D osa - tom. 1373 | Medica - Odontologica | Turku 2018

Turun yliopisto
University of Turku

VASCULAR ADHESION PROTEIN-1, ITS LIGANDS AND ROLE IN CARDIOVASCULAR DISEASE PREDICTION

Kristiina Santalahti

TURUN YLIOPISTON JULKAISUJA – ANNALES UNIVERSITATIS TURKUENSIS
Sarja - ser. D osa - tom. 1373 | Medica - Odontologica | Turku 2018

University of Turku

Faculty of Medicine
Institute of Biomedicine
Medical Microbiology and Immunology
Turku Doctoral Programme of Molecular Medicine (TuDMM)
and National Doctoral Programme in Nanoscience
MediCity Research Laboratory

Supervised by

Professor Sirpa Jalkanen, M.D., Ph.D.
MediCity Research Laboratory,
Medical Microbiology and Immunology
University of Turku
Turku, Finland

Professor Marko Salmi, M.D., Ph.D.
MediCity Research Laboratory,
Medical Biochemistry and Genetics
University of Turku
Turku, Finland

Reviewed by

Professor Emeritus Petri Kovanen, M.D., Ph.D.
Experimental Atherosclerosis
Wihuri Research Institute
Helsinki, Finland

Professor Emeritus Olli Vainio, M.D., Ph.D.
Research Unit of Biomedicine
University of Oulu
Oulu, Finland

Opponent

Professor Markku Savolainen, M.D., Ph.D.
Biocenter Oulu and Department of Internal
Medicine, University of Oulu and Medical Research Center,
Oulu University Hospital
Oulu, Finland

Cover photo by Jukka Juurinen

The originality of this thesis has been checked in accordance with the University of Turku quality assurance system using the Turnitin OriginalityCheck service.

ISBN 978-951-29-7323-1 (PRINT)
ISBN 978-951-29-7324-8 (PDF)
ISSN 0355-9483 (PRINT)
ISSN 2343-3213 (PDF)
Painosalama Oy – Turku, Finland 2018

To Ville, Effi, Mamma, Moffa, Amma, Susse

You have to know the past to understand the present
–Carl Sagan

ABSTRACT

Kristiina Santalahti

Vascular adhesion protein-1, its ligands and role in cardiovascular disease prediction

University of Turku, Faculty of Medicine, Institute of Biomedicine, Medical Microbiology and Immunology, Turku Doctoral Programme of Molecular Medicine, National Doctoral Programme in Nanoscience, MediCity Research Laboratory

Annales Universitatis Turkuensis, Turku, Finland, 2018

To study the pathogenesis and prevention of diseases, population studies in which hundreds of measurements are done from the same persons have a crucial role. A biomarker is any measurable characteristic that gives information on the biological state of the body. At its best a biomarker can predict future disease events. Cardiovascular diseases (CVDs) are chronic diseases in which one feature is harmful leukocyte trafficking.

In this thesis project, I studied vascular adhesion protein-1 (VAP-1), a molecule involved in leukocyte trafficking. I wanted to identify the ligands on the surface of leukocytes to which VAP-1 binds to and thus helps the leukocytes to migrate from blood to tissues. A soluble form of VAP-1 (sVAP-1) is present in the blood. To study sVAP-1 as a biomarker, I developed two different assays to measure the sVAP-1 levels in a high throughput way. This enabled the measurements of the sVAP-1 levels in two population cohorts and examine whether sVAP-1 associates with early phases of CVDs. Furthermore, I investigated the ability of sVAP-1 levels to predict future cardiovascular events in a Finnish population.

In this thesis, the first leukocyte ligands for VAP-1 were identified. Sialic acid binding Ig-like lectins Siglec-10 and Siglec-9 are expressed on different leukocytes and were able to bind to VAP-1. In addition, the sVAP-1 levels from nearly 5000 Finns were measured with the newly developed assays. The statistical analyses revealed that increased levels of serum sVAP-1 correlated with early manifestations of atherosclerosis. Additionally, sVAP-1 levels could predict future cardiovascular events and even improved the reclassification of patients to correct risk categories.

Keywords: cardiovascular diseases, leukocyte trafficking, ligand, biomarker, population study

TIIVISTELMÄ

Kristiina Santalahti

Vaskulaarinen adheesioproteiini-1, sen ligandit ja rooli sydän- ja verisuonitautien ennustamisessa

Turun yliopisto, Lääketieteellinen tiedekunta, Biolääketieteen laitos, Lääketieteellinen mikrobiologia ja immunologia, Molekyylilääketieteen tohtoriohjelma, Valtakunnallinen nanotieteiden tutkijakoulu, MediCity-tutkimuslaboratorio

Annales Universitatis Turkuensis, Turku, Suomi, 2018

Sydän- ja verisuonitaudit ovat suomalaisten kansantauteja. Näille sairauksille ominaista on häiriintynyt valkosoluliikenne. Näiden tautien kehittymisestä ja ennaltaehkäisystä saadaan tietoja kansallisilla väestötutkimuksilla, joissa ihmisestä voidaan mitata niin kutsuttaja biomarkkereita, jotka antavat tietoa elimistön tilasta. Parhaimmillaan biomarkkerit ennustavat tulevia tautitapahtumia vuosien päähän näytteenottohetkestä.

Tässä väitöskirjatyössä keskeisessä roolissa oli soluliikenteessä vaikuttava biomolekyyli, vaskulaarinen adheesioproteiini-1 (VAP-1). Työssä etsittiin valkosolujen pinnalla esiintyviä molekyylejä, ligandeja, joihin VAP-1 sitoutuu, ja näin auttaa valkosoluja siirtymään verestä kudoksiin. Lisäksi kahta veren liukoisen VAP-1:n määrää mittaavaa menetelmää kehitettiin väestötutkimuksiin sopivammaksi VAP-1:n biomarkkeri-roolin selvittämiseksi. Näillä high-throughput -menetelmillä oli tarkoitus selvittää assosioituuko VAP-1 sydän- ja verisuonitautien alkuvaiheisiin ja voidaanko VAP-1:n tasoilla ennustaa tulevia sydän- ja verisuonitautitapahtumia suomalaisessa väestössä.

Tutkimuksissa löysimme ensimmäiset valkosoluligandit VAP-1:lle. Siaalihappoihin sitoutuvat immunoglobuliini-tyyppiset lektiinit, Siglec-10 ja Siglec-9 ilmentyvät eri valkosolujen pinnalla ja sitoutuvat VAP-1:een. Kehittämiemme menetelmien avulla määritimme VAP-1-tasot lähes 5000:lta väestötutkimuksiin osallistuneelta suomalaiselta. VAP-1-tulosten tilastollinen analyysi muiden väestötutkimuksissa määritettyjen muuttujien ohella osoitti, että VAP-1-tasot korreloivat kaulavaltimon seinämäpaksuuden kanssa. Lisäksi VAP-1-tasoilla pystyttiin selittämään tulevien sydäntautitapahtumien riskiä ja parantamaan tilastollisen ennustemallin uudelleenluokittelukykyä.

Avainsanat: sydän- ja verisuonitaudit, valkosoluliikenne, ligandi, biomarkkeri, väestötutkimukset

TABLE OF CONTENTS

ABBREVIATIONS

Amino acids

A	Ala	alanine
C	Cys	cysteine
D	Asp	aspartic acid
E	Glu	glutamic acid
F	Phe	phenylalanine
G	Gly	glycine
H	His	histidine
I	Ile	isoleucine
K	Lys	lysine
L	Leu	leucine
M	Met	methionine
N	Asn	asparagine
P	Pro	proline
Q	Gln	glutamine
R	Arg	arginine
S	Ser	serine
T	Thr	threonine
V	Val	valine
W	Trp	tryptophan
Y	Tyr	tyrosine

AGE	advanced glycation end product
AOC	amine oxidase, copper dependent
AUC	area under the ROC curve
CAD	coronary artery disease
CD	cluster of differentiation
CHD	coronary heart disease
CHO	Chinese hamster ovary cells
CRP	C-reactive protein
CVD	cardiovascular diseases
DM	diabetes mellitus
EC	endothelial cell
EDTA	ethylenediaminetetraacetic acid
ELISA	enzyme-linked immunosorbent assay

ESL	endothelial surface layer
FR02	The National FINRISK 2002 study
GFP	green fluorescent protein
HDL	high-density lipoprotein
HEV	high endothelial venule
HR	hazard ratio
HRP	horseradish peroxidase
ICAM-1	intercellular adhesion molecule 1
IDI	integrated discrimination improvement
IFN-γ	interferon gamma
Ig	immunoglobulin
IL	interleukin
IMT	intima-media thickness
KO	knockout
LDL	low-density lipoprotein
LEC	lymphatic endothelial cell
LN	lymph node
mAb	monoclonal antibody
MACE	major adverse cardiovascular event
NRI	net reclassification improvement
PBS	phosphate buffered saline
PET	positron emission tomography
RCT	reverse cholesterol transport
ROC	receiver operating characteristic
Siglec	sialic acid binding Ig-like lectin
SLO	secondary lymphoid organ
SMC	smooth muscle cell
SPB	sodium phosphate buffer
SSAO	semicarbazide-sensitive amine oxidase
sVAP-1	soluble VAP-1
TLO	tertiary lymphoid organ
TNF-α	tumor necrosis factor alpha
TPQ	topaquinone (2,4,5-trihydroxyphenylalanine)
VAP-1	vascular adhesion protein-1
VCAM-1	vascular cell adhesion molecule 1
VEGF	vascular endothelial growth factor
WT	wild type
YFS	the Cardiovascular Risk in Young Finns study

LIST OF ORIGINAL PUBLICATIONS

This work is based on the following original publications, which are referred to in the text by Roman numerals (I-IV).

I Kivi, E., Elima, K.*, Aalto, K.*, Nymalm, Y., Auvinen, K., Koivunen, E., Otto, D.M., Crocker, P.R., Salminen, T.A., Salmi, M. and Jalkanen, S. Human Siglec-10 can bind to vascular adhesion protein-1 and serves as its substrate. *Blood*. 2009 Dec 17;114(26):5385-92.

II Aalto, K.*, Autio, A.*, Kiss, E.A., Elima, K., Nymalm, Y., Veres, T.Z., Marttila-Ichihara, F., Elovaara, H., Saanijoki, T., Crocker, P.R., Maksimow, M., Bligt, E., Salminen, T.A., Salmi, M., Roivainen, A. and Jalkanen, S. Siglec-9 is a novel leukocyte ligand for vascular adhesion protein-1 and can be used in PET-imaging of inflammation and cancer. *Blood*. 2011 Sep 29;118(13):3725-33.

III Aalto, K., Maksimow, M., Juonala, M., Viikari, J., Jula, A., Kähönen, M., Jalkanen, S., Raitakari, O.T. and Salmi, M. Soluble Vascular Adhesion Protein-1 Correlates With Cardiovascular Risk Factors and Early Atherosclerotic Manifestations. *Arterioscler Thromb Vasc Biol.* 2012 Feb;32(2):523-32.

IV Aalto, K., Havulinna, A.S., Jalkanen, S., Salomaa, V. and Salmi, M. Soluble vascular adhesion protein-1 predicts incident major adverse cardiovascular events and improves reclassification in a Finnish prospective cohort study. *Circ Cadiovasc Genet.* 2014 Aug;7(4):529-35.

*Equal contribution.

1 INTRODUCTION

Cardiovascular diseases (CVDs) were estimated to be responsible of nearly 18 million deaths worldwide in 2015, with an estimated 423 million prevalent CVD cases (Roth et al. 2017). In order to prevent these events and to better understand the pathogenesis of the diseases, population studies are carried out around the globe. In a typical epidemiological population study, thousands of randomly selected participants answer questionnaires and take part in a physical examination involving the collection of blood samples. Depending on the study design, the participants are then followed-up through linkages to national registries or by re-examinations in the study centers. Any measurable variable which gives information on the status of the body is called a biomarker.

Human circulatory system entwines the cardiovascular and lymphatic systems together. Human cardiovascular system consists of heart, blood vessels, and blood, whereas lymphatic system consists of lymphoid tissues, lymphatic vessels and lymph. Together these systems transport nutrients (including lipids) around the body, maintain the fluid homeostasis, and effectively protect the body from pathogens and environmental threats by distributing the cells and molecules of the immune system (OpenStax 2013).

The cells of the immune system are called leukocytes. In a process called leukocyte trafficking, leukocytes patrol through the whole body in the search of pathogens. Blood vessels are lined by endothelium, a heterogeneous population of cells, which are able to actively interact with the leukocytes. Endothelial cells express adhesion molecules, which in turn attach to their counterparts on the leukocytes and thus help the leukocytes to migrate into the surrounding tissue. (Abbas 2018). Atherosclerosis, the disease preceding CVDs, is a chronic inflammatory disease combining endothelial dysfunction and harmful leukocyte trafficking (Aspelund et al. 2016).

Vascular adhesion protein-1 (VAP-1) is an adhesion molecule expressed by vascular endothelium, smooth muscle cells, and adipocytes, and is present in circulation as a soluble form (Salmi and Jalkanen 2017). VAP-1 can assist leukocytes to migrate through vascular endothelium, but the leukocyte counterparts for VAP-1 have remained unknown. VAP-1 is also an enzyme producing hydrogen peroxide, ammonia and aldehydes, all of which are known to be detrimental for the vascular endothelia. In an attempt to prevent harmful cell trafficking, more is needed to know on the counterpart of VAP-1. Soluble VAP-1, a biomarker, has been measured in various disease states (Salmi and Jalkanen 2017), but its role in CVDs remains unclear.

2 REVIEW OF LITERATURE

2.1 Human circulatory system

The human circulatory system consists of the cardiovascular system and the lymphatic system. Both systems are designed to transport fluids and its contents throughout the human body, and they are intertwined together to accomplish this task, as seen in Figure 1. In steady state, the fluids in human body continuously flow between the plasma, interstitial fluid, and the lymph. The fluid turnover is estimated to be ~8L/day, meaning that once every 9 h the entire plasma volume (~3L) leaves the blood circulation (Levick and Michel 2010). In non-steady states the fluid flow alters to accommodate the situation. In acute hemorrhages the fluid is absorbed to bloodstream from the interstitial space to secure the cardiac output, whereas in acute inflammation the permeability of the vessel walls changes to assist more leukocytes on the inflammatory site, causing swelling at the site.

Human cardiovascular system includes the heart, the blood vessels and the blood. The main function of the cardiovascular system is to transport oxygen, nutrients, and cells to tissues while removing the waste products from the periphery. First, in the pulmonary circulation the blood high in carbon dioxide is pumped from the right side of the heart to the lungs for oxygenation and back to the left side of the heart, as seen in Figure 1. Next, in the systemic circulation the left side of the heart pumps the oxygenated blood to arteries, which carries the blood to tissues in relatively high pressure. In the tissues the gases are exchanged, and the deoxygenated, but high in carbon dioxide blood then returns to the right side of the heart via veins in a relatively small pressure thus completing the systemic circulation.

In contrast to cardiovascular system, lymphatic system is linear, not circular, as depicted in Figure 1. The lymphatic system consists of the lymphatic vessels, lymphoid tissues, and the lymph. The lymphatic system maintains the tissue fluid homeostasis. Fluid leaks from the blood capillaries into the interstitial space as the result of hydrostatic pressure. Some fluid is reabsorbed through the post-capillary venules, but the fluid left behind is called interstitial fluid. The fluid flows into the lymphatic capillaries as the result of the pressure gradient. The fluid is now called the lymph. In addition to blood-derived molecules and cells, the lymph entails products of metabolic/catabolic activity of the specific organ (Clement et al. 2011; Clement et al. 2013; Hansen et al. 2015). The smooth muscle cell and skeletal muscle contractions together with intraluminal valves of the collecting lymph vessels transport the lymph to the lymph nodes, the meeting

points of antigens and lymphocytes. Finally, the lymph returns back to the blood via the thoracic and right lymphatic ducts at the subclavian vein. In addition, the lymphatic system regulates the absorption of gastrointestinal lipids.

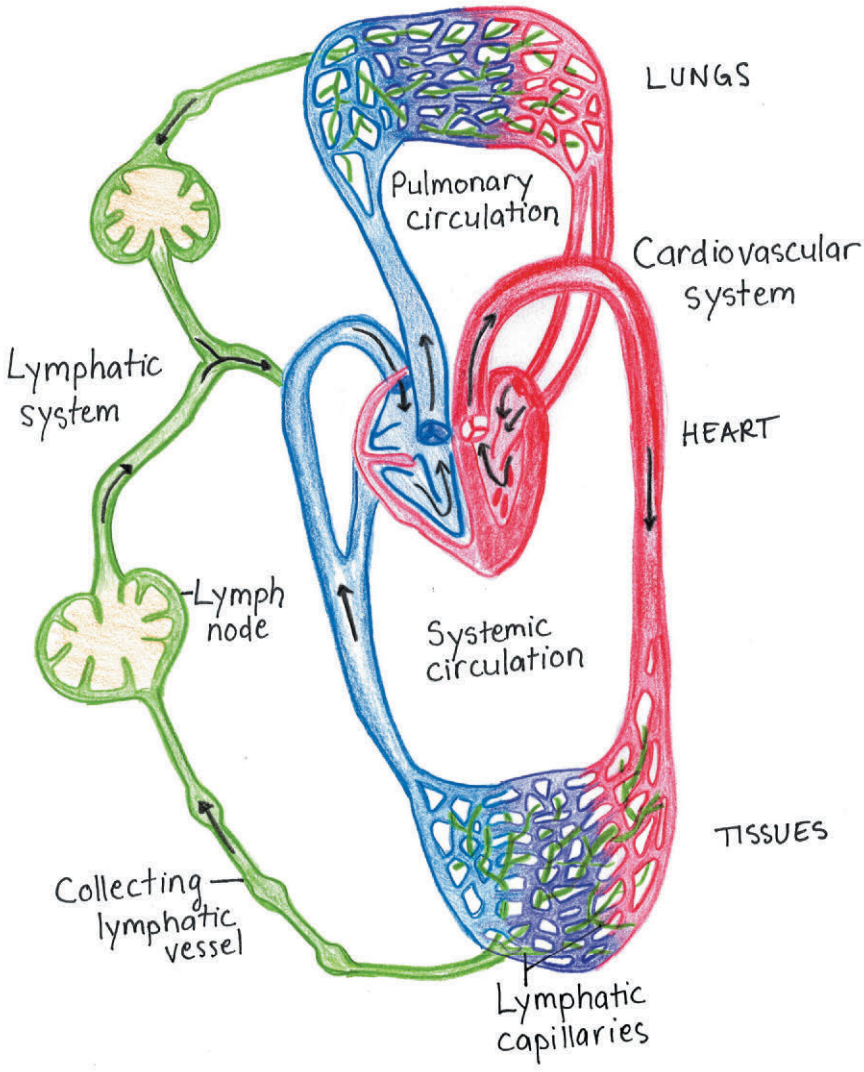

Figure 1. Illustration of the blood and lymph circulation in the human body. The blood is oxygenated in the pulmonary circulation, and then pumped to tissues through the systemic circulation. In the tissues the arterial capillaries transform into venous capillaries. The gases and nutrients are exchanged, and the fluid is leaked into the interstitial space. The excess fluid is taken up by the lymphatic capillaries, and the resulting lymph is returned to the heart through lymph nodes and lymphatic vessels. The deoxygenated blood is returned to the heart through venous vessels.

2.1.1 Human cardiovascular system

The human cardiovascular system (including heart, blood vessels, and blood) has several functions such as transportation of nutrients, gases and cells; defense against external threats by blood clotting and immune cell trafficking; and maintaining temperature, pH, and fluid homeostasis. Diseases involving blood vessels and heart are called CVDs. A vast majority of CVDs are caused by atherosclerosis, a condition where plaques are formed in the arterial wall and the vascular elasticity is diminished (Head et al. 2017).

2.1.1.1 Blood

Blood consists of extracellular matrix and cellular elements. The extracellular matrix in blood, called plasma, is mostly water (92%). The second largest component (7%) of plasma consists of different proteins (albumins, globulins, and fibrinogen). A study by Clement et al. revealed that the plasma proteome consisted of extracellular proteins (45%), cytoplasmic proteins (17%), plasma membrane proteins (12%), and nucleus-derived proteins (8%) (Clement et al. 2013). Functionally the plasma proteome contains proteins associated with coagulation (61%), and lipid metabolism and molecular transport (18%). In addition, the plasma contains gases (such as oxygen and carbon dioxide); nutrients (such as glucose, amino acids, and fatty acids); ions (such as calcium, potassium, and sodium) and metabolic wastes (such as urea and lactic acid).

The cellular element of blood consists of erythrocytes, platelets, and leukocytes. Erythrocytes constitute the largest part (99%) of the blood's cell entity and they are responsible for the transportation of gases. Platelets are small cell fragments which promote blood clotting (also known as hemostasis). Leukocytes are specific cells with a key role in immune defense against pathogens and in repair of injured tissues. Leukocytes are divided into two categories according to their morphology. Granular leukocytes include neutrophils, eosinophils and basophils, whereas lymphocytes and monocytes constitute the agranular group. Most leukocytes are involved in non-specific immunity, whereas lymphocytes are capable of specific immune defense by producing antibodies (B cells) and forming effector and memory cells (B and T cells). (Abbas 2018). The immune defense mechanisms of blood leukocytes are discussed further later on.

The variety of substances found in blood reflects the diversity of functions of the blood. In addition to oxygen carbon dioxide –transportation, blood transports nutrients for cells to use and waste products for the body to excrete. Moreover, hormones are released from endocrine glands and carried in bloodstream to their

target sites. The blood electrolytes are involved in modification of membrane potential. Blood also has a significant role in maintaining the homeostasis in the body by buffering against pH changes. In addition, the plasma proteins maintain the osmotic pressure of the blood; function as transport vehicles for hydrophobic molecules, and mediate immune responses with leukocytes. Taken together, it is not surprise, that the clinical analysis of blood is a widely used diagnostic procedure since the blood reflects the state of an individual's physiology (Geyer et al. 2017). Blood is thus an abundant source of biomarkers.

2.1.1.2 Systemic blood vessels

Systemic blood vessels are the scene of the beginning and progression of CVDs. Atherosclerosis, the disease behind the life-threatening complications such as myocardial infarction and stroke, affects the walls of large and medium-sized arteries, whereas smaller vessels are the site of molecule and cell trafficking.

Structurally, the larger blood vessels consist of three layers (tunicas): intima, media and externa (also knowns as adventitia) illustrated in Figure 2. The tunica intima is lined by endothelial cells forming the endothelium. Endothelium is not merely a barrier between blood and the extravascular compartment, but an active multifunctional organ with key aspects regarding vascular health. The endothelium is thus further discussed in the following chapter. Beneath the endothelium are basal lamina and a thin layer of connective tissue with elastic and collagenous fibers to give the vessel flexibility and strength.

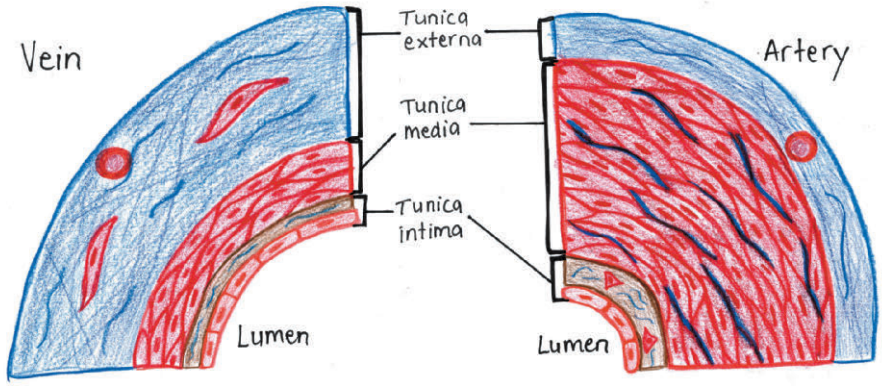

Figure 2. The three layers of blood vessels. On the left is an illustration of a medium-sized vein, and on the right an illustration of a muscular artery. Usually the lumens of veins are larger in diameter than the lumens in arteries. Tunica intima consists of endothelium, basal lamina and a connective tissue layer with elastic fibers. The tunica media contains smooth muscle cells (SMCs; red diamond shaped cells) and especially in the arteries, elastic tissue (blue lines). The outer layer, the tunica externa, is mostly collagen with some SMCs, elastic fibers, and vasa vasorum.

The tunica media, the middle layer of the vessel wall, consists of mainly smooth muscle cells (SMCs) and circular layers of elastic tissue. In the outer part of the media the SMCs form layers of longitudinal muscle. As the SMCs contract and relax in response to various stimuli, the lumen of the vessel decreases and increases, respectively. This affects the pressure and flow of the blood; as the smooth muscles contract and the lumen narrows, the blood flow decreases and pressure increases. The opposite happens as the smooth muscles relax. Collagenous fibers bind the media to the intima and externa tunics. In general, the tunica media is the most prominent part of arterial walls, and the thickness decreases with the distance from the heart. In veins the media is always thinner than in arteries. The outmost layer of blood vessel, the tunica externa or adventitia, is made out of collagen and some elastic fibers. In veins, the externa is usually the thickest. Within the tunica externa of larger vessels are vasa vasorum, small blood vessels that supply the cells in vessel walls with oxygen and nutrients, and remove waste products. Recently, the role of vasa vasorum, and especially the neovascularization of these vessels, in atherosclerotic plaque instability has become clearer (Chistiakov et al. 2017). The accumulation of inflammatory leukocytes, thickening of intima, and intraplaque haemorrhages leading to lesion ruptures, atherothrombosis, and finally to acute cardiovascular events, are processes involving vasa vasorum (Chistiakov et al. 2017).

In normal arteries, medial and adventitial layers of the wall contain lymphatic vessels, whereas in atherosclerotic lesions lymphatic vessels are found in the intima as well (Kholova et al. 2011). In atherosclerotic arteries the number of lymphatics increased in intima and media according to the progression of atherosclerosis, although angiogenesis was increased more in these areas than lymphangiogenesis (Kholova et al. 2011). In normal and in atherosclerotic arteries, lymphatic vessels are found in the vicinity of vasa vasorum in the adventitia (Kholova et al. 2011).

As the heart muscle contracts, the blood is pushed into the systemic arteries in a pulsatile flow. The pressure pulse travels inside the closed system of systemic blood vessels causing the blood to press against the inner walls of the vessels. This force is called the blood pressure, and as the distance from the heart grows the pressure lessens. The fine structure of the vessel wall changes as well, as the distance from the heart increases. The blood leaves the heart in a large vessel called aorta, an example of an elastic artery. Elastic arteries (diameter >1 cm) have high amount of elastic tissue in their walls in order to even the blood flow. As the heart pumps the blood forcefully to arteries (systole), the elastin in the vessel wall is stretched and the wall is dilated. After the contraction, in the diastole, the arterial pressure is maintained as the elastin rebounds passively and the heart valves prevent the blood to flow back to heart. As the distance from the

heart increases, the diameters of the vessels decrease. In addition, the elastin proportion of the arteries gradually decreases and the smooth muscle proportion increases and the arteries are called muscular arteries. In the muscular arteries (diameter 0.5mm-1 cm), the vessel wall contains mainly smooth muscle cells and some elastic fibers. This structure reflects the key part the muscular arteries play in the vasoconstriction. As the diameter of the arteries further decreases, the vessels are called arterioles (diameter 0.03-0.5 mm). Arterioles play an important role in the vascular resistance, as they are very responsive for the neural and chemical stimuli.

The smallest vessels in the blood circulatory system are capillaries (diameter 5-10 μm), formed by a single layer of endothelial cells (ECs) encased by pericytes here and there. They form a network of microvasculature where arteries change into veins while they supply the surrounding tissue with blood in a process called perfusion. The main function of capillaries thus is to permit the transfer of oxygen from blood to tissues and carbon dioxide from tissues to blood. The rate and mode of molecule relocation through endothelium are in proportion to the fine structure of capillaries. In continuous capillaries molecules are transported in a regulated manner through transcytosis. In fenestrated capillaries the exchange of water and small solutes between plasma and interstitial fluid is fast since the ECs have intracellular pores covered with a diaphragm. Under the ECs the basement membrane is still complete as is the case in continuous capillaries as well. Instead, in sinusoidal capillaries both the EC lining and the basal lamina have gaps resulting in free exchange of water and large solutes between plasma and interstitial fluid. (Augustin and Koh 2017; Potente and Makinen 2017). From the capillaries the blood starts the journey back to heart. In general, veins have larger lumen sizes and thinner walls, than arteries. The blood drains into postcapillary venules (diameter 10-25 μm) from the capillaries. The venules merge to form small veins (diameter <1mm) which in turn join to form medium-sized veins (diameter 1-10 mm). In venules and in veins valves prevent the blood to flow backwards.

2.1.1.3 Vascular endothelium

A heterogeneous population of endothelial cells (ECs) forms the inner lining of the entire cardiovascular system. This organ called endothelium is large in surface (350 m^2) while weighing only 110 g (Pries et al. 2000; Sumitran-Holgersson and Holgersson 2010). Morphologically vascular ECs are flat and long with average dimensions of 0.1-0.5 μm thick, 10-15 μm wide and 20-40 μm long (Cahill and Redmond 2016). However, the shape, thickness and alignment

of the ECs, as well as the thickness of the glycocalyx (a layer of membrane-bound proteoglycans and glycoproteins) coating the ECs, as seen in Figure 3, varies across the vascular tree (Aird 2007). This variation in the structure of the cells reflects the variety of functions ECs have. For example, endothelium acts as a semipermeable barrier between blood and the extravascular space; regulates vasomotor tone by sensing the hemodynamic forces; controls hemostasis; and allows leukocytes to pass to the underlying tissue (Rajendran et al. 2013; Cahill and Redmond 2016).

Endothelium executes its various tasks by producing vast amount of different signaling molecules making it a paracrine, endocrine, and autocrine organ (Hadi et al. 2005). ECs produce vasodilating mediators (such as nitric oxide), cytokines, chemokines, and growth factors, as well as receptors for cytokines, chemokines, and growth factors (Sumitran-Holgersson and Holgersson 2010). In addition, endothelium expresses several adhesion molecules involved in leukocyte recruitment, such as E- and P-selectin, intercellular adhesion molecule 1 (ICAM-1), vascular cell adhesion molecule 1 (VCAM-1), vascular adhesion protein-1 (VAP-1), and platelet endothelial cell adhesion molecule-1 (PECAM-1). Endothelial dysfunction is a state where the normal physiology of endothelium is altered resulting in impaired endothelium-dependent vasodilation, and activation of EC's characterized by proinflammatory process (Hadi et al. 2005).

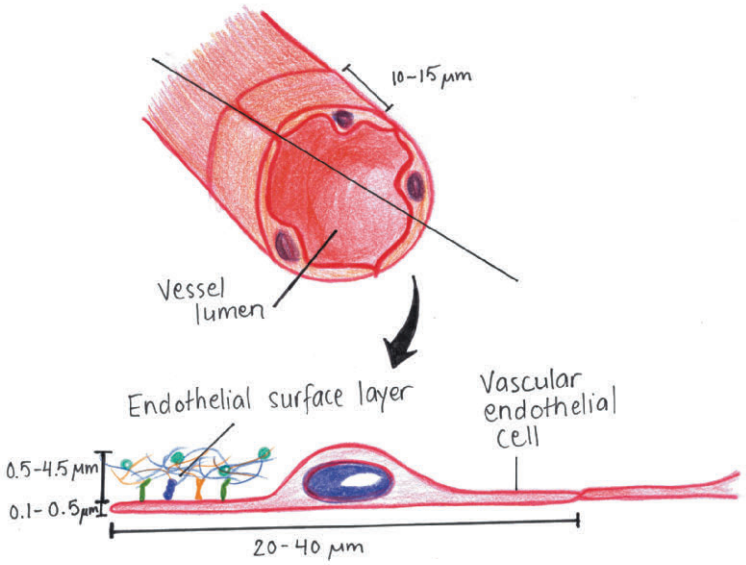

Figure 3. An illustration of the dimensions (not drawn to scale) of vascular endothelial cell (EC) and the endothelial surface layer (ESL). The blood vessel is sectioned by the black line and the flat layer of ECs is examined. Vascular ECs are 0.1-0.5 µm thick, 10-15 µm wide and 20-40 µm long. The thickness of ESL varies according to the location in the blood circulatory tree.

The intracellular structure of ECs clearly demonstrates the selective barrier function of endothelium between intravascular and extravascular spaces. ECs have various vesicle organelles to accomplish the endocytosis and transcytosis pathways. The intercellular structures of the endothelium reflect the permeability function of the endothelium as well. ECs are anchored to the extracellular matrix (basal lamina) and to each other through transmembrane proteins. Integrins and extracellular matrix proteins link the ECs to the extracellular matrix and to the filaments in the matrix. Junctional proteins link the cells to each other forming the cell monolayer of endothelium. These interendothelial junctions physically restrict proteins to passively diffuse from blood through the vessel wall and thus maintain the tissue-fluid homeostasis (Komarova et al. 2017; Radeva and Waschke 2017). The regulated transport of fluids and solutes across the endothelium can be basal or inducible. In basal conditions, the flux of materials between blood and interstitium is continuous, and happens primarily in the capillaries. The basal permeability differs spatially, and one reason for this is the number and complexity of tight junctions, which is inversely proportional to permeability (Aird 2007). The induced permeability occurs in acute and chronic inflammation, and mainly in the postcapillary venules. Thus, for example in acute allergic reactions, activation of mast cells with consequent release of histamine and of vasoactive compounds, endothelial gaps are formed, so increasing endothelial permeability particularly in the postcapillary venules (Ashina et al. 2015).

EC alignment differs across vascular tree as well. In the straight segments of arteries the ECs are aligned in the direction of blood, and this flow-dependent alignment of cells happens in response to hemodynamic stress (Flaherty et al. 1972). However, the branching of the arteries to smaller arteries causes irregularities in blood flow in the sharp turns and branched areas of the blood vessels. Thus, in the branch area of an artery, the ECs are irregular in shape and in orientation (Lupu et al. 2005). These changes in ECs are caused by the mechanical forces such as fluid shear stress (the frictional force caused by the flowing blood per unit area) and blood pressure (the force of blood flow against the vessel wall). It is known, that the alignment of cells renders some part of the vasculature more vulnerable for vascular diseases (Tarbell 2010). The inner wall of vessel curvature, near branch points, and the lateral walls of bifurcations are typical sites for the atherosclerotic plaques to occur (Head et al. 2017). Hahn and Schwartz reviewed the role of mechanotransduction in vascular physiology and especially in atherogenesis (Hahn and Schwartz 2009). Vascular endothelial cadherin, together with vascular endothelial growth factor receptor (VEGFR)2 and platelet endothelial cell adhesion molecule-1 (PECAM-1) comprise a mechanosensory complex, which in fluid flow studies was shown to align ECs in the direction of flow (Tzima et al. 2005). In addition to shear stress and blood

pressure, the transmigration of leukocytes generates mechanical forces that impact the ECs (Dorland and Huveneers 2017). The phosphorylation of vascular endothelial cadherin has a pivotal role in the opening of endothelial junctions in inflammation allowing leukocytes to extravasate into the tissue (Wessel et al. 2014).

2.1.1.4 Glycocalyx and endothelial surface layer

Virtually all ECs have a structure called endothelial surface layer (ESL) on the luminal surface of the endothelium. The ESL actually consists of two physically different layers, a glycocalyx and a superficial layer denoted as outer layer of ESL (Pries et al. 2000; Marki et al. 2015). The endothelial glycocalyx is roughly 100-nm-thick layer of carbohydrate-rich extracellular domains of membrane-bound glycoproteins (proteins with covalently bound short and branched carbohydrate moieties in N-glycosyl or O-glycosyl linkages) and proteoglycans (proteins with long unbranched sugar side chains with O-glycosyl linkages) (Becker et al. 2010) shown in Figure 4. Furthermore, shorter projections from the cell membrane, mainly membrane receptors and adhesion molecules are accounted to the glycocalyx as well. The outer layer of ESL consists of proteins, peptides, and polysaccharides, as seen in Figure 4. These molecules are either plasma or membrane derived and include glycosaminoglycans such as heparan sulfate and hyaluronic acid, plasma proteins such as albumin and fibrinogen, and secreted proteoglycans such as syndecan-1 and biglycan (Marki et al. 2015).

Some researchers refer to ESL by the name of glycocalyx and vice versa creating confusion. For example, Reitsma et al. reported the thickness of the glycocalyx coating to differ across the blood circulatory tree ranging from 0.5 μm thickness in muscle capillaries to 4.5 μm in carotid arteries (Reitsma et al. 2007). In another review by Marki et al., the same dimensions were reported for the ESL (Marki et al. 2015). In this dissertation, the ESL refers to the two layers together, the glycocalyx and the outer layer of ESL, as seen in Figure 4. Nevertheless, in some pathophysiological situations, such as ischemia/reperfusion, and in chronic inflammation in atherosclerosis, the glycocalyx and the whole ESL are damaged (Becker et al. 2010). This implies to the importance of the ESL in normal physiology. Pries and co-workers reviewed the several vascular functions regulated by the ESL (Pries et al. 2000). The fluid shear stress affects the ECs via ESL and the mechanotransduction is transmitted through transmembrane proteins of the glycocalyx, which in turn are attached to the cytoskeleton. In addition, regulation of blood flow, the barrier function of ECs, coagulation, and interactions with leukocytes are mentioned in regard the role of ESL.

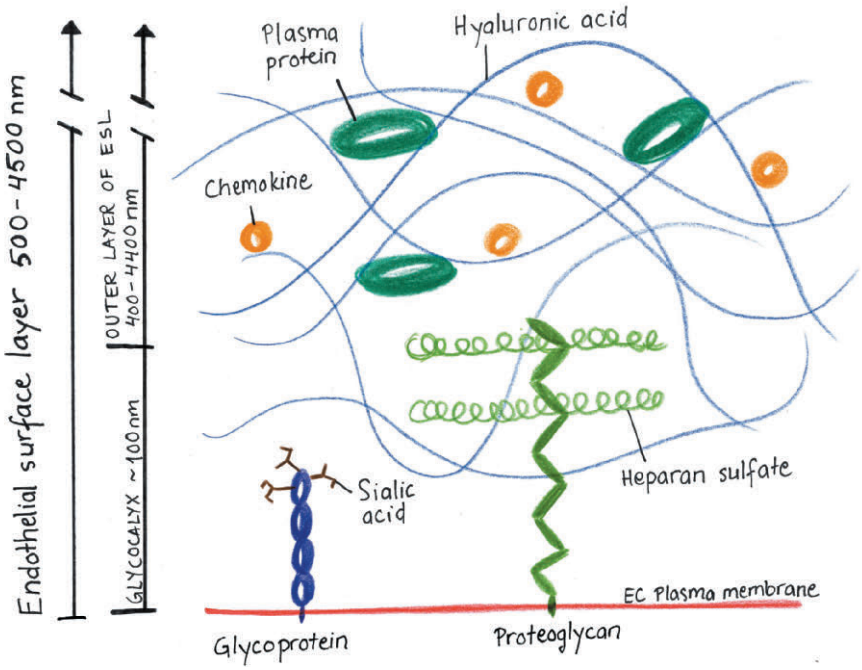

Figure 4. Glycocalyx together with an outer layer constituting of hyaluronic acid and adsorbed plasma proteins form the endothelial surface layer (ESL). Glycoproteins and proteoglycans form the glycocalyx (~100 nm thick), whereas the plasma proteins and glycosaminoglycans constitute the outer layer of the 500-4500 nm thick ESL. In inflammatory conditions the ESL is shed in part, leaving approximately 200 nm thick layer, as depicted in the picture. Secreted chemokines are bound to the outer layer initiating the contacts with leukocytes. Even when the ESL is partly shed, the adhesion molecules (glycoproteins mainly) reach only ~50 nm into the lumen.

Especially important is the role of ESL in vascular permeability. The size and steric hindrance in addition to electrostatic charges created by the glycocalyx and ESL affect the extravasation of fluids and solutes (Reitsma et al. 2007). The negative charges of the glycosaminoglycan side chains in the ESL prevent the adhesion of the circulating platelets and red cells, and the steric hindrance prevents leukocytes to interact with the endothelial adhesion molecules (Chelazzi et al. 2015). In addition, the plasma-derived soluble molecules docked to the ESL can change the local environment by increasing the local concentration of different substances.

As mentioned, damages in ESL have severe consequences. Intravenous injection of oxidized low-density lipoproteins (LDL) to hamsters reduced the ESL by 60% in the capillaries of the cremaster muscle, when studied by intravital microscopy. As a result, an increased number of platelets adhered to endothelium compared to LDL-treated hamsters (Vink et al. 2000). The glycosaminoglycans can be shed from the ESL by inflammatory mediators resulting in an increased adhesion of leukocytes to the endothelium (Mulivor and Lipowsky 2004). It was also shown,

that tumor necrosis factor-α was able to modify the ESL independently of leukocyte adhesion, resulting in increased macromolecule penetration (Henry and Duling 2000). Chelazzi and co-workers reviewed the effects of pro-inflammatory mediators and oxidative stress in inflammatory injury of the glycocalyx (Chelazzi et al. 2015).

2.1.2 Human lymphatic system

The lymphatic system transports lymph from nearly all organs back to the bloodstream thereby maintaining the tissue fluid homeostasis (Trevaskis et al. 2015). It also produces, maintains, and transports the players of the immune system, and thus facilitates innate and adaptive immune responses (Abbas et al. 2016). Finally, the lymphatic system transports dietary lipids and fat-absorbed vitamins (Bernier-Latmani and Petrova 2017). Taken together the tasks performed by the lymphatic system, it is not surprising that recently the role of lymphatic system in the pathogenesis of CVDs has emerged (Aspelund et al. 2016). Cardiac lymphatics, or lymphatic vasculature in the heart, have several processes important for the heart function (Vuorio et al. 2017). For example, the atherosclerotic plaque formation can be delayed by the development of new lymphatics (lymphangiogenesis) presumably by improving the reverse cholesterol transport (RCT) (Martel et al. 2013; Vuorio et al. 2017). In addition, studies have shown a beneficial role of lymphangiogenesis after myocardial infarction (MI) in resolving the edema and clearing the inflammatory cells from the cardiac tissue (Henri et al. 2016).

During the last decade it has become clearer that the lymphatic system is not just a secondary transport system where the lymph flows passively (against pressure gradients), but an actively regulated and energy consuming process (Zawieja 2009). In addition, recently many previously ‘alymphatic’ organs have been proven to have lymphatic vessels. For example cornea (Aspelund et al. 2014) and the central nervous system (Aspelund et al. 2015; Louveau et al. 2015) have lymphatic vessels.

2.1.2.1 Lymph

Even though the lymphatic vessels and the lymph were described by Hippocrates (460-377 BCE) 2400 years ago, the exact content of lymph has remained without much attention (Choi et al. 2012). In fact, it has just been assumed that the lymph and the plasma would have similar protein composition (Hansen et al. 2015).

Still, lymph is known to be derived from the interstitial fluid, which contains the metabolic products of the organ as well as the fluid leaked out of the vascular vessels (Hansen et al. 2015). Thus in general, the lymph contains products of tissue metabolism, catabolism and remodeling, ultrafiltrate of proteins and molecules originated from the blood, apoptotic cells, and possible pathogens (Zolla et al. 2015). However, the content of the lymph is modified by the anatomical region it is derived from, as well as pathological conditions, especially sepsis, inflammation, and trauma (Hansen et al. 2015). The intestinal lymph contains chylomicrons, protein and lipid packages produced by the enterocytes from the food-derived fatty acids and cholesterol. It is worth noticing, that due to this arrangement, only lipids are transported through mesenteric lymph nodes and through heart and lung vasculature before entering the liver, whereas all other nutrients from the diet are directly entered into the portal venous circulation of liver (Randolph and Miller 2014). It is worth noticing, that other chylomicron targeted macromolecules such as drugs and environmental toxins go through the systemic circulation before entering the portal circulation (Randolph and Miller 2014).

2.1.2.2 Lymphatic vessels

Lymphatic endothelial cells (LECs) line all lymphatic vessels, and are in direct contact with the extracellular matrix, and thus make the initial contacts with the macromolecules, immune cells and pathogens, and small molecules arriving to the lymphatic system from the periphery. As their blood vascular equivalents, LECs are covered by a glycocalyx layer as well (Zolla et al. 2015). LECs are able to control the lymph flow, and thus the delivery of leukocytes and antigens to lymph node, by expressing chemokines, adhesion molecules, and secreting nitric oxide (Card et al. 2014). It has been revealed, that LECs are able to express major histocompatibility class I and II molecules, thus enabling them to potentially act as antigen presenting cells and cause peripheral tolerance (Liao and von der Weid 2015; Aspelund et al. 2016).

Lymphatic capillaries, also called initial lymphatic vessels, are ~50 μm in diameter and are constituted solely of LECs, meaning that they do not have any basement membrane, SMCs, pericytes, nor continuous interendothelial junctions (Huxley and Scallan 2011). Instead, LECs overlap each other creating button-like junctions (Baluk et al. 2007). The button-like appearance is formed by adherens and tight junctions. Increase in the interstitial pressure tenses the anchoring filaments attached to the LECs opening the flaps (Figure 5). The appearing holes (2-3 μm in diameter) allow extracellular fluid as well as all the molecules and

particles with less than 1 μm diameter in size to freely enter the lymphatic capillary from the interstitium. This means that the resulted lymph can contain bacteria and viruses, foreign antigens, as well as a pool of self-antigens from the surrounding tissue. (Liao and von der Weid 2015).

Gradually the morphology of the lymph vessels change as the LEC junctions become zipper-like, basement membrane becomes continuous, and SMCs cover the vessel as seen in Figure 6. These changes reflect the functional change from gathering surrounding fluids and solutes to transporting these toward the lymph node. These vessels are called collecting lymphatic vessels. To facilitate the movement toward the lymph nodes, luminal valves are disposed along the way with lymphangions constituting the section between two valves. To pump the lymph, the smooth muscle cells surrounding lymphangions contract spontaneously as a consequence of action potential initiated by the pacemaker cells (von der Weid and Zawieja 2004; Trevaskis et al. 2015). In coordination with the muscle contractile activity the intraluminal valves close thus preventing the backflow of the lymph.

Older age and obesity are linked to CVDs, and some studies imply that lymphatic system might have a role in this link. Zolla et al. demonstrated how older rats had degenerated lymphatic collectors with less extracellular matrix in the valves, decreased vessel functionality, and altered glycocalyx coating of LECs resulting in impaired pathogen clearance and permeability of lymphatic collectors (Zolla et al. 2015). In addition to age, obesity can cause impairment of lymphatic vessels' function (Blum et al. 2014; Garcia Nores et al. 2016; Escobedo and Oliver 2017), but fortunately by losing weight these detrimental changes are reversible (Nitti et al. 2016). Some studies implicate that aberrations in lymphatic vessel function could cause obesity, one of the risk factors for CVDs (Aspelund et al. 2016). The lymphatic vessels of the intestines of the VEGF-C-deficient mice regressed, resulting in reduced lipid uptake and simultaneous increase in lipid excretion through feces (Nurmi et al. 2015). Even though these mice were fed a high-fat diet, their glucose-metabolism improved after the VEGF-C deletion and the obesity was counteracted.

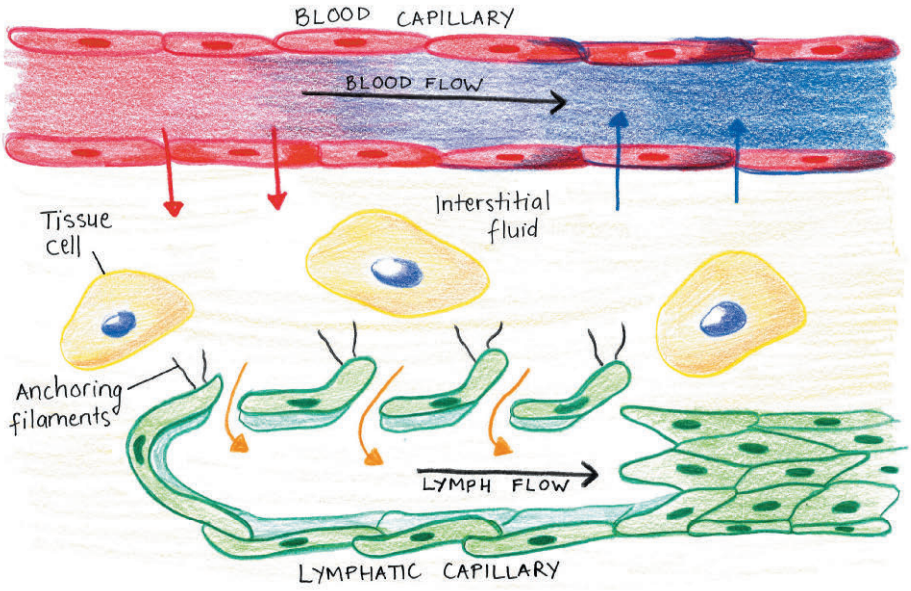

Figure 5. The transcapillary flow of fluids. This oversimplified scheme illustrates how the fluid leaks out of the blood capillary (→) into the interstitial space increasing the pressure of interstitial fluid. This in turn tenses the anchoring filaments attached to the connective tissue from the flaps of the LECs of lymphatic capillary, opening them. Some fluid reabsorbs to the postcapillary venule (→) but according to the latest hypothesis, most of the fluid is taken up by the lymphatic capillary (→), which returns the fluid back to the bloodstream through the subclavian vein.

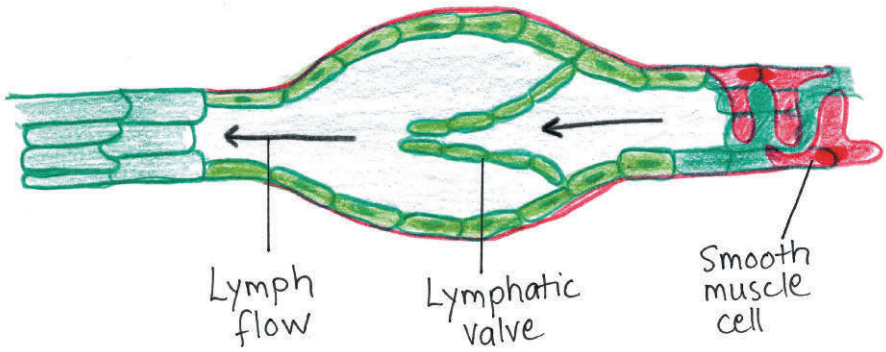

Figure 6. Lymphatic valves and zipper-like junctions in collecting lymphatic vessels. In collecting vessels the lymphatic endothelial cells have zipper-like appearance and smooth muscle cells cover the vessel. The lymphatic valve facilitates the fluid movement by opening and closing according to the contractions of SMCs.

2.1.2.3 Lymph nodes and adventitial tertiary lymphoid organs

The secondary lymphoid organs (SLOs) include the encapsulated lymph nodes, and spleen, and the cutaneous and mucosal immune systems. These organs are developed during ontogeny, and are highly compartmentalized with special areas for T and B cells, antigen-presenting cells, stromal cells, and blood and lymph vessels (Ruddle 2014). Specific features of SLOs (except spleen) are the high-endothelial venules (HEVs), through which the lymphocytes egress the blood and enter the lymphoid organs. The ECs in HEVs are cuboidal in morphology with thick apical glycocalyx and they express addressins (lymphocyte homing receptors) on their apical surface (Ager and May 2015). Non-lymphoid organs can develop HEVs during chronic inflammation (Ager and May 2015).

The raison d'être of lymph nodes (LNs) is to bring together the antigen from the periphery and the lymphocytes from the blood circulation which then elicit a proper immune response. In humans, LNs are 1-25 mm in length and bean-shaped. The fine structure of LNs is designed to facilitate the encounter of antigens and lymphocytes by forming a meshwork of lymph-filled sinuses to reach the LN parenchyma (von Andrian and Mempel 2003). Structurally, LN can be divided into four layers starting from the outmost: capsule, cortex, paracortex, and medulla. LNs are located outside the organs they drain and constantly receive information of the state of the tissue (Card et al. 2014). Throughout the body the LNs are situated in critical places to be able to filter out the antigens and pathogens before reaching vital organs and to collect the antigens from the periphery. Thus the respiratory and digestive systems and urogenital tract areas are concentrated with LNs responding to the high exposure to external substances.

In chronic inflammation lymphoid cells can accumulate to almost any non-lymphoid tissue as a result of environmental cues similar to those in LN development. These organs have similarities to SLOs, especially LNs, and are referred to as tertiary lymphoid organs (TLOs) (Ruddle 2014). TLOs have organized lymphatic vessels and HEVs, and are thus able to recruit lymphocytes from the blood (Akhavanpoor et al. 2018). TLOs are usually disease-associated findings, and the size of the TLOs have been reported to correlate with disease severity (Yin et al. 2016). In aged atherosclerosis-prone hyperlipidemic apolipoprotein E-deficient mice, lymphoid aggregates called artery tertiary lymphoid organs (ATLOs) are found in the adventitia of the atherosclerotic arteries (Yin et al. 2016). In humans, cellular infiltrates in the adventitia of atherosclerotic arteries were described already in 1962 (Schwartz and Mitchell 1962). Other studies have implied an association of immune cell infiltration to adventitia with adverse cardiovascular events (Kohchi et al. 1985; Akhavanpoor

et al. 2018) and that vulnerable plaques have more lymphocyte infiltration than stable plaques (Tavora et al. 2010). Akhavanpoor et al. staged the human adventitial TLOs similarly to the mice ATLO staging (Grabner et al. 2009): in Stage I T cell aggregates are present; in Stage II separate T- and B-cell areas are evident; and in Stage III ectopic germinal centers are found in addition to separate T- and B-cell areas (Grabner et al. 2009; Akhavanpoor et al. 2018). In the same study, a positive correlation between the sizes of TLOs and plaque size and instability was reported (Akhavanpoor et al. 2018). In addition, the fatal lesions presented stage III TLOs, and the media and intima adjacent to the TLO were infiltrated with inflammatory cells and structural and cellular destruction was evident at these sites as well (Akhavanpoor et al. 2018). These results indicate, that a massive inflammatory cell invasion precedes the plaque rupture, which might be involved with the intraplaque neovascularization as a route for the inflammatory cells (Chistiakov et al. 2017; Akhavanpoor et al. 2018). Thus, at least in atherosclerosis, the presence of TLOs is linked to plaque ruptures and subsequent acute cardiovascular events.

2.1.2.4 Reverse cholesterol transport by lymphatic system

Lymphatic system transports lipids from the intestine to the blood circulation and thus finally to the peripheral tissues (Dixon 2010). Interestingly, lymphatic system also removes the excess cholesterol from the interstitial space of peripheral tissues, a process called the reverse cholesterol transport (RCT) (Martel and Randolph 2013; Huang et al. 2015; Vuorio et al. 2017).

In RCT the excess cholesterol is removed from the peripheral tissues by macrophages and transported as HDL for excretion in the liver (Lim et al. 2013; Martel et al. 2013; Huang et al. 2015). As an example, the excess cholesterol in the form of cholesteryl ester-rich lipoprotein in the arterial wall is taken up by the macrophages in the intima. A vast accumulation of cholesteryl esters into the macrophages' cytoplasm converts them into foam cells. The cholesteryl esters are then hydrolyzed to free cholesterol. In the RCT, the excess free cholesterol is actively transported (through ATP-binding cassette A1 or G1, or scavenger receptor BI expressed on the surface of macrophages) or passively diffused into the interstitial space (Wang and Rader 2007). The free cholesterol is bound by mature high-density lipoprotein (HDL) or by apolipoprotein A-I to form HDL, where the free cholesterol is again esterified to maintain the gradient of free cholesterol from macrophages to acceptors (Wang and Rader 2007). The size range of the small discoidal HDL-molecules found in the interstitial fluid is 3.8 to 5.4 nm, directing it to the lymphatic rather than blood vasculature (Randolph

and Miller 2014). Surprisingly, Lim et al. showed that at least partly, the entry of HDL particles to the lymphatics is an actively controlled process (Lim et al. 2013). LECs express HDL transporters on their surface, and interfering the scavenger receptor BI expression impaired HDL uptake to the lymphatics by 80%, and antibody-blocking of the same receptor prevented the specific transport of HDL through the LEC monolayer (Lim et al. 2013). Martel et al. demonstrated that the cholesterol efflux from the aortic plaques through the adventitial lymphatic vessels could be blocked by anti-VEGFR3-antibodies (Martel et al. 2013). Once in the lymphatic system, the cholesterol-carrying HDL-particle travels through the collecting lymphatic vessels and finally enters the blood circulation via thoracic duct. In the last stage of RCT, the liver takes up the HDL and secretes the cholesterol to bile to be excreted via the feces. Through RCT, the lymphatic system can actually facilitate the cholesterol efflux from a plaque (Aspelund et al. 2016).

2.1.3 Leukocyte circulation between blood, lymphoid organs, and other tissues

The main purpose of leukocyte recirculation is to allow naïve lymphocytes to search for their specific antigens in confined spaces distributed around the body and to then allow the effector cells to migrate into tissues from which the antigen originated from. In addition, monocytes and neutrophils migrate to inflammatory sites in case of infection or tissue injury. Thus, an essential feature of leukocyte recirculation is the variability in the timing and location of leukocyte extravasation from the blood to enter either an SLO or an inflamed tissue. This specificity to recognize the site of extravasation is tightly regulated by changing the expression of adhesion molecules on the surface of endothelium as well as on the leukocytes (Butcher and Picker 1996). By varying the timing, amount, and combinations of just a few trafficking molecules, the immune system can either enable or restrict the access of specific leukocytes to relevant sites. This sequential process is called adhesion cascade, and it is reviewed in details in the next chapter. Each leukocyte subpopulation has its special role in immune surveillance, and the migratory tendencies of the leukocytes belonging to the various subpopulations vary in physiological and inflammatory circumstances. In short, naïve B and T lymphocytes migrate from blood to SLOs, whereas the cells of the innate immunity (dendritic cells, monocytes, and neutrophils for example) readily enter tissues upon inflammatory signals. Later on, the cells of the adaptive immunity (effector and memory B and T cells) enter the inflammatory sites as well. (Abbas et al. 2016).

2.1.3.1 Leukocyte trafficking across inflamed endothelium

In general, venules are the site of leukocyte transmigration (Nourshargh et al. 2010). The following is a description of leukocyte trafficking across the endothelium in inflamed and/or damaged tissues. The same steps, with slightly different adhesion molecules, are taken when lymphocytes enter LN through HEVs (von Andrian and Mempel 2003). In particular monocytes, neutrophils, and effector T cells are required to enter the interstitium to eliminate the inflammatory trigger and help repairing the tissue. For this to happen, several steps involving leukocyte stimulation and shape changes, as well as destruction of the endothelium while preventing plasma leakage need to be taken, all while under the hydrodynamic forces of the blood flow. This highly controlled process has been reviewed in great detail recently (Nourshargh and Alon 2014; Vestweber 2015). A simplified illustration of the cascade is shown in Figure 8.

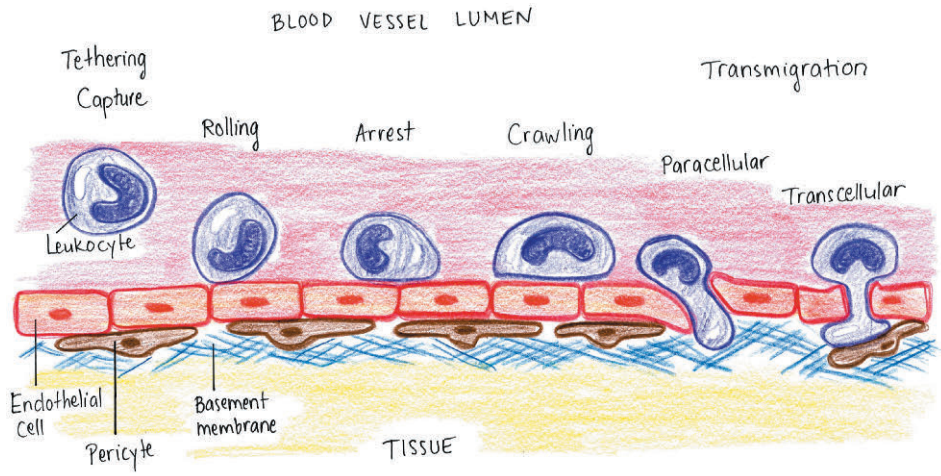

Figure 8. The leukocyte adhesion cascade. The cascade starts as the endothelial cells express certain adhesion molecules on their surface. The bypassing leukocytes first tether on the vascular wall and start to roll on the endothelium. The activated endothelial cells and leukocytes express new adhesion molecules leading to firmer attachment. The leukocyte crawls on the endothelium in search of an appropriate transmigration site and finally extravasates the blood vascular lumen and enters the tissue.

The whole cascade of events starts as exogenous (micro-organisms, allergens, toxic compounds etc.) or endogenous (signals originated from stressed, damaged, or malfunctioning tissue) inducers are released to the interstitium (Medzhitov 2008). The resident cells of the innate immune system and other local cells respond to this stimulus by releasing cytokines and other pro-inflammatory mediators, which in turn activate the ECs of the post-capillary venules in the

tissue (Vestweber 2015). Activated ECs express first P-selectin and later E-selectin as well, on their surface, causing the bypassing leukocytes to take initial contacts (tethering) to the endothelium via P-selectin glycoprotein ligand-1 and L-selectin expressed on the leukocyte surface. This capture of leukocytes leads to rolling of leukocytes on the endothelium. Vascular adhesion protein-1 (VAP-1) an adhesion molecule expressed by ECs is involved in the tethering and rolling phases of the adhesion cascade as well (Salmi and Jalkanen 2017). P- and L-selectin depended rolling requires the shear stress of blood flow, and allows the movement of leukocyte as new bonds are formed before the old ones are broken (Ley et al. 2007). In addition to selectins, integrins play an important role in the rolling, as well as the firm adhesion stages of the cascade in a leukocyte subtype specific manner (Evans et al. 2009; Hogg et al. 2011). As ECs express certain chemokines on their surface, the rolling leukocytes get activated leading to the activation of integrins on the leukocyte surface. The activated integrins are then able to bind intercellular adhesion molecule 1 (ICAM-1) and vascular cell adhesion molecule 1 (VCAM-1) expressed on the activated endothelium. These interactions first slow the rolling down, and finally arrest the leukocyte. Next, the leukocytes crawl on the vessel wall presumably in search of an exit place (Vestweber 2015). Especially neutrophils, monocytes and T-cells can crawl long distances on the luminal surface of the blood vessel. Interestingly, some monocytes patrol the blood vessels even in non-inflamed tissues (Auffray et al. 2007), and scavenge microparticles (Carlin et al. 2013). Finally the leukocytes have reached the transmigration site to extravasate the blood and cross the endothelium. The transmigration itself can happen by paracellular (between ECs) or transcellular (through an individual EC) route. Some studies suggests, that no matter what route, the ECs form actin filament-containing membrane extensions called docking structures (Barreiro et al. 2002). Another study showed how *in vivo* by binding to ICAM-1 on the surface of ECs the leukocyte triggers a signaling cascade involving cortactin and Ras homology growth-related, which results in the clustering of ICAM-1 molecules into a ring-like structure around the leukocyte (Schnoor et al. 2011). This action is required for the diapedesis process.

2.2 Atherosclerosis, the underlying cause of several CVDs

Atherosclerosis is a chronic, inflammatory, and progressive disease which is accountable for the majority of CVDs (Head et al. 2017). The mechanisms and pathways behind atherosclerosis are complex, with particular emphasis on the role of endothelium as the regulator of blood flow and leukocyte migration for instance. In atherosclerosis, the lumen of a large- or medium-sized artery narrows

in consequence of plaque build-up in the arterial wall. The origin of atherosclerosis lies in 1) the dysfunctional mechanotransduction of endothelium in disturbed flow areas, 2) the entailing disrupted lipid accumulation to the intima of the blood vessel as a result of increased permeability and hyperlipidemia, and 3) the maladaptive immune response to the situation, seen as an inappropriate leukocyte trafficking (Galkina and Ley 2009). As the intima thickens, hypoxia entails, resulting in the formation of immature, leaky neovessels (Chistiakov et al. 2017). These neovessels are responsible for recruiting more leukocytes to the scene which has been shown to associate with adverse cardiac events. In addition, the intraplaque neovessels can cause intraplaque hemorrhages, thus destabilizing the plaque (Chistiakov et al. 2017). Indeed, the stability of the forming plaque determines whether the plaque progression completes with a rupture leading to acute cardiovascular events.

Atherosclerosis manifests itself in the clinic as ischemic heart disease (in which an obstruction in the coronary arteries of the heart restricts the blood supply to the heart; also known as coronary artery disease (CAD) or coronary heart disease (CHD)), ischemic stroke (in which an obstruction in the cerebral arteries restricts the blood supply to the brain; also known as cerebrovascular disease), and as peripheral artery disease (in which atherosclerosis restricts blood supply to lower limbs, stomach, or arms) (Herrington et al. 2016). Despite the vast understanding of the biology and genetics behind atherosclerosis, CVD alone is accounted for nearly half of the deaths in Europe (Nichols M 2012; Townsend et al. 2015), suggesting that we are not able to intervene the course of the disease early enough, or that we are not accurately identifying the individuals at risk for future CVD. Indeed, approximately 60% of the persons classified to low or low-intermediate risk for future CAD had a CAD event (Elosua et al. 2013). This suggests that new biomarkers for CVD are needed.

2.2.1 Pathogenesis of atherosclerosis

Atherosclerosis is a long process, origins of which are found already in the childhood (Tabas et al. 2007; Juonala et al. 2013). Atherosclerosis is now known to be a complex chronic inflammatory disease (shown in Figure 9), which starts by dysfunction of ECs exposed to external forces such as disturbed flow in the branch points of the aortic tree (fluid shear stress), hypertension, free radicals, smoking, or dyslipidemia. This leads to the activation of endothelium, following expression of adhesion molecules and chemokines, and subsequently leukocyte (especially monocyte and T lymphocyte) adherence and transmigration. At the same time, changes in the permeability of the endothelial barrier allow

cholesterol-carrying low-density lipoprotein (LDL) particles to enter the extracellular matrix beneath the endothelium. The protein part of the particles, apolipoprotein B-100, interacts with the proteoglycans of the extracellular matrix. This leads to the retention of LDL-particles to the intima layer and subsequently predisposes these particles to the attacks of oxidative enzymes and reactive oxygen species generating oxidized LDL. The oxidized LDL presents danger-associated molecular patterns (DAMPs) that activate the cells of the innate immune system as well as the vascular cells (Ketelhuth and Hansson 2016). Additionally, the oxidative stress can accelerate the reactions between reducing sugars and the free amino groups of proteins leading to advanced glycation end (AGE) products, which in turn increase the production of inflammatory cytokines (Galkina and Ley 2009; Nowotny et al. 2015). Activated ECs release macrophage colony-stimulating factor (MCSF) which stimulates monocytes to differentiate into scavenger receptor expressing macrophages, while activated T-cells release inflammatory cytokines, such as interferon gamma (IFN-γ) to further activate the ECs and macrophages (Hansson and Hermansson 2011). These macrophages are able to take up oxidized LDL particles and turn into lipid-rich foam cells, which form the initial lesion called a fatty streak. The early lesion develops neovessels in respond to the hypoxia and inflammation resulting from the thickening of the vessel wall, and facilitating the recruitment of leukocytes (Moreno et al. 2006; Galkina and Ley 2009). As the lesion progresses, some foam cells and SMCs die of apoptosis, releasing lipids and cell debris which accumulates and forms the necrotic core. SMCs, resident and the ones recruited from the tunica media, form a fibrous cap above the necrotic core by producing collagen, proteoglycans, and elastin. Some advancing lesions may undergo a thinning of the cap as the interferon-γ produced by T-cells is inhibiting the synthesis of cap-stabilizing collagen and as macrophages are producing collagenases. This may lead to a fracture in the cap, which brings the blood components into a close contact with the plaque components. The following thrombosis and partial or total occlusion of the affected artery may be the first clinical manifestation of the asymptomatic, subclinical atherosclerosis. (Hansson and Hermansson 2011; Libby et al. 2011; Libby 2013; Libby et al. 2013).

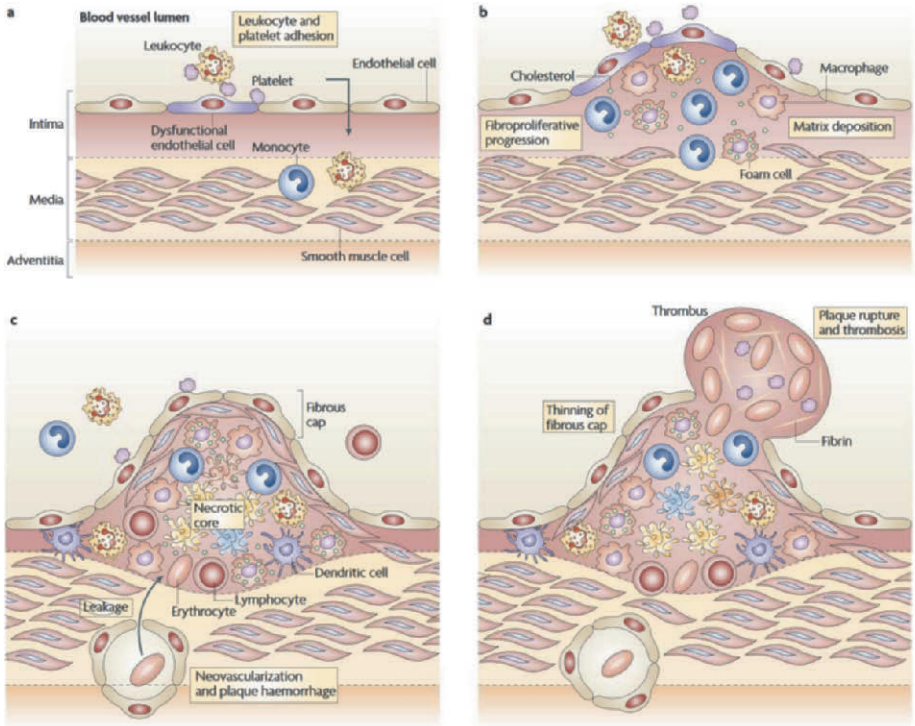

Figure 9. The process of atherosclerosis. a) High blood pressure, hyperlipidaemia, smoking, free radicals, and diabetes lead to dysfunction of endothelium. Endothelial cells (ECs) release adhesion molecules, and the permeability of endothelium increases. b) Leukocytes and cholesterol enters intima. Activated ECs release chemokines and growth factors. LDL-particles are oxidized. Monocytes recruited to the intima transform into macrophages. Macrophages accumulate the lipids, forming foam cells, which make up the early lesions called fatty streaks. c) Fibrous cap and SMC layer forms. Neovessels are formed to feed the thickening wall. Necrotic core forms from the apoptotic foam cells. The lumen of the blood vessel narrows. d) Matrix degradation due to proteases and time thins the fibrous cap. Plaque ruptures, and blood coagulation factors encounter the debris from the plaque, which leads to thrombosis, arterial occlusion, and myocardial infarction or stroke. Reprinted by permission from Springer Nature: Springer Nature, Nature Reviews Immunology, *The multifaceted contributions of leukocyte subsets to atherosclerosis: lessons from mouse models.* Weber, C., Zernecke, A. and Libby, P. 2008. License number: 4283050451709.

The numerous roles of T and B cells, as well as monocyte-macrophages and dendritic cells in atherosclerosis have been recently reviewed (Cybulsky et al. 2016; Ketelhuth and Hansson 2016; Tabas and Lichtman 2017). In addition to the devastating role of immune cells to the progress of atherosclerosis, the lymphatic vessels have numerous paths to affect the atherogenesis process as well, as they are involved in the dietary fat absorption and metabolism, in the inflammation of adipose tissue, in obesity, in RCT, and in generally in innate and adaptive immunity (Milasan et al. 2015; Aspelund et al. 2016). In humans, lymphatic vessels are present in the adventitia of aorta (Drozdz et al. 2008), and

in the intima of atherosclerotic lesions (Kholova et al. 2011).The dense network of lymphatic vessels in arteries seems to be atheroprotective, probably because of the RCT (Kutkut et al. 2015). Several studies have shown that the TLOs in arteries are associated with the severity of atherosclerosis (Schwartz and Mitchell 1962; Kohchi et al. 1985; Tavora et al. 2010; Akhavanpoor et al. 2018).

2.2.2 Atherosclerosis as a foundation bed of CVD risk factors

The term 'risk factor' was introduced in 1961 in Framingham Study (Kannel et al. 1961), and in many occasions it is described as a factor that increases the probability of developing a disease. In this dissertation, the term 'risk factor' means that the factor has causal effect on the disease progression and that this has been proven at least in Mendelian randomization experiments (Herrington et al. 2016). The causality of at least smoking, high blood pressure, dyslipidemia, and diabetes mellitus to future CVD have been established (Herrington et al. 2016), and are considered as traditional risk factors in this dissertation. In addition, male sex and older age are considered as traditional risk factors for CVDs in this dissertation (D'Agostino et al. 2008). Most of the traditional risk factors for CVDs are considered as lifestyle-associated, and CVDs are often seen as lifestyle-dependent modern diseases of Western society. Recent studies however have reported atherosclerosis-like arterial changes in mummies of ancient societies challenging the previous hypothesis, and other studies have determined that age itself is the strongest risk factor for atherosclerosis, and thus for CVDs (Head et al. 2017; Niiranen et al. 2017). Interestingly, endothelial dysfunction is associated with smoking, hypercholesterolemia, hypertension, aging, and diabetes (Hadi et al. 2005; Rajendran et al. 2013). Since the results from intervention studies concerning diet, physical activity, alcohol intake, social connections, sleep, and psychological stress in association of CVD events are somewhat controversial (Doughty et al. 2017), this review of literature concentrates on the traditional risk factors of CVDs and the environmental factors as risk factors of CVDs.

Smoking. According to World Health Organization, smoking alone accounts for 10% of CVD events (Messner and Bernhard 2014). The evidence for causal effect of cigarette smoking to CVD has been easily proven, since the predisposing to this particular risk factor is rather straightforward, as a person either smokes or does not. In addition, by quitting cigarette smoking the risk for CVD events is decreased (Messner and Bernhard 2014). Since tobacco smoke can contain up to 4000 different chemicals, the physiological pathways to which these agents affect to are still mostly unclear. Smoking causes several pro-

atherogenic changes in the vasculature. It decreases the endothelium-dependent flow-mediated dilatation (a marker of endothelial dysfunction) measured by ultrasound, increases serum total cholesterol while decreasing HDL cholesterol, and increases the oxidative modification of lipids (Hadi et al. 2005; Messner and Bernhard 2014). In addition, smokers have elevated levels of proinflammatory cytokines and leukocytes in blood circulation, and furthermore, the endothelium of smokers expresses more adhesion molecules than non-smokers endothelium, thus facilitating leukocyte recruitment (Messner and Bernhard 2014). Finally, smoking has pro-atherothrombotic effects as it activates the coagulation system (Csordas and Bernhard 2013).

High systolic blood pressure. Hypertension is such a major risk factor for CVD, that in 2017 the threshold for hypertension was lowered to ≥130/80 mmHg from the previous ≥140/90 mmHg (Whelton et al. 2017). The regulation of blood pressure takes place mainly in the small resistance arteries (lumen diameter <300μm) (Touyz et al. 2018). The vascular SMCs are plastic, switching phenotype from differentiated contractile cells to dedifferentiated, proliferative phenotype. Inflammation in the vasculature is thought to contribute to hypertension by increasing the proliferation of SMCs. The proliferative SMCs express low levels of contractile markers, but high levels of signaling molecules associated with migration, inflammation, fibrosis, and cell growth leading to accumulation of SMCs in the vascular wall, and ultimately to vascular stiffness (Touyz et al. 2018). However, the etiology of hypertension is far from clear (Leibowitz and Schiffrin 2011). Hypertension is a complex state which is influenced by factors such as age, sex hormones, and lifestyle, and recently the differences in the key systems of activation among men and women, and their contribution to different effects on hypertension and CVD risk have been studied (Colafella and Denton 2018).

High levels of modified LDL. The causality of cholesterol to atherosclerosis, and thus to CVD, is well established (Steinberg 2013; Di Pietro et al. 2016), and some even suggest that the lipoprotein retention is the root cause of atherosclerosis (Tabas et al. 2007). LDL consists of cholesteryl ester, free cholesterol, phospholipids, triglycerides, and an apolipoprotein B-100 protein, and it is the main lipid transporter in circulation. The LDL particles enter the intima via transcytotic pathway through endothelium, but since the intima lacks lymphatic vessels which would remove excess LDL, the LDL not taken up by the cells accumulates in the arterial intima (Pentikainen et al. 2000). Indeed, the nearest lymphatic vessels are located in the medial layer, and in order to reach them LDL particles have to pass the extracellular matrix of intima (Pentikainen et al. 2000). The subendothelial LDL is modified proteolytically, lipolytically, and oxidatively, creating modified LDL particles. The macrophages in the intima

remove the modified LDL and form foam cells (Matsuura et al. 2006). The modified LDL in turn can further activate the endothelium and SMCs by increasing the expression of adhesion molecules and chemokines, thus perpetuating the inflammatory cycle (Steinberg 2002; Galkina and Ley 2009).

Low levels of plasma HDL. Low levels of plasma HDL are associated with increased risk of CVD (Rosenson et al. 2016). This originates in the role of HDL in many antiatherosclerotic processes. HDL, and its main protein component apolipoprotein A1 are the main acceptors of free cholesterol from macrophages in RCT (Martel and Randolph 2013; Lee-Rueckert et al. 2016). HDL can enhance the production of nitric oxide from ECs thus ameliorating the endothelial dysfunction. HDL particles range in size from 7 nm to 14 nm, with the largest particles containing largest amounts of cholesterol (He et al. 2018). Nevertheless, HDL as a population is heterogeneous with each sub-population having possibly distinct functions and routes of metabolism (He et al. 2018).

Type 2 diabetes mellitus (DM) is a metabolic disease which manifests as hyperglycemia caused by insulin resistance and beta-cell impairment (De Rosa et al. 2018). Type 2 DM is an independent risk factor for CVD (Grundy et al. 1999), although several pathophysiological features are shared by type 2 DM and CVD, such as hypertension, obesity and dyslipidemia (De Rosa et al. 2018) and thus it is hypothesized that these diseases have a ‘common soil’ (Stern 1995). The prevalence of type 2 DM is rising with the Western diet of high-caloric intake which has been shown to induce vascular abnormalities due reactive oxygen species production (Rajendran et al. 2013). Insulin has vasodilatory effects (widening of the vessel lumen) through enhanced production of nitric oxide causing increase in blood flow, which is especially important in the microvasculature where nutrients, hormones, and insulin itself is transported into the tissues (Rajendran et al. 2013). In insulin resistance the microvascular circulation is disturbed leading to further peripheral endothelial dysfunction (Hadi et al. 2005). In addition, chronic hyperglycemia results in glycation of macromolecules and proteins, oxidation of lipids and proteins, all of which are contributing to endothelial dysfunction and are thus atherogenic (Hadi et al. 2005).

Male sex. There are sex differences in the incidence of CVD events as well as in the clinical spectrum of events. In a Finnish population study, men had more major adverse cardiovascular events (MACEs), four times more fatal coronary heart disease events and three times more non-fatal coronary heart disease events than women (Lehto et al. 2014). In addition, the clinical spectrum varied as coronary heart disease was the most common type of MACE in men, whereas in women heart failure was the most common type (Lehto et al. 2014). However,

contemporary studies on gender has evoked new perspectives on how much the male sex and how much the male gender as a social determinant, is behind these differences seen in the CVD vulnerability (O'Neil et al. 2018). O'Neil and co-workers speculated that as the gender is socially produced, the roles for boys and girls are adopted already in the early childhood, affecting the risk of CVD events in adulthood through societal pressure for smoking, physical activity, and alcohol consumption. In adulthood the gender, rather than the biological sex, modifies the risk of CVD events via experiences of work, home and financial stress (O'Neil et al. 2018).

Aging. The inevitable aging of vessels leads to vascular remodeling evident as thickening of intima and media, and loss of arterial elasticity resulting in arterial stiffness, and subsequently hypertension (Wang and Bennett 2012). In arteries, aging can be seen as a chronic, low-grade inflammation (Wang et al. 2014) Aged vessels have increased amounts of collagen, matrix metalloproteinase enzyme activity, and glycated proteins, while decreased amounts of SMCs and elastin in arterial wall have been reported (Wang and Bennett 2012). In addition, both SMCs and ECs in aged vessels have shown to secrete augmented amounts proinflammatory cytokines, and ECs of aged vessels express increased levels of leukocyte adhesion molecules. All these detrimental changes are accelerated in atherosclerosis (Wang and Bennett 2012).

Environmental factors, such as air pollution (combustion byproducts released from motor vehicles, particulate matter from coal burning and other fossil fuel usage) and nonessential metals (arsenic, cadmium, and lead), are considered risk factors of CVD (Cosselman et al. 2015; Bhatnagar 2017). According to WHO, air pollution attributed 3.7 million deaths in 2012, and 4 out 5 deaths were CVD-related (Cosselman et al. 2015). The environmental agents can be inhaled, ingested, or absorbed through skin, and they evoke inflammation, and alter cell signaling and gene expression. Like the air pollutants, the nonessential metal pollutants can act through oxidative stress, inflammation, and altered ion channel activity leading to endothelial dysfunction, increased blood pressure, and decreased heart-rate variability, ultimately resulting in atherosclerosis and hypertension (Cosselman et al. 2015).

2.2.3 Biomarkers of CVD

In this thesis, a biomarker and a risk factor are defined as follows. For a character to be called a risk factor, this character has to have proven effect to affect the beginning or the progress of the disease, i.e. causality has been proven (Libby and King 2015). A biomarker however may or may not contribute to the

disease progression itself, but merely reflects the state of the disease (Libby and King 2015). In this regard, cardiovascular risk factors are high age, high total and low HDL cholesterol, smoking, high systolic blood pressure, presence of diabetes mellitus, and male sex for example, whereas some of the biomarkers of cardiovascular diseases with their pathophysiological pathways (given in brackets after the respective risk factor) are high-sensitivity CRP (inflammation), homocysteine (endothelial dysfunction), cardiac troponins (cardiomyocyte injury), natriuretic peptides (hemodynamic stress), plasminogen activator inhibitor-1 (thrombosis), and lipoprotein(a) (lipid metabolism) for example (Wang et al. 2006; Vasan 2006; Zethelius et al. 2008; Wang 2011; Cahill et al. 2015; Wang et al. 2017).

New potential biomarkers for coronary artery disease are extracellular vesicles containing lipids, proteins, noncoding RNA and nuclear material, which are known to accumulate in atherosclerotic plaques, and released by ECs, leukocytes, platelets, and erythrocytes (Boulanger et al. 2017). Another new area of biomarkers for CVD are the markers of endothelial glycocalyx dysfunction, especially the proteoglycans of glycocalyx, such as Syndecan-1 (Kim et al. 2017). Flow-mediated vasodilation is a potential marker for endothelial dysfunction as it measures the diameter of the artery in endothelium-dependent (reactive hyperemia induced by cuff) and in endothelium-independent (response to nitroglycerin) dilatation (Raitakari and Celermajer 2000; Kim et al. 2017).

Biomarkers of CVD are needed, because the current risk prediction leaves out the persons with none of the traditional risk factors or with only one traditional risk factor, who however do experience a CVD event (Khot et al. 2003; Wang 2011). Recently, biomarkers identifying the individuals at the “low and intermediate” risk of CVD events have acquired much interest since the individuals in high risk for CVD get intervention in any case, whereas the individuals with only a few risk factors as a population account for the most CVD events (Khot et al. 2003; Wang et al. 2012; Folsom 2013). Indeed, in numbers most of the CVD events happen in this group of people, yet they are not targeted for any preventive measures according to traditional risk factors (Wang 2011).

2.2.4 Technical considerations regarding an ideal biomarker of CVD

According to Biomarkers Definitions Working Group a biomarker is defined as “A characteristic that is objectively measured and evaluated as an indicator of normal biological processes, pathogenic processes, or pharmacological responses to a therapeutic intervention” (Atkinson et al. 2001). Biomarkers are used to discover new pathogenic pathways, to discover new therapeutic targets, to

discriminate ‘cases’ and ‘non-cases’, to categorize individuals to different risk categories of future event, and in precision medicine, to help indicate the responsiveness of the patient for a drug dosage, for example (Libby and King 2015). When considering a new biomarker for CVD, the biomarker should be easily and cost-effectively measurable, have an association with the outcome, add information to old tests, and help the clinician to manage the patients (Morrow and de Lemos 2007).

There are several methods to obtain biomarker information from an individual (Vasan 2006). First, a biomarker can be quantified from a biosample, such as blood, urine or tissue. Second, biomarker information can be recorded from a person like blood pressure. Third, the biomarker can be the result of an imaging test, such as ultrasound. This review of literature concentrates on the biomarkers obtained from blood sampling. When considering blood biomarkers several issues need to be addressed. Pre-analytical variability stems from the blood sampling as such (effect of hemolysis for example), the anticoagulants used (the effect of chelating agents), the stability of the analyte in different storage temperatures and for different lengths of time (Vasan 2006; Libby and King 2015). The assays measuring the biomarkers need some consideration as well, as they are the source of analytical variation. Accuracy and precision of the assay are pivotal in biomarker assay validation and can be controlled through use of reference materials and coefficients of intra-assay variation (calculated from the duplicates on the same plate) and inter-assay variation (describes the plate-to-plate variation, and is calculated from the mean values of high and low controls on different plates) (Vasan 2006). In addition, the costs of a biomarker assay are to be considered when transferring the assay to a clinical environment.

2.2.5 Statistical considerations regarding an ideal biomarker of CVD

For a CVD biomarker, a few characteristics are considered invaluable. Regardless the causality or non-causality of the CVD biomarker, a novel biomarker should add information above and beyond the classical risk factors in prediction equations of CVD events (Wang 2011; Folsom 2013). For researchers to demonstrate the ability of a novel biomarker to add incremental value to the elevated risk of an outcome, the already established risk factors must be accounted for in multivariable models. The hazard ratios (HRs) obtained from Cox proportional hazard models with the values of the probability test of significance are one way to present the results (Vasan 2006).

Classically, the goodness of a novel biomarker has been measured by its performance in discrimination (i.e. the tests’ ability to distinguish those who will

get the disease from those who will not) by improving the concordance statistics (Wang 2011). Concordance statistics measures the area under the receiver operating characteristics (ROC) curve (AUC), which is drawn based on the ranks of the individuals who developed the disease and those who did not (Vasan 2006). The concordance statistics introduces two inherently important aspects of any screening test; sensitivity ("the ability to detect disease when it is present") and the specificity ("the ability to exclude disease when it is absent") (Wang 2011). Since the model including the traditional risk factors explain nearly 80% of the CVD events (D'Agostino et al. 2008), it's fairly difficult to add new predictive biomarkers for this model (Pencina et al. 2008). In addition, the area under the ROC curve (also known as AUC and C-statistics) has gained criticism for not being suitable for clinical use, since it was developed for a different purpose (during World War II to analyze radar data in order to differentiate signal noise and enemy aircraft) (Streiner and Cairney 2007; Cook and Ridker 2009; Grund and Sabin 2010). After the World War II, the ROC analysis has been used to compare diagnostic tests, with the emphasis on true positive rate against the false positive rate (Janes et al. 2008). The ROC analysis is based on the rank-orders of the predicted risks rather than the size of the risks, and additionally, ROC-analysis assumes that both high sensitivity and high specificity are equally meaningful (Grund and Sabin 2010). However, in clinical settings the size of the actual risk of an individual may be important, and furthermore, a clinician is rarely asked to compare the risks of a pair of subjects (Janes et al. 2008). To address these before mentioned defects, Pencina and co-workers introduced two new measures to evaluate the usefulness of a new marker, since statistically significant relation of a new marker to the outcome does not imply improvement in model performance nor clinical significance (Pencina et al. 2008; Wang 2011). The first measure is called net reclassification improvement (NRI) and it is based on *a priori* decided risk categories (0-5, 5-10, 10-20, and >20 per cent risk categories for CVD events in the next 10 years for example). The movement of subjects who develop an event to a higher risk category is considered as an improvement in classification, whereas movement of an event subject to a lower risk category is considered worse reclassification. The same reclassification tables are calculated for the non-events (i.e. those subjects who do not develop the event) but with opposite interpretation of the movements (downward improves reclassification and upward movements worsens it). The sum of proportional movements in the right direction for subjects with and without an event minus the sum of proportional movements in the wrong direction for both groups quantifies the improvement in reclassification and this measure is called the NRI (Pencina et al. 2008). The drawback of NRI is that it requires the use of pre-existing risk categories. To overcome this, Pencina and co-workers introduced another measure, called integrated discrimination

improvement (IDI), a category-free measure for quantifying the overall improvement in specificity and sensitivity based on the difference in discrimination slopes of the old and new (with the new biomarker) models (Pencina et al. 2008). These measures have since been developed further (Pencina et al. 2011), and the usefulness of these measures in clinical point of view has been a subject of debate (Leening et al. 2014; Leening et al. 2014; Sniderman et al. 2015).

In addition to the abilities to discriminate and reclassify, the risk prediction model with the new biomarker should be well calibrated, meaning that the predicted risks and the observed risks actually go hand-in-hand, and this can be measured with Hosmer-Lemeshow test (P values >0.05 means that there is not a significant difference between the predicted and observed risks and the model is thus well calibrated) (Wang 2011). Finally, the findings related to a novel biomarker need a validation; a test how well the results obtained from the training study population would fit to another study population called the validation data set. The validation tells how well the model performs in practice. In ideal circumstances, the model is trained and validated in two independent data sets, but this is rarely possible, and to circumvent this a cross-validation protocol is used (Picard and Cook 1984). In cross-validation the data set is first divided to k subsets with equal sizes. For example, in 10-fold cross validation, the model is trained in 9 subsets and then the intercepts and parameter estimates acquired from the 9 training folds are used in the remaining subset, called the validation data set. This process is repeated 10 times, with each subset as the validation data set once.

2.3 Vascular adhesion protein-1

As mentioned before, a hallmark of leukocyte trafficking is the adhesion of leukocytes to the vascular endothelial cells. In normal circumstances lymphocytes migrate to peripheral lymph nodes and mucosal lymphoid organs through HEVs. Instead, upon inflammation the endothelium of any location is activated and adhesion molecules are expressed and or transported onto the luminal side. In 1992 Salmi and Jalkanen produced monoclonal antibodies (mAb) against human synovial vessels. In immunohistological stainings of inflamed synovial membranes, peripheral lymph node, and tonsil, one mAb stained HEV-like venules. The antigen was named vascular adhesion protein-1 (Salmi and Jalkanen 1992).

2.3.1 Basic characteristics

In humans, VAP-1 was first discovered as a 90-kDa protein on the luminal surface, as well as in intracellular granules of endothelial cells, and in smooth muscle cells of arteries, veins and bowel wall (appendix) (Salmi and Jalkanen 1992). A larger, 150-180-kDa form of VAP-1 was detected soon after the first discovery (Jalkanen and Salmi 1993). In 1998, a circulating form of VAP-1 was detected in human serum samples, allowing the quantitation of soluble VAP-1 in patients (Kurkijarvi et al. 1998). Surprisingly, the cloning of VAP-1 revealed an unexpected similarity to the copper-containing amine oxidase family (Smith et al. 1998), and further studies confirmed that the D4 domain of VAP-1 is the catalytic site of the enzyme (Salminen et al. 1998). The enzymatic activity of VAP-1 is referred as semicarbazide-sensitive amine oxidase (SSAO)-activity stemming from the notion that semicarbazide inhibits the reaction (Bergeret et al. 1957). In summary, VAP-1, the adhesion molecule involved in the leukocyte-adhesion, was discovered in 1992, but the enzyme, the copper-containing amine oxidase, has been known since the 1950's (Bergeret et al. 1957), and finally in 1998 they were shown to be the same molecule.

Structurally, VAP-1 is a type II transmembrane protein, a homodimer with each identical monomer consisting of domains D2, D3, and D4, and with sialic acid decorations on the surface at the end of the glycans (Salminen et al. 1998; Smith et al. 1998; Airenne et al. 2005; Maula et al. 2005). The crystallographic studies on VAP-1 have shown that all 6 possible *N*-glycosylation sites are occupied and that on the surface of VAP-1 molecule, an RDG motif is found (Airenne et al. 2005; Jakobsson et al. 2005).

VAP-1 molecule is found on various cell and tissue types in relation to the various functions of VAP-1. In the vessels of tonsil and peripheral lymph node, VAP-1 is expressed on the cells of HEVs (Salmi et al. 1993) where VAP-1 exerts its function as an adhesion molecule of leukocyte trafficking (Salmi and Jalkanen 1992). Instead, in the larger vessels (aorta and vena cava for example) VAP-1 is present in the smooth muscle cells of the vessel wall (Salmi et al. 1993; Jaakkola et al. 1999). On adipocytes VAP-1 is present on the plasma membrane as well as in intracellular glucose transporter type 4 containing vesicles (Enrique-Tarancon et al. 1998) in line with VAP-1's role in glucose transportation in adipocytes, and in leukocyte infiltration to white adipose tissue (Zorzano et al. 2003; Bour et al. 2007; Bour et al. 2009). In human liver, VAP-1 is a heavily sialylated glycoprotein, which is constitutively expressed on vascular and sinusoidal endothelium, and the anti-VAP-1-mAb 1B2 is able to inhibit T cell binding to hepatic endothelium (McNab et al. 1996). In addition, VAP-1 is found on a subset of venules in kidney, skin, heart, and brain (Salmi et al. 1993).

The expression of VAP-1 was elevated in inflamed human tissue samples, but none of the known inflammatory mediators were able to induce the VAP-1 expression *in vitro* (Salmi et al. 1993). Instead, in an organ culture of human tonsillar tissue, interleukin-4 (IL-4), IFN-γ, tumor necrosis factor alpha (TNF-α), and lipopolysaccharide were able to up-regulate the endothelial VAP-1 expression (Arvilommi et al. 1997). Interestingly, this induced increase in endothelial VAP-1 expression was not achieved in an organ culture of human appendix, nor in the SMCs of these tissues (Arvilommi et al. 1997). In *in vivo* experimental inflammations of skin and joint, the results indicated that the up-regulation of VAP-1 occurred in 60 minutes after an inflammatory stimulus, and that in the normal tissues the VAP-1 molecule was not present on the luminal surface of the endothelium, but was intracellularly stored (Jaakkola et al. 2000). Weston and co-workers developed a GFP-fusion protein of VAP-1 and demonstrated that VAP-1 is localized in subcellular vesicles throughout the cytoplasm of hepatic sinusoidal ECs, liver myofibroblasts, and hepatic stellate cell line (Weston et al. 2013). Interestingly, Sallisalmi and co-workers measured the amounts of SSAO-activity and syndecan-1 in 20 septic shock patients and showed that the glycocalyx injury and circulating VAP-1 levels coincident thus suggesting that endothelial injury activated VAP-1 on the endothelium (Sallisalmi et al. 2012). Curry et al. reviewed the several consequences of glycocalyx injury on the microvascular permeability and the following inflammatory cascade leading to leukocyte adherence (Curry and Noll 2010).

When comparing naturally occurring VAP-1 in vessels to cultured endothelial cells, several differences were noticed. In tonsil HEV, VAP-1 is 170-kDa in size, has sialic acid as well as O- and N-linked glycans as decorations, and is localized in large cytoplasmic granules, which are not Weibel-Palade bodies (Salmi and Jalkanen 1995). Instead, in cultured endothelial cells (e.g. EaHy-926 and human umbilical vein endothelial cells) these post-translational modifications were absent, and the 180-kDa VAP-1 molecule was expressed solely in small cytoplasmic granules, and was not inducible (Salmi and Jalkanen 1995; Arvilommi et al. 1997). These differences in VAP-1 post-translational modifications could be due to the difference in the inherent properties of different endothelial cells; cells of HEVs have ample glycocalyx and larger intercellular junctions suitable for lymphocyte trafficking, whereas no leukocyte migration occurs through human umbilical veins in normal circumstances. The various sialidase and glycosidase digestions revealed the abundancy of sialic acid and oligosaccharide decorations on VAP-1 (Salmi and Jalkanen 1996). The importance of these sialic acid decorations for VAP-1 function became evident, when neuraminidase or O-sialoglycoprotease treatment abrogated VAP-1-dependent lymphocyte binding to tonsil HEV on frozen sections under conditions of shear stress (Salmi and Jalkanen 1996). In addition, experiments with mutated

Ax endothelial cells demonstrated the particular importance of the three apical N-glycans in lymphocyte adherence to endothelium (Maula et al. 2005). The above-mentioned differences of endothelial cells bring a twist in the experimentation concerning adhesion molecules of HEV, and thus affect the result interpretation as well.

Generation of two mice lines expressing full-length human VAP-1 on the surface of endothelial cells or adipocytes, respectively (Stolen et al. 2004), and the creation of VAP-1 KO mice (Stolen et al. 2005) brought new tools to study VAP-1. The mice overexpressing VAP-1 had higher amounts of SSAO reaction product H_2O_2 in adipose tissue and liver lysates (Stolen et al. 2004). In general, the VAP-1 KO mice (*AOC3*$^{-/-}$) develop normally with no differences in the body weight nor in the life span compared to wild type (WT) mice (Stolen et al. 2005). In addition, the leukocyte numbers in the blood and in the secondary lymphoid organs were comparable (Stolen et al. 2005). The VAP-1 KO mice have generally normal lymphocyte recirculation (Salmi and Jalkanen 2017). However, the granulocytes and lymphocytes roll faster, adhere less, and transmigrate less in the VAP-1 negative blood vessels, but these effects were not due to changes in other adhesion molecules (Stolen et al. 2005). The blood pressure, heart rate, and the pulse pressure are normal in *SSAO*$^{-/-}$ mice (Mercier et al. 2006). Although the diameters of carotid arteries were found to be higher in *SSAO*$^{-/-}$ animals compared to WT mice, the arterial stiffness and the mechanical strength of the vascular wall were similar, suggesting that the smooth muscle function and the endothelial function were normal (Mercier et al. 2006).

2.3.2 VAP-1, an enzyme

As mentioned earlier, when VAP-1 was cloned, it was revealed to be an enzyme (Smith et al. 1998). The correct name for the gene product of *AOC3* gene is Membrane primary amine oxidase (EC:1.4.3.21), although it has been known as copper amine oxidase (one Cu^{2+} ion in each subunit (Airenne et al. 2005)) and as semicarbazide-sensitive amine oxidase (SSAO) as well (the reaction can be inhibited with semicarbazide (Smith et al. 1998)). Even though the current name specifies the enzyme to be membrane-related, the soluble form of endothelial VAP-1 harbors the SSAO-activity as well (Kurkijarvi et al. 2000).

VAP-1 belongs to the enzyme family of human copper amine oxidases with four other genes (*AOC1*, *AOC2*, and *AOC4*) belonging to the same gene family (Finney et al. 2014). *AOC1* encodes a diamine oxidase, an enzyme with main responsibilities to metabolize ingested histamine and putrescine (Kaitaniemi et al. 2009; Finney et al. 2014). *AOC2* encodes a retina-specific amine oxidase,

which prefers *p*-tyramine and tryptamine as substrates (Kaitaniemi et al. 2009; Finney et al. 2014). The *AOC4* is a pseudo-gene and due to an internal stop codon the *AOC4* encodes a non-functional protein in humans (Schwelberger 2010). The proteins encoded by *AOC1, AOC2* and *AOC3* share 38%-65% identity, with main conserved areas in the active-site (Finney et al. 2014). The *AOC3* comprises 7008 base pairs, has 4 exons, and is located in chromosome 17 (GeneCards 2018).

In this thesis, the enzymatic activity of VAP-1 is referred to as SSAO. The SSAO reaction catalyzed by VAP-1 involves the deamination of primary amines to corresponding aldehydes while releasing hydrogen peroxide and ammonium. Crucial for the enzymatic reaction is a topaquinone (TPQ) cofactor, which is derived from a tyrosine in a post-translational modification requiring copper and molecular oxygen (Shepard and Dooley 2015). The SSAO reaction is divided to two half-reactions. First, in the reductive half-reaction the substrate (a primary amine) reacts with the TPQ to form a Schiff base. Subsequently, the product aldehyde is released through hydrolysis, and the remaining TPQ is reduced. In the second half-reaction, molecular oxygen then reoxidizes the reduced TPQ in the presence of copper ion, producing H_2O_2 and ammonium. (Shepard and Dooley 2015). The enzymatic reaction is illustrated in Figure 10 on page 47.

Endogenous substrates of SSAO include methylamine, aminoacetone, cysteamine, and β-phenylethylamine (Dunkel et al. 2008; Heuts et al. 2011). These substrates are products of metabolism or ingested from drink, food, or through inhaling cigarette smoke (Yu et al. 2003). In addition to semicarbazide, several small-molecule inhibitors of the SSAO reaction are known, including hydroxylamine, hydralazine, phenelzine, aminoguanidine, and zimeldine, for example (Dunkel et al. 2008). One of these inhibitors, hydroxylamine, a by-product of normal cell metabolism, acted as a local vasodilator eliciting hypotension in rats partly by its conversion to nitric oxide, and partly by its inhibitory effect to SSAO-activity decreasing the local amount of released H_2O_2 (Vidrio and Medina 2007).

The wide array of functions related to the SSAO activity in humans, namely the metabolism of endogenous amines, involvement in the leukocyte adhesion cascade and angiogenesis, and participation in glucose transport and adipocyte differentiation (Yu et al. 2003; Dunkel et al. 2008; Salmi and Jalkanen 2017), have been a promising target for drug discoveries. Nevertheless, the effectors of the enzymatic activity of an SSAO are the cytotoxic products of the reaction, as discussed in the Chapter 2.3.5 VAP-1 in atherosclerosis.

To study the effect of the SSAO-activity in different functions, a cell line overexpressing enzymatically inactive VAP-1, where the crucial tyrosine is

mutated to phenylalanine (CHO-VAP-1-Y471F) has been developed (Koskinen et al. 2004). In flow-dependent experiments the enzyme inactive mutant VAP-1 molecules were unable to mediate the transmigration of granulocytes, demonstrating the importance of the SSAO-activity for the adhesive function of VAP-1 (Koskinen et al. 2004). In addition, mice with the corresponding Y471F mutation have been generated (Noonan et al. 2013). These mice were healthy and expressed normal amounts of VAP-1, but they had a defect in cell trafficking as fewer neutrophils trafficked in a sterile peritonitis model induced by tumor necrosis factor alpha (Noonan et al. 2013). Furthermore, in an arthritis model, the mutant mice with enzyme inactive VAP-1 had smaller mean arthritis scores than the WT mice, suggesting a less severe inflammation (Noonan et al. 2013). These studies thus point to an important role of SSAO-activity in physiological functions of VAP-1.

2.3.3 VAP-1, an adhesion molecule

As previously stated, VAP-1 was found in a quest to discover endothelial adhesion molecules assisting lymphocyte homing (Salmi and Jalkanen 1992). The mAb stainings readily showed VAP-1 to be located at the luminal surface of HEVs in synovial membranes, lymph nodes, and tonsil. The functionality of VAP-1 to assist lymphocyte binding to before mentioned HEVs was proved by inhibiting the interactions with the mAb. In addition, a small decrease on granulocyte binding to inflamed tonsil HEVs was seen. The HEVs of mucosa-associated lymphatic tissues were not as VAP-1-positive as the HEVs of peripheral lymph nodes in normal circumstances, but instead at the sites of inflammation the expression of VAP-1 was increased, and VAP-1 was shown to assist the binding of lymphocytes to the venules of inflamed lamina propria (Salmi et al. 1993). Thus, already the early data on VAP-1 indicates the diverse role of VAP-1 under normal conditions, i.e. in lymphocyte homing, and at the sites of inflammation in non-lymphoid organs.

The role of VAP-1 in the initial tethering and rolling phases of the lymphocyte trafficking to lymph node HEVs was elegantly showed in an intravital microscopy assay (Salmi et al. 1997). Furthermore, the crucial role of VAP-1 in granulocyte extravasation came apparent in *in vivo* experiments of acute inflammation, where the mAbs against VAP-1 increased the rolling velocity of the granulocytes, leading to decreased number of firmly bound and extravasated granulocytes (Tohka et al. 2001). In addition to the acute inflammation, VAP-1 was shown to be involved in a mouse model of diabetes as an example of chronic inflammation (Merinen et al. 2005).

The importance of SSAO enzyme activity for the leukocyte adhesion was first seen in experiments where primary endothelial cells were pre-incubated with SSAO inhibitors resulting in reduced number of lymphocytes rolling on and adhering to the endothelium (Salmi et al. 2001). In the same experiments it was shown that the tethering, i.e. the first transient contacts between lymphocyte and endothelium, was not dependent on the SSAO-activity (Salmi et al. 2001). In addition, the number of adhered and transmigrated lymphocytes on human hepatic endothelial cells decreased in the presence of enzyme activity inhibitor (Lalor et al. 2002). Similarly, in experiments with inhibitors of SSAO-activity, enzymatically inactive VAP-1 mutant, and mAbs against VAP-1, the results showed that the number of granulocytes rolling on and transmigrating through EC layer was diminished (Koskinen et al. 2004). The dualistic role of VAP-1 and its enzyme activity in leukocyte trafficking is summarized in Figure 10, where the substrate for the enzymatic reaction is provided by the leukocyte adhering to the endothelial cells.

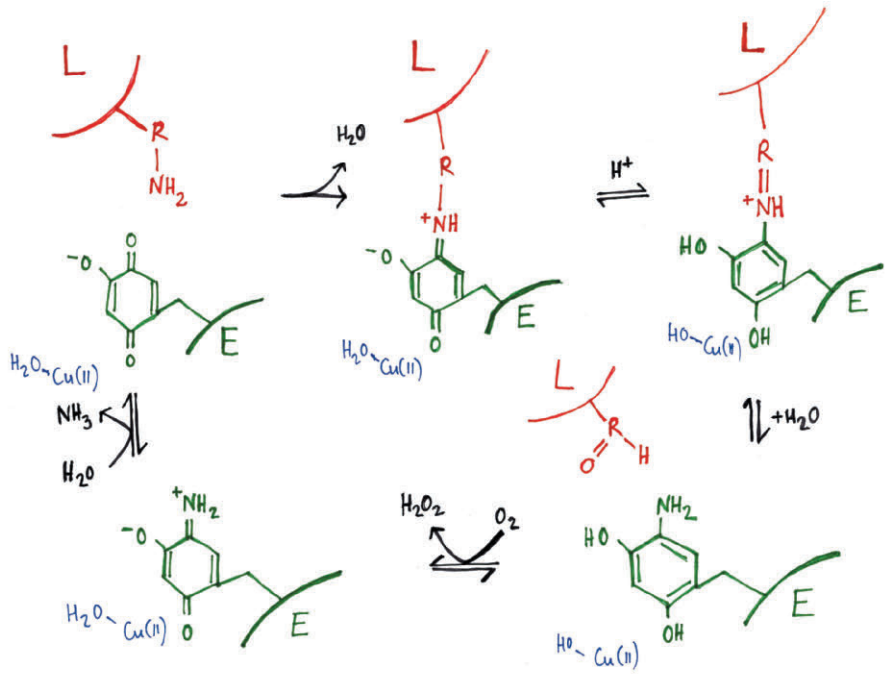

Figure 10. Enzyme activity of VAP-1 in leukocyte adhesion cascade. The substrate primary amine (in red) is provided by the leukocyte ligand of VAP-1 (denoted by L) as the leukocyte adheres to the endothelium (E). The endothelial cells express VAP-1 on their surface. The topaquinone (TPQ) of the catalytic center of VAP-1 is shown in green. Through an intermediary Schiff base formation, an aldehyde is produced with the release of hydrogen peroxide and ammonia. The enzymatic activity of VAP-1 is important for the adhesion cascade. The copper ion (in blue) is the inorganic cofactor common for all copper-containing amine oxidases.

To date, the experimental evidence for the adhesive function of VAP-1 is vast. In liver, VAP-1 is known to mediate the binding of T cells to hepatic endothelium (McNab et al. 1996), adhesion and transendothelial migration of lymphocytes on human hepatic ECs (Lalor et al. 2002), rolling and adhesion of CD4-positive type 2 T helper (Th2) cells in inflamed liver sinusoids (Bonder et al. 2005), recruitment of inflammatory cells to liver (Weston et al. 2015), and adhesion of gut-tropic lymphocytes to hepatic endothelial cells (Trivedi et al. 2017). In inflammatory settings other than in liver, and in disease models other than cancer, VAP-1 has been shown to mediate adhesion of lymphocytes to inflamed skin vasculature (Arvilommi et al. 1996), binding of granulocytes to vessels in ischemic human heart (Jaakkola et al. 2000), binding of granulocytes to inflamed peritoneum in rabbits (Tohka et al. 2001), binding of lymphocytes to renal vessels in chronically rejected kidney (Kurkijarvi et al. 2001), transmigration of granulocytes to inflamed peritoneum and migration of monocytes to inflamed air pouch (Merinen et al. 2005), migration of neutrophils to inflamed lung (Foot et al. 2013), infiltration of macrophages to choroidal neovascularization lesions (Yoshikawa et al. 2012), leukocyte trafficking in aneurysmal subarachnoid hemorrhage (Xu et al. 2014), accumulation of macrophages to atherosclerotic plaques (Silvola et al. 2016), infiltration of neutrophils, but not macrophages or T cells, to renal ischemia/reperfusion injury site (Tanaka et al. 2017), extravasation of neutrophils to inflamed brain (Becchi et al. 2017), and infiltration of inflammatory cells to inflamed retina (Matsuda et al. 2017). In addition, in tumor models VAP-1 mediates the adhesion of tumor-infiltrating leukocytes, lymphokine-activated killer cells, and natural killer (NK) cells to the vasculature of cancer tissue (Irjala et al. 2001), the migration of Gr-1+CD11b+ myeloid cells into tumor (Marttila-Ichihara et al. 2009), and the accumulation of CD8+ lymphocytes to tumors (Marttila-Ichihara et al. 2010). Instead, in non-inflamed circumstances VAP-1 does not mediate the binding of CD4-positive T cells to HEVs of popliteal lymph nodes (Salmi et al. 1998), but VAP-1 mediates binding of CD8 positive T cells and NK cells to endothelium of popliteal lymph nodes under shear (Salmi et al. 1997) and the infiltration of macrophages, NK cells, T cells, and NKT cells to white adipose tissue (Bour et al. 2009).

2.3.4 Soluble VAP-1

In order to use VAP-1 as a biomarker, it has to be readily measurable. Fortunately, VAP-1 is found as a soluble form in the blood (Kurkijarvi et al. 1998), and the soluble form harbors the catalytic SSAO activity thus allowing the fluorometric detection of sVAP-1 in blood samples (Kurkijarvi et al. 2000). The

levels of sVAP-1 in human blood samples have been associated to several conditions, such as diabetes, heart failure, and liver diseases (Salmi and Jalkanen 2017). The origin of soluble VAP-1 has been studied in mice overexpressing VAP-1. Under normal physiologic conditions, the endothelial VAP-1 was the source of sVAP-1 found in the serum, whereas in experimental diabetes the adipocytes released VAP-1 to the circulation as well (Stolen et al. 2004). Interestingly, the same study revealed that the male mice overexpressing transmembrane VAP-1 had higher levels of sVAP-1 in the serum than the female mice overexpressing VAP-1, and the amount of sVAP-1 in circulation could be genetically regulated (Stolen et al. 2004). In humans, sVAP-1 is released by liver sinusoidal ECs (Kurkijarvi et al. 2000), and in human adipose tissue explants the release of sVAP-1 from the adipocyte membrane was regulated by tumor necrosis factor alpha and insulin (Abella et al. 2004). In addition, the shedding of VAP-1 from the adipocyte membrane was metalloproteinase-dependent (Abella et al. 2004). Yoshida et al, showed that matrix metalloproteinase-2 and -9 shed VAP-1 from retinal capillary ECs after stimulation with VEGF, TNF-α, or IL-1β (Murata et al. 2012; Yoshida et al. 2018).

Soluble forms of several adhesion molecules are found in the circulation, often as the result of sheddases cleaving the extracellular part of the adhesion molecules on the endothelial cell surface. In addition to cleaving VAP-1 on cell surface, matrix metalloproteinases cleave CD44 and ICAM-1 as well (Salmi and Jalkanen 2012). Soluble forms of L-selectin, VCAM-1, and vascular endothelial cadherin instead are released by members of the disintegrin and metalloproteinase (ADAM) family (Salmi and Jalkanen 2012). The soluble forms of adhesion molecules are known to regulate the cell trafficking in various ways, such as altering the activation of leukocytes and competing for the binding sites on the vascular endothelium and thus limiting the inflammation (Smalley and Ley 2005). Since the levels of soluble forms of adhesion molecules are fairly constant in the circulation, the shedding must be tightly regulated, yet altered levels of soluble adhesion molecules are found in several diseases (Salmi and Jalkanen 2012).

2.3.5 VAP-1 in atherosclerosis

Atherogenesis, the progression of atheroma formation as seen in the Figure 9, is a long process with several steps to which VAP-1 can contribute to. First of all, VAP-1 present on the SMCs in the tunica media of muscular arteries, are capable of producing hydrogen peroxide (H_2O_2) (Jaakkola et al. 1999), aldehydes (Yu and Deng 1998), and ammonia, all of which can contribute to endothelial

dysfunction (Yu and Zuo 1993; Magyar et al. 2001; Dunkel et al. 2008) and thus exacerbate the local inflammation. The H_2O_2 and aldehydes are involved in lipid peroxidation and aldehyde modifications of proteins and oligosaccharides (AGE products), and the H_2O_2 induces other adhesion molecules, chemokines, as well as direct cytotoxic effects on endothelium (Yu and Zuo 1993; Yu and Deng 1998; Lalor et al. 2002; Jalkanen et al. 2007; Sole et al. 2008; Liaskou et al. 2011). Secondly, VAP-1 can promote atherosclerosis by recruiting more leukocytes to the scene. In fact, atherosclerotic plaques are shown to have upregulated gene expression of VAP-1 (Anger et al. 2007), and the neovessels of human atherosclerotic plaque are VAP-1 positive (Silvola et al. 2016). This allows VAP-1 to assist monocytes and macrophages to infiltrate into the atherosclerotic plaque, thus further aggravating the atherogenesis. Indeed, by inhibiting the VAP-1's SSAO-activity by a small molecule inhibitor, less macrophages infiltrated to inflamed atherosclerotic plaques in mice (Silvola et al. 2016).

As mentioned, amine oxidases have been subjects of investigations since 1950' and thus already in the 1980's it became evident, that SSAO was found in the plasma membrane fraction of rat aorta (Wibo et al. 1980) and that the vascular smooth muscle cells were the source of SSAO-activity (Lyles and Singh 1985). In humans, elevated amounts of SSAOs in conditions related to atherosclerosis have been found in the plasma samples of patients with diabetes (Boomsma et al. 1995) and congestive heart failure (McEwen and Harrison 1965; Boomsma et al. 1997). The SSAO-activity or sVAP-1 levels were positively correlated to carotid plaque score and IMT in healthy subjects, and to severity of carotid stenosis in patients of type 2 DM (Karadi et al. 2002) and in patients with calcific aortic stenosis (Altug Cakmak et al. 2015). Fernanda et al. noticed, that the homogenates of vascular tissue of type 2 DM patients had significantly less SSAO-activity than those derived from the subjects without type 2 DM, whereas the plasma SSAO activity was higher in patients with type 2 DM compared to subjects without type 2 DM (Nunes et al. 2010). It seems insulin might regulate the shedding of endothelial VAP-1 (Salmi et al. 2002). In addition, in patients with type 2 DM, the sVAP-1 levels predicted 10-year CVD mortality (Li et al. 2011). In relation to ischaemic strokes, all the vessels in human brain from post-capillary venules to large-size arteries express VAP-1 on the ECs as well as SMCs, and an acute cerebral ischemia triggered the release of VAP-1 from the brain vasculature leading to increased sVAP-1 in circulation and decreased expression of VAP-1 in infarcted brain areas (Airas et al. 2008). This might be due to the loss of integral elements of basal lamina, or by the increased tumor necrosis factor alpha amounts in ischemic brain enhancing the clearance of VAP-1 (Abella et al. 2004). Nevertheless, the cholesterol lowering drug simvastatin is able to attenuate the sVAP-1 release in experimental models of cerebral

ischemia, and block the VAP-1-mediated leukocyte adherence (Sun et al. 2018). Interestingly, some other drugs, such as hydralazine for hypertension and aminoguanidine for diabetes mellitus, can inhibit the SSAO-activity (Boomsma et al. 2005).

In cultured endothelial cells, methylamine deaminated to formaldehyde by the SSAO in human serum led to endothelial damage measured in cell viability and growth (Yu and Zuo 1993). As both the amount of methylamine and the SSAO activity are elevated in the blood of diabetic individuals, the authors suggested that the metabolism of methylamine could be behind the endothelial injury, leading to atherosclerotic plaques, and to subsequent CVD events among diabetic patients (Yu and Zuo 1993). An interesting note is, that formaldehyde produced in blood is not further metabolized since the dehydrogenase is missing from blood, leaving the formaldehyde to interact with proteins and single-stranded deoxyribonucleic acid forming cross-linked complexes (Yu et al. 2003). The by-product of oxidative deamination of aminoacetone by SSAO is methylglyoxal, with similar cross-linking properties as formaldehyde (Yu et al. 2003). When taking into account the co-existence of H_2O_2 and formaldehyde under physiological pH, free radicals are generated, which in turn could result in the oxidation of LDL, for example (Trezl and Pipek 1988; Yu et al. 2003).

The first evidence of VAP-1 causing vascular complications in *in vivo* came apparent in experiments studying the long-term effects of SSAO-activity in transgenic mice overexpressing VAP-1 on endothelium (Stolen et al. 2004). The increased SSAO-activity was shown to cause increased amounts of AGE products, elevated blood pressure, as well as higher BMI and increased fat pad weight (Stolen et al. 2004). The transgenic mice had fewer atherosclerotic lesions in the aortas compared to non-transgenic mice, but interestingly, the total area of lesions were equal, indicating that the lesions were larger in transgenic mice (Stolen et al. 2004). This unexpected result was repeated by Zhang et al., who discovered that by inhibiting SSAO activity in $LDLR^{-/-}$ mice (animal model for human atherosclerosis) they developed larger lesions than mice without inhibition (Zhang et al. 2016). The current hypothesis is, that without SSAO activity, the SMCs switch from quiescent contractile phenotype to active synthetic phenotype, thus exacerbating atherosclerotic lesion progress (Peng et al. 2016; Zhang et al. 2016).

3 AIMS OF THE STUDY

Cardiovascular diseases are a global burden affecting the lives of hundreds of millions of people. The origin of these diseases lies in the vascular endothelium. Vascular adhesion protein-1 (VAP-1) is an adhesion molecule assisting leukocyte trafficking across endothelium into inflamed tissues. In addition, VAP-1's enzymatic activity produces substances which are harmful to endothelium. Thus, VAP-1 has the characteristics to have an important role in the beginning of atherosclerosis, the hallmark of atherosclerotic cardiovascular diseases. As VAP-1 is present in the blood as a soluble form, it is possible to measure the level of VAP-1 in different populations.

The aim of this study was to elucidate the role of VAP-1 in atherosclerosis. The specific aims were:

I To find the molecules on the leukocyte surface to which the endothelial VAP-1 attaches to, and verify this interaction

II To develop methods suitable for soluble VAP-1 level measurements in large population studies

III To study the association of VAP-1 to CVD risk factors and the potentiality of soluble VAP-1 to function as a biomarker of early manifestations of atherosclerosis

IV To test the biomarker ability of VAP-1 by investigating whether soluble VAP-1 levels can predict cardiovascular events in a normal population

4 MATERIALS AND METHODS

The materials and methods used in this study are summarized here and described in more detail in the original publications, which will be denoted in Roman numerals.

4.1 Materials

4.1.1 Antibodies

Table 1. Characteristics of antibodies used in the study.

Antigen	Clone	Isotype	Conjugate	Source/reference	Used in
chicken T-cell	3G6	mouse IgG1		(Salmi and Jalkanen 1992)	I, II
human CD14		mouse IgG2a	FITC	Southern Biotech	II
human CD19		mouse IgG1	FITC	eBioscience	I
human CD44	Hermes-1, 9B5	rat IgG2a		(Jalkanen et al. 1986)	I, II
human CD66b		mouse IgM	FITC	BD Biosciences	II
human IgG		mouse IgG1		BD Bioscience	I
human leukocyte antigen A,B,C	HB-116	mouse IgG1		ATCC	II
human VAP-1	TK8-18	mouse IgG2a		(Kurkijarvi et al. 1998)	I, IV
human VAP-1	Jg-2.10	rat IgG2a		Gift from E. Butcher	I, II
human VAP-1	1B2	mouse IgM		(Salmi and Jalkanen 1992)	III
human VAP-1	TK8-14	mouse IgG2a		(Kurkijarvi et al. 1998)	IV
human VAP-1		rabbit polyclonal		(Maula et al. 2005)	I, II
mouse IgG		goat IgG	Alexa 546	Molecular Probes	II

Table 1. (continued)

Antigen	**Clone**	**Ig class**	**Conjugate**	**Source/reference**	**Used in**
mouse PV-1	Meca-32	rat IgG2a		gift from E. Butcher	II
mouse VAP-1		rat IgG2b		(Merinen et al. 2005)	II
P-selectin		sheep polyclonal	FITC	R&D Systems	I
rabbit IgG		sheep tai goat polyclonal	FITC	Sigma-Aldrich	I, II
rat IgG		goat IgG	Alexa 546	Invitrogen	I, II
rat IgG		rabbit tai goat polyclonal	FITC	Sigma-Aldrich	I,II
sheep IgG		donkey polyclonal	Alexa 546	Invitrogen	I
Siglec-9		polyclonal		gift from P. Crocker	II
Siglec-9	K8	mouse IgG1		(Zhang et al. 2000)	II
Siglec-10	5G6	mouse IgG1		(Munday et al. 2001)	I
Siglec-10		sheep polyclonal		(Munday et al. 2001)	I

In addition, two chimeric Ig molecules were used in the study I: a human CD44-IgG (descripted in the thesis of Maula, SM, in 2003), and a Siglec-10 Ig (Munday et al. 2001) .

4.1.2 Peptides

All the peptides used in this study were from PolyPeptide Group.

Table 2. Peptides used in the study.

Sequence	Description	Used in
CVKWRGVVVC	phage display hit	II
CWSFRNRVLC	phage display hit	I
biot-CARLSLSWRGLTLC	biotinylated cyclic Siglec-9	II
CARLSLSWRGLTLCPSK-biot	biotinylated cyclic Siglec-9	II
CAALSLSWAGLTLCPS	mutated cyclic Siglec-9 without arginines	II
CAALSLSWRGLTLCPS	mutated cyclic Siglec-9 without arginine in site 284	II
CARLSLSWAGLTLCPS	mutated cyclic Siglec-9 without arginine in site 290	II
CATLSWVLQNRVLSSCK-biot	biotinylated cyclic Siglec-10	I
CATLSWVLQNAVLSSCK-biot	biotinylated, mutated cyclic Siglec-10 without arginine	I

4.1.3 Cells

Table 3. Cells and cell lines used in the study.

Cell / Cell line	Description	Source/ reference	Used in
CHO	Chinese hamster ovary cells	American Type Culture Collection (ATCC)	I, II
CHO mock	Chinese hamster ovary cells transfected with vector only	(Salmi et al. 2000)	I, II
CHO-VAP-1	Chinese hamster ovary cells expressing human VAP-1	(Smith et al. 1998)	I, II
CHO-VAP-1-Y471F	Chinese hamster ovary cells expressing enzymatically inactive mutant VAP-1	(Koskinen et al. 2004)	I, II
CHO-VAP-1-D728A	Chinese hamster ovary cells expressing RGD mutant VAP-1	(Salmi et al. 2000)	I

Table 3. (Continued)

Cell / Cell line	Description	Source/ reference	Used in
CHO-Siglec-10	Chinese hamster ovary cells expressing Siglec-10	(Munday et al. 2001)	I
CHO-Siglec11-GFP	Chinese hamster ovary cells expressing extracellular region of Siglec-11 fused to the green fluorescent protein	(Angata et al. 2002)	I
CHO-Siglec-G-GFP	Chinese hamster ovary cells expressing extracellular region of Siglec-G fused to the green fluorescent protein	(Hoffmann et al. 2007)	I
CHO-Siglec-9	Chinese hamster ovary cells expressing Siglec-9	(Zhang et al. 2000)	II
CHO-mVAP-1	Chinese hamster ovary cells expressing mouse VAP-1	(Bono et al. 1999)	II
CHO-Siglec-E	Chinese hamster ovary cells expressing mouse Siglec-E	(Zhang et al. 2004)	II
B16	Mouse melanoma cell line	Xenogen	II

4.1.4 Animals

Table 4. Animals used in the study.

Animals	Description	Source/ reference	Used in
Mouse, C57Black	Wild type		II
Mouse, VAP-1 KO, mouse VAP-$1^{-/-}$ human VAP-$1^{-/-}$, 1296S/ FVB/N and C57BL/6N	Mouse lacking endogenous VAP-1 and human VAP-1	(Stolen et al. 2004; Jalkanen et al. 2007)	I, II
Mouse, VAP-1 KO-TG, mouse VAP-$1^{-/-}$ human VAP-$1^{+/-}$, 1296S/ FVB/N and C57BL/6N	Mouse lacking endogenous VAP-1, but expressing human VAP-1 under the control of mouse Tie-1 promoter	(Stolen et al. 2004; Jalkanen et al. 2007)	I, II
Rat, Sprague-Dawley	Wild type	Central Animal Laboratory, Turku University, Finland	II

4.1.5 Nationwide study populations

4.1.5.1 The Cardiovascular Risk in Young Finns Study, YFS

The Cardiovascular Risk in Young Finns Study (YFS) is a prospective longitudinal study. It was started in 1980 as a counteraction to the high incidence of coronary heart diseases in Finland and as a response to the World Health Organization Recommendation of 1978 declaring that atherosclerosis predisposition should be studied in children (reviewed in (Raitakari et al. 2008). The main focus is to study how childhood lifestyle, psychological, and biological measures contribute to the risk of CVD in adulthood. The study involves five university cities with medical schools, and their surroundings. From the population register 4320 children of age 3, 6, 9, 12, 15 and 18 years were randomly chosen from these areas. Out of these, 3596 children and adolescents participated in the first cross-sectional study conducted in 1980. The participants answered structured questionnaires, donated blood sample and their body measurements were taken. After the baseline study, the participants have been followed up 3 to 9 years apart by repeating the questionnaires and physical examinations. The blood samples used for sVAP-1 measurements were collected in 2007 from 2183 participants. Thus, the participants were at the time 30, 33, 36, 39, 42 and 45 years old, respectively. The strength of this study cohort is the longitudinal research frame, which allows the scientists to study the association of lifetime burden of risk factors to vascular ageing progression (Raitakari et al. 2008). In addition, it allows studying the stability, or on the contrary, changes of risk factor levels from childhood to adulthood.

4.1.5.2 The FINRISK 2002

The National FINRISK Studies are prospective population surveys focused on studying the protective as well as the risk factors of chronic non-communicable diseases in the Finnish population. The study started as the North Karelia Project in 1972 and is conducted every fifth year since (Borodulin et al. 2015; Jousilahti et al. 2016; Puska et al. 2016). Each year the participants are randomly chosen from the national register and a physical examination with blood drawing and a background questionnaire are carried out. After the baseline examination the participants are followed up through linkages to National Hospital Discharge Register, National Causes of Death Register, and National Drug Reimbursement Register. In 2002 the areas included in the study were province of North Karelia, province of North Savo, Turku-Loimaa district, Helsinki-Vantaa, province of

Oulu and province of Lapland. The participants were randomly chosen from the population aged 25-64 years in a 10-year and gender adjusted way. In addition, in the provinces of North Karelia and Lapland, and in the Helsinki-Vantaa area a subpopulation of 65-74 year old participants was included (250 women and 250 men). The study sample used in this study was a subpopulation of all the 51-74 year old participants of the 2002 FINRISK with a blood sample (n=2775).

4.2 Methods

Table 5. Methods used in the studies.

Method	**Used in**
Adhesion assays with peptides, proteins, chimeras	I, II
Adhesion assays with transfectants	I, II
Cell isolation and culture	I, II
ELISA (enzyme-linked immunosorbent assay)	IV
Ex vivo frozen section binding assay	I, II
Expression induction	II
FACS (fluorescence-activated cell sorting)	I, II
Fluorescence microscopy imaging	II
Immunohistochemistry	I, II
Intravital video microscopy	II
Modeling and docking simulation	I, II
Mouse inflammation models, cremaster and skin	II
Mouse tumor model, melanoma	II
PET imaging	II
Phage display screening	I, II
Rat inflammation model, turpentine	II
SSAO activity assay, transfectants cells	I
SSAO activity assay, blood samples	III
Statistical analysis	I, II, III, IV
Surface plasmon resonance assay	II

4.2.1 96-well plate based peptide – protein adhesion assay (I)

The wells of a Nunc MaxiSorp flat bottom white 96-well plate (Nunc, Roskilde, Denmark) were coated with 400 ng of either recombinant VAP-1 protein or bovine serum albumin in 100 µl of 0.1 M $NaHCO_3$, and left at +4 °C overnight. In the following morning, the plate was incubated in RT for an hour. Next the liquids were aspirated from the wells and blocked with 200 µl/well 2 % bovine serum albumin in phosphate buffered saline (PBS) for 90 minutes in +37 °C. The wells were washed 6 times with Wallac Delfia Microplate washer (PerkinElmer, Waltham, USA) with 0.1% Tween-PBS as a washing solution to remove the un-immobilized bovine serum albumin. Next, 10 µg/ml of biotinylated peptides (wild type sialic acid binding Ig-like lectin-10 (Siglec-10) and mutated Siglec-10 without arginine) were added to the wells in 100 µl of 2 % bovine serum albumin in PBS. A specific anti-VAP-1 antibody (1 µg/ml TK8-18) was used as a positive control. After 90 minutes incubation in RT, the wells were washed as told previously. The bound peptides and antibody were detected with 1:1000 dilution of streptavidin-horseradish peroxidase (HRP) in PBS. 15 minutes before the end of the last incubation, BM Chemiluminescence ELISA substrate (POD; Sigma-Aldrich, Saint Louis, USA) solutions A and B were mixed in 1:100 proportions. After 60 minutes incubation in RT the wells were washed again and the freshly mixed ELISA substrate solution was added to the wells. The luminescence of the bound peptides and antibody were measured after 3 minutes with a multimode plate reader (Tecan Infinite M200, Tecan, Männedorf, Switzerland). The experiment was done on three different days with three replicates of each peptide-protein or antibody-protein pair.

4.2.2 Cell – cell adhesion assays (I, II)

Labelled cells in suspension were introduced to a layer of cultured cells, incubated, and after washes the adherence of the cells was quantified by measuring the fluorescence of the labelled cells. In more details, 50 000 - 90 000 cells (CHO-VAP-1, CHO-VAP-1Y471F, CHO-VAP1D720A, CHO-mVAP-1 and CHO-mock transfectants) were plated on 96-well plates (ViewPlate, Perkin Elmer, Waltham, USA) the previous night and cultured to confluence the next day. The wells were blocked with 1% bovine serum albumin in phosphate buffered saline (PBS) for 10 min in +4 °C, and then washed with 10% fetal calf serum (FCS) in RPMI-medium. CHO-Siglec-9, CHO-Siglec-10, and CHO-Siglec-E cells were detached, counted, and labelled with carboxyfluorescein succinimidyl ester (final concentration 0.5 µM) in warm HEC-medium (RPMI 1640 medium with 4 mM L-glutamine, 10% FCS, 100 IU/ml penicillin, and 100

µg/ml streptomycin) for 20 min in +37 °C, and then washed three times with warm HEC-medium. CHO-Siglec-11-GFP and CHO-Siglec-G-GFP were detached and counted, but not stained with carboxyfluorescein succinimidyl ester since they were attached to GFP. The labelled cells (200000/well) were added in 50 µl volume of 10% FCS in RPMI-medium. The cells were incubated in +37 °C for 30 minutes in gentle shaking. After the incubation the cells were imaged with Axiovert 200 M microscope with Hamamatsu ORCA camera and the fluorescence was measured with Tecan Infinite M200 microplate reader (Tecan, Männedorf, Switzerland). The wells were washed by running warm 10% FCS in RPMI medium along the wells wall for 9 times. Between each wash the fluorescence was measured to quantify the amount of adherent cells, and after the washes the wells were imaged again to visualize the amount of adherent cells.

4.2.3 SSAO-activity measurements of YFS samples (III)

The enzymatic activity of sVAP-1, and thus the amount of sVAP-1 molecules in human plasma is possible to quantify by measuring the amount of one of the reaction end products, hydrogen peroxide (H_2O_2) in the sample solution. The high-throughput method used in this study was developed based on an old fluorometric detection protocol performed on 96-well microplates (Salmi et al. 2001). The enzymatic reaction and the following detection reaction used in this study are depicted in the Figure 11. Benzylamine was used as the substrate for sVAP-1 molecules in the sample. As the catalytic reaction of VAP-1 transforms the primary amine to benzaldehyde, ammonia and hydrogen peroxide are released. In the coupled reaction, HRP converses Amplex Red reagent (10-acetyl 3,7-dihydroxyphenoxazine) to highly fluorescent resorufin (7-hydroxyphenoxazin-3-one). The stoichiometry of the reaction is 1:1, as for each hydrogen peroxide molecule produced by the oxidase activity of VAP-1 one molecule of Amplex Red is transferred to one molecule of resorufin. The development of the high-throughput enzyme activity assay is discussed in more detail in the results.

The series of samples measured in this study, the YFS, composed of 2204 serum samples. With the new high-throughput assay 112 samples could be measured on a 384-well microplate simultaneously. One assay took 2 to 3 hours, and thus each day two assay plates (224 samples) were processed. The whole series was measured in 10 days. The finalized protocol for measuring the SSAO-activities of the YFS samples was as follows.

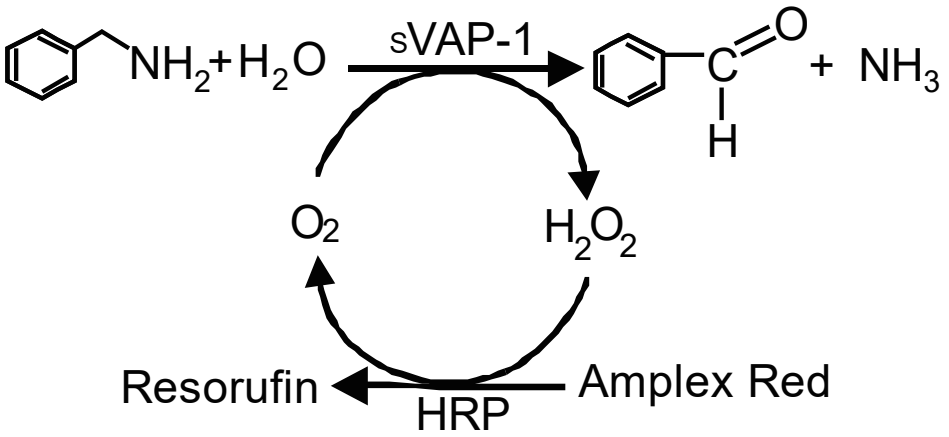

Figure 11. The SSAO-activity assay is based on coupled catalytic reactions of sVAP-1 and HRP. The coupled reactions of oxidation of benzylamine and the following conversion of Amplex Red into highly fluorescent resorufin are illustrated. In the activity assay the upper part of the reaction is catalyzed by the sVAP-1 molecules in the plasma samples. HRP=horseradish peroxidase.

The assay was built on a black 384-well microplate (Perkin Elmer, Waltham, USA). Two 96-well white non-treated microplates (Nunc, Roskilde, Denmark) were used to pre-dilute the samples. The layouts of the pre-dilution plates and the assay plate are shown in Figure 12. The final volume on the assay plate wells was 80 µl. For each sample, two separate wells were pipetted, either without the inhibitor (yellow wells) or with the inhibitor (blue wells). In this study the inhibitor was hydroxylamine in the final concentration of 5 µM. In both wells the substrate, benzylamine, was present at the final concentration of 0.5 mM. To speed up the process, all buffer solutions were dispensed with a Multidrop Combi reagent dispenser (Thermo Fisher Scientific, Waltham, USA). After each dispensing, the tubes of Multidrop Combi were carefully cleaned by running MQ water through the system.

The night before the measurements, the sera (224 sample tubes) were taken from -135 °C to +4 °C overnight. The assay buffer was 0.1 M sodium phosphate buffer (SPB) pH 7.4. One liter of SPB was reached by combining 95 ml of 0.2 M sodium dihydrogen phosphate, 405 ml of 0.2 M disodium hydrogen phosphate, and 500 ml MQ water. This solution was kept at room temperature.

The reagents were weighted and diluted freshly every morning for each assay plate. The SSAO-specific inhibitor and substrate were weighted and diluted in the buffer. More specifically, 10 mM solution of hydroxylamine hydrochloride (Sigma Aldrich, Saint Louis, USA) and 4 mM solution of benzylamine hydrochloride were prepared.

Pre-dilution plates:

	1	2	3	4	5	6	7
A	1	9	17	25	33	41	49
B	2	10	18	26	34	Pool	50
C	3	11	19	27	35	43	51
D	4	Low	20	28	36	44	52
E	5	13	21	29	37	45	53
F	6	14	22	30	38	46	54
G	7	15	23	31	39	47	55
H	8	16	24	32	40	48	56

	1	2	3	4	5	6	7	8
A	57	65	73	81	89	97	105	Pool
B	58	66	High	82	90	98	106	Pool
C	59	67	75	83	91	99	107	Pool
D	60	68	76	84	92	100	108	Pool
E	61	69	77	85	93	101	109	Pool
F	62	70	78	86	94	102	110	Pool
G	63	71	79	87	95	103	Mid	Pool
H	64	72	80	88	96	104	112	Pool

Assay plate:

	1	2	3	4	5	6	7	8	9	10	11	12	13	14	15	16	17	18	19	20	21	22	23	24
A	1	9	17	25	33	41	49				1	9	17	25	33	41	49				Pool	Pool	Pool	Pool
B	57	65	73	81	89	97	105				57	65	73	81	89	97	105				Pool	Pool	Pool	Pool
C	2	10	18	26	34	Pool	50				2	10	18	26	34	Pool	50				Pool	Pool	Pool	Pool
D	58	66	High	82	90	98	106				58	66	High	82	90	98	106				Pool	Pool	Pool	Pool
E	3	11	19	27	35	43	51				3	11	19	27	35	43	51				Pool	Pool	Pool	Pool
F	59	67	75	83	91	99	107				59	67	75	83	91	99	107				Pool	Pool	Pool	Pool
G	4	Low	20	28	36	44	52				4	Low	20	28	36	44	52				Pool	Pool	Pool	Pool
H	60	68	76	84	92	100	108				60	68	76	84	92	100	108				Pool	Pool	Pool	Pool
I	5	13	21	29	37	45	53				5	13	21	29	37	45	53				Pool	Pool	Pool	Pool
J	61	69	77	85	93	101	109				61	69	77	85	93	101	109				Pool	Pool	Pool	Pool
K	6	14	22	30	38	46	54				6	14	22	30	38	46	54				Pool	Pool	Pool	Pool
L	62	70	78	86	94	102	110				62	70	78	86	94	102	110				Pool	Pool	Pool	Pool
M	7	15	23	31	39	47	55				7	15	23	31	39	47	55				Pool	Pool	Pool	Pool
N	63	71	79	87	95	103	Mid				63	71	79	87	95	103	Mid				Pool	Pool	Pool	Pool
O	8	16	24	32	40	48	56				8	16	24	32	40	48	56				Pool	Pool	Pool	Pool
P	64	72	80	88	96	104	112				64	72	80	88	96	104	112				Pool	Pool	Pool	Pool

Figure 12. The layouts of the pre-dilution and assay plates of the SSAO-activity assay. Dilutions of the serum samples numbered 1-112 were done on the pre-dilution plates. 'Low', 'Pool', 'Mid', and 'High' denote the control sera used on every plate. From the pre-dilution plates the diluted samples were transferred to the assay plate with an 8-channelled manual pipette. On the assay plate the samples were incubated without (columns 1-7) or with (columns 11-17) a SSAO inhibitor, hydroxylamine. The wells in columns 21-24 indicate the standard wells in which pooled serum was in the same dilution as the samples in the sample wells. All the sample wells contained the substrate, benzylamine.

The final volumes of the solutions needed to be large enough to account for the dead volume in the tubes of the automatic dispenser. The inhibitor solution, substrate solution and 150 ml of SPB were tempered in +37 °C for at least 30 minutes, or until used.

The samples were taken from the +4 °C to room temperature. The containers including the sample tubes were first pound against the table top in order to make sure the serum was completely detached from the walls and the cap of the sample tube. Next the sample tubes were vortexed individually and then centrifuged at 4000 round per minutes for 3 minutes. For the pre-dilution plates, 255 µl of SPB was dispensed with the Multidrop Combi (large volume cassette). According to the plate layout, 45 µl of serum samples were pipetted by hand into the wells of the pre-dilution plates.

Next, a 100 µM solution of hydroxylamine was prepared in the buffer, which was further diluted to the final concentration of 9 µM by adding buffer to yield a final volume of 11 ml. With the automatic dispenser 45 µl of SPB was dispensed on the assay plate wells in the columns 1-10, and 55, 50, 45 and 40 µl of SPB to the wells in the columns 21, 22, 23, and 24, respectively (small cassette). After washing the tubes, 45 µl of the previously prepared 9 µM hydroxylamine

solution was dispensed to the wells in the columns 11-20. Next, the pre-dilution plates were shaken with the Multidrop Combi for 15 seconds, and then 16 µl of the samples were transferred with an 8-channelled manual pipet to the assay plate according to the plate layout shown in Figure 12. The assay plate was shaken with Multidrop Combi for 15 seconds, sealed with an adhesive film, and incubated at +37 °C with a pre-heated iron plate on top of the plate for 30 minutes. In the mean-time, the plate reader (Tecan Infinite M200) was started and pre-heated to +37 °C.

After the incubation, the SPB, plate and substrate were taken from the incubator. All the subsequent reagents were prepared just before the usage. 10 ml of 5 µM H_2O_2-solution was prepared from 3 % H_2O_2-solution, and 5, 10 and 15 µl of the solution were dispensed with Multidrop Combi to the assay plate (columns 22, 23, and 24, respectively). Next a 15 ml solution of Amplex Red reagent (final concentration of 8 µM; Sigma-Aldrich, St. Louis, USA) and HRP (1:125; Peroxidase, Type VI from horseradish, 1KU in 1 ml of PBS, Sigma-Aldrich) was prepared and 10 µl of this solution was dispensed to all wells on the assay plate. Finally, 10 µl of the 4 mM benzylamine solution was dispensed to all the sample wells.

The amount of fluorescent resorufin formed in the wells by the conversion of the H_2O_2 formed by the enzymatic activity of VAP-1 in the samples, or by the H_2O_2 pipetted in the standards, was measured with the Tecan Infinite M200 plate reader. For 60 minutes, in 5 minutes interval the fluorescence was measured at the emission wavelength of 590 nm, with the excitation wavelength of 545 nm.

The 4992 numeric values obtained from the one hour kinetic measurement were transferred to a sheet called ‘raw data’ on a self-made Excel macro. In addition, the macro included sheets for each time interval (0-5 min, 5-10 min, etc.) and a summary sheet collecting all the results. From the raw data sheet the values were automatically transferred to corresponding analyzing sheets. An example of the analyzing sheet with the formulas is shown in Figure 13. The same sheet with actual values from the YFS 2007 is shown in Figure 14. The specific activity in the sample was analyzed by calculating the change in the fluorescence during the 5 minutes interval in the wells without and with the inhibitor, and changing these values to corresponding amounts of H_2O_2 formed by dividing with the slope of the standard line. The specific H_2O_2 was the difference of the H_2O_2 formed in the wells with and without the inhibitor. Finally the specific H_2O_2 was transformed to activity by taking into account the volume of the sample, total volume, and time as shown in Figures 13 and 14.

Formed fluorescence in the standard wells in 5 minutes										
V1 µl	c1 µM	V2 µl	C2 nM	RFU at 0 min	RFU at 5 min	ΔRFU				
0	5	80	=A3*B3/C3*1000							
5	5	80		=AVERAGE(data!X2:X17)						
10	5	80			=AVERAGE(data!Y19:Y34)					
15	5	80				=AVERAGE(E6:F6)-AVERAGE($E$3:$F$3)				
V serum µl		2.4	**Slope**	=SLOPE(G3:G6;D3:D6)						
V final ml		0.08	**t min**	5						
	RFU at 0 min	RFU at 5 min	ΔRFU	formed H2O2 nM	RFU at 0 min with HA	RFU at 5 min with HA	ΔRFU with HA	formed H2O2 nM	specific H2O2 nM	activity nmol/ml/h
1	=data!C2	=data!C19	=C11-B11	=D11/$E$8	=data!M2	=data!M19	=G11-F11	=H11/$E$8	=E11-I11	=(J11*60*1000*$C$9)/(1000*$C$8*$E$9)
2	=data!C3	=data!C20	=C12-B12	=D12/$E$8	=data!M3	=data!M20	=G12-F12	=H12/$E$8	=E12-I12	=(J12*60*1000*$C$9)/(1000*$C$8*$E$9)
3	=data!C4	=data!C21	=C13-B13	=D13/$E$8	=data!M4	=data!M21	=G13-F13	=H13/$E$8	=E13-I13	=(J13*60*1000*$C$9)/(1000*$C$8*$E$9)
4	=data!C5	=data!C22	=C14-B14	=D14/$E$8	=data!M5	=data!M22	=G14-F14	=H14/$E$8	=E14-I14	=(J14*60*1000*$C$9)/(1000*$C$8*$E$9)
5	=data!C6	=data!C23	=C15-B15	=D15/$E$8	=data!M6	=data!M23	=G15-F15	=H15/$E$8	=E15-I15	=(J15*60*1000*$C$9)/(1000*$C$8*$E$9)
6	=data!C7	=data!C24	=C16-B16	=D16/$E$8	=data!M7	=data!M24	=G16-F16	=H16/$E$8	=E16-I16	=(J16*60*1000*$C$9)/(1000*$C$8*$E$9)
7	=data!C8	=data!C25	=C17-B17	=D17/$E$8	=data!M8	=data!M25	=G17-F17	=H17/$E$8	=E17-I17	=(J17*60*1000*$C$9)/(1000*$C$8*$E$9)
8	=data!C9	=data!C26	=C18-B18	=D18/$E$8	=data!M9	=data!M26	=G18-F18	=H18/$E$8	=E18-I18	=(J18*60*1000*$C$9)/(1000*$C$8*$E$9)
9	=data!C10	=data!C27	=C19-B19	=D19/$E$8	=data!M10	=data!M27	=G19-F19	=H19/$E$8	=E19-I19	=(J19*60*1000*$C$9)/(1000*$C$8*$E$9)
10	=data!C11	=data!C28	=C20-B20	=D20/$E$8	=data!M11	=data!M28	=G20-F20	=H20/$E$8	=E20-I20	=(J20*60*1000*$C$9)/(1000*$C$8*$E$9)

Figure 13. The Excel macro for calculating the VAP-1 activity. The formulas used in the macro are shown. 'Data' refers to the sheet to which the data from the measurement had been copied to. RFU=relative fluorescence unit, the values obtained from the multimode microplate reader.

Formed fluorescence in the standard wells in 5 minutes

V1 µl	c1 µM	V2 µl	C2 nM	RFU at 0 min	RFU at 5 min	ΔRFU
0	5	80	0	3310	3853	0
5	5	80	312.5	11143	11902	7941
10	5	80	625	18335	19300	15236
15	5	80	937.5	25609	26717	22582
			Slope		24.01	
V serum µl	2.4		**t min**	5		
V final ml	0.08					

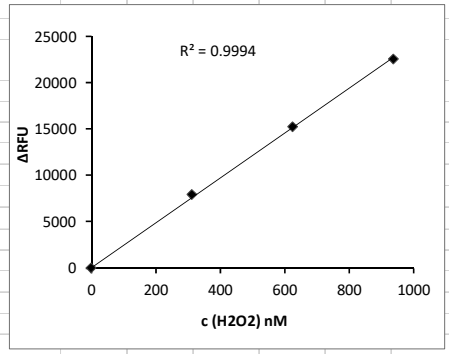

	RFU at 0 min	RFU at 5 min	ΔRFU	formed H2O2 nM	RFU at 0 min with HA	RFU at 5 min with HA	ΔRFU with HA	formed H2O2 nM	specific H2O2 nM	activity nmol/ml/h
1	2785	4263	1478	61.55	3863	4540	677	28.19	33.4	13.3
2	2258	3520	1262	52.55	3178	3829	651	27.11	25.4	10.2
3	2352	3347	995	41.44	3289	3767	478	19.91	21.5	8.6
4	2774	4056	1282	53.39	4423	5024	601	25.03	28.4	11.3
5	2798	4804	2006	83.54	3698	4349	651	27.11	56.4	22.6
6	2282	3490	1208	50.31	3346	3848	502	20.91	29.4	11.8
7	2646	4057	1411	58.76	3901	4383	482	20.07	38.7	15.5
8	2291	3612	1321	55.01	2958	3431	473	19.70	35.3	14.1
9	2808	3910	1102	45.89	4022	4432	410	17.07	28.8	11.5
10	3256	4799	1543	64.26	4254	4594	340	14.16	50.1	20.0

Figure 14. An example of the Excel macro for calculating the VAP-1 activities in the samples. The values are from the YFS 2007 series. RFU=relative fluorescence unit; HA=hydroxylamine.

Finally the macro calculated the activities for each sample in each time interval and collected the results on a summary sheet. The final results were the averages from the 13 intervals. Each plate included control samples (high, low, pool, middle) to inspect the validity of the plate.

4.2.4 Enzyme-linked immunosorbent assay (ELISA) (IV)

The enzyme-linked immunosorbent assay (ELISA) used in this study was developed on the basis of an original quantitative sandwich ELISA method for sVAP-1 (Kurkijarvi et al. 1998) performed on a 96-well plates and used in the research laboratory of Jalkanen and Salmi. The new ELISA protocol was developed in order to measure more samples during a normal working day (previously 8 samples, now 150 samples), while maintaining a pleasant workflow. In Figure 15, the basic principle of a sandwich ELISA is demonstrated. The capture and the detection antibodies are both specific mAbs against VAP-1, the target protein.

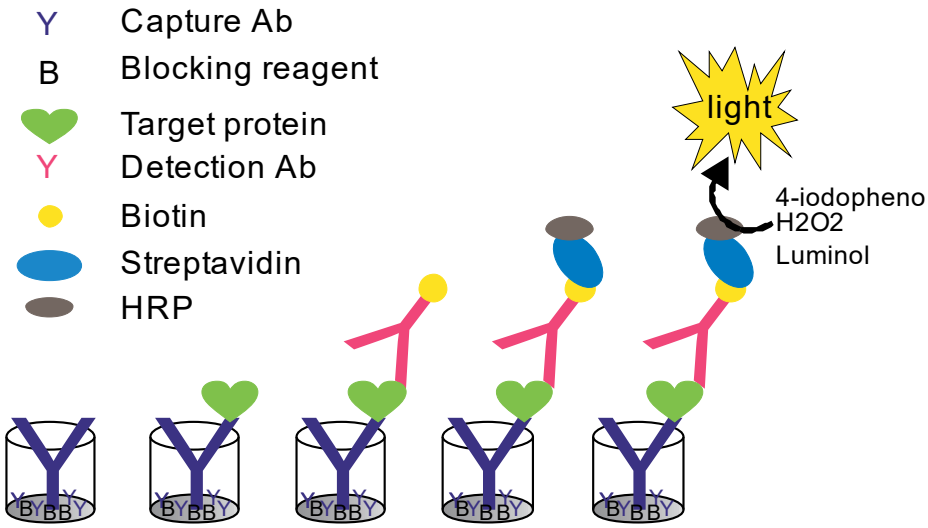

Figure 15. A schematic overview illustrating the principle of the in-house sandwich ELISA used in this study. The whole reaction chain is shown for one capture antibody (Ab) while in reality the same chain evolves for most of the capture antibodies. For more details, please see text.

The following modifications were done during the assay development. In the original protocol, all the samples, controls, and the standards were on the plate in triplicates. In addition, for each specific anti-VAP-1 mAb well, a negative antibody well was pipetted in order to get the background values and to identify the rare cases were the patient sample would have autoantibodies. In the new protocol, each sample, and standard was on the plate as a single well and thus only the sVAP-1 molecules detected by specific anti-VAP-1 mAb pair (capture antibody TK8-18 and detection antibody TK8-14) were measured. This was achieved by carefully examining the sources of the largest influencers on the

intra- and inter-assay variations, explained in more detail in the results section. To quantify the sVAP-1 levels in the samples, three dilutions of human tonsil lysates were used to produce the standard curve in the original protocol. In the new protocol an 8-point linear standard curve generated by recombinant human VAP-1 was used. The dilutions of samples, biotinylated detecting antibody (TK8-14), and streptavidin-peroxidase were changed as well compared to the original protocol. The new ELISA protocol was used to measure the sVAP-1 levels of the 2775 heparin plasma samples of the National FINRISK 2002 Study subpopulation as described in the next paragraph. The method development itself is discussed in more detail in the Results section.

All the reagents were prepared freshly for each day. During one work day 2 assay plates were measured with 75 samples per plate, 150 samples per day consequently. All the 2775 samples were measured in 19 days, 2 days a week for 10 weeks. The day before the measurement, two Nunc MaxiSorp flat bottom white 96-well plates (Nunc, Roskilde, Denmark) were coated with the capture Ab, 10 µg/ml anti-VAP-1 mAb (TK8-18) in 0.1 M $NaHCO_3$ (pH 9.6) solution. The 100 µl volume was pipetted into the wells with an electronic Biohit Proline 100-5000 µl pipettor (Sartorius, Göttingen, Germany) without touching the sides of the wells. The plates were sealed with a sticker and incubated at +4°C overnight. The following morning the previously coated assay plates were taken from +4°C and incubated in +37°C for an hour. The once thawed sample tubes were taken from -70 °C and let thaw at room temperature. The blocking reagent was prepared by dissolving 3 g gelatin into 300 ml PBS by boiling the solution in two patches for at least 10 minutes in a microwave oven. After cooling the solution in cold water bath, 3 g of milk powder was dissolved into the solution. All the subsequent reagents were diluted into the blocking reagent and all the steps were done in room temperature. The assay plates were washed 6 times with the Wallac Delfia Microplate washer (PerkinElmer, Waltham, USA) with 0.1% Tween-PBS as washing solution, after which the free spaces in the wells were blocked with the blocking reagent for 45 min.

The thawed samples were centrifuged at 5000 rounds per minute for 3 minutes. The 1:100 dilution of samples were done by dispensing 495 µl of blocking reagent to an auxiliary plate (Deep Well Storage plate, U-bottom, 1.2 ml, 4titude Limited, Wotton, UK) with Multidrop Combi Reagent Dispenser (ThermoFischer), adding 10 µl of samples with a Biohit mLine 1-10 µl pipette, shaking the plate vigorously with Multidrop, and dispensing another 495 µl of blocking reagent into the wells. The standards were diluted in FACS-tubes, and thereafter transferred to an auxiliary plate. A serial dilution of recombinant human VAP-1 (R&D Systems, Minneapolis, USA) was done in the blocking reagent with the final concentrations of 44, 33, 22, 11, 5.5, 2.8, and 0.7 ng/ml.

VAP-1-depleted plasma (i.e. plasma from which VAP-1 molecules had been removed) was added into each standard dilution to a ratio of 1:100.

After blocking the assay plates, the plates were washed again as described above. It is important, that the washing remnants were left to the wells and not tapped against cellulose paper, nor allowed them to dry before transferring the standards or samples from the auxiliary plates. The pre-diluted standard and sample solutions were mixed by pumping with a manual 8-channelled Biohit mLine 30-300 µl pipette and subsequently transferred from the auxiliary plates to the assay plates. The standard and sample solutions were incubated for an hour, and then washed as described previously. Next the detecting antibody, a biotinylated anti-VAP-1 mAb (TK8-14) was diluted in the blocking reagent in 1:200, and then pipetted 100 µl/well with an electronic 8-channelled Biohit eLine 10-300 µl pipette. After 60 minutes incubation, the plates were washed and a 1:500 dilution of streptavidin-HRP conjugate (GE Healthcare Life Sciences, Chicago, USA) in the blocking reagent was added to the wells of the assay plates with an electronic 8-channelled pipette, and incubated for an hour. At least 15 minutes before the end of the incubation time, BM Chemiluminescence ELISA substrate (POD; Sigma-Aldrich, Saint Louis, USA) solutions A and B were mixed in 1:100 proportions. After the final washing step, 100 µl of the chemiluminescent reagent was added to the wells with an electronic 8-channelled pipette. After a 3-minute waiting period, the luminescence values of the assay plate wells were measured with Tecan Infinite M200 plate reader.

After the reduction of blank values (1:100 dilution of VAP-1-depleted plasma in the blocking reagent) the sVAP-1 levels were calculated by subtracting the intercept of the linear standard curve from the luminescence value and divided the result with the slope of the linear standard curve. A high and low control plasmas were as triplicates on each plate for quality control and for intra- and inter assay variation controls. After all the 37 plates were measured, those plates which controls were not inside the pre-decided ±15% range from the average of the whole series were replicated.

5 RESULTS

5.1 Siglec-10 and Siglec-9 are first natural ligands for VAP-1 and the interactions are dependent on arginines (I, II)

Although VAP-1 has been known to mediate the trafficking of lymphocytes and granulocytes for a while (Salmi and Jalkanen 1992; Tohka et al. 2001), the counter-receptor(s) for VAP-1 on these cell populations has remained unknown. In order to solve the mystery, a CX_8C phage peptide library was introduced to immobilized recombinant VAP-1. The phages bound to VAP-1 were sequenced and the resultant sequences revealed similarities to Sialic acid binding Ig-like lectin-10 (Siglec-10) and Siglec-9. Siglec-10 is a glycoconjugate binding protein found on the surface of monocytes, eosinophils, and B cells (Munday et al. 2001), whereas Siglec-9 is found on monocytes, neutrophils, dendritic cells, and natural killer cells (Zhang et al. 2000; Macauley et al. 2014). Siglecs, as well as selectins, bind to sialic acids. The predominant sialic acid in humans is the *N*-acetylneuraminic acid, Neu5Ac, but in general sialic acid term is used on 43 different derivatives of the 9-carbon acidic sugar of neuraminic acid. Sialic acids are usually the capping sugars at the end of the glycan chains of all cell surfaces and secreted proteins (Varki 2008).

The interactions of VAP-1 with Siglecs were further validated in numerous *in vitro* experiments involving peptides, proteins, and cells expressing VAP-1, Siglec-9 or Siglec-10. The possibility of lymphocytes to use Siglec-10 and granulocytes to use Siglec-9 in order to bind to endothelial VAP-1 were demonstrated in *ex vivo* frozen section assays. By pretreating the isolated human B cells with anti-Siglec-10 mAb and granulocytes with anti-Siglec-9 mAb, less of them bound to the vessels of mesenteric lymph nodes of KOTG mice expressing hVAP-1. Vice versa, when the heart sections of hVAP-1 KOTG mice were pretreated with Siglec-10-Ig, less anti-VAP-1-mAb bound to the heart vasculature. In addition, through intravital microscopy imaging the rolling of granulocytes on VAP-1 positive inflamed endothelium was visualized. This experiment also suggested that Siglec-9 has a role in the early phases of the extravasation cascade.

Furthermore, the ability of Siglec-10 and -9 to bind to VAP-1's enzymatic groove and to study the interactions of VAP-1 and Siglec-9 and Siglec-10 on molecular level, a series of experiments with mutated peptides and recombinant proteins, or transfectants were performed. The relevant sequences are shown in Table 2 in Methods and in Table 6.

Table 6. Sequences in Siglecs relevant to VAP-1 binding.

Description	Sequence
Siglec-10	WVLQNRVLSS
Siglec-11	WVLQDRVLSS
Siglec-G	WVLEDQVLSW
Siglec-9	DSNPPARLSLSWRGLT
Siglec-E	DSYPPANLSWSWDNLT

All of these experiments revealed the necessity of arginines (denoted as R in Table 6 and Figure 16) in the interactions between Siglec-10 or -9 and VAP-1. First of all, Siglec-10 was able to act as a substrate for VAP-1 as H_2O_2 was produced in the presence of Siglec-10 cells and purified VAP-1. Presumably the arginine 293 of Siglec-10 interacts with the TPQ of VAP-1. Furthermore, Siglec-10 expressing cells failed to adhere to cells expressing enzymatically inactive VAP-1 where the TPQ precursor, tyrosine 471, was mutated to phenylalanine (see Figure 16 for the structures of amino acids). Surprisingly, Siglec-9 failed to act as a substrate for VAP-1, and even though the adhesion of Siglec-9 expressing cells to cells expressing enzymatically inactive VAP-1 was decreased compared to the wild type VAP-1 expressing cells, the decrease was not as much as with mock-transfected cells.

A cyclic peptide containing the residues 284-297 (ATLSWVLQNRVLSS) of Siglec-10 was shown to bind to recombinant VAP-1 in an ELISA assay. When the arginine in Siglec-10 peptide was mutated to alanine, a dramatically lesser amount of the peptide was bound to immobilized recombinant VAP-1 ($P<0.01$). The sequence binding to VAP-1 in Siglec-10 is located in the flexible CE loop of Siglec-10 protein. Interestingly, in Siglec-11 there is only one amino acid change in this area, an aspartic acid instead of the asparagine in Siglec-10. Remarkably, the change of primary amide to a carboxylate (both in ionic states in physiological circumstances) is enough to prevent the binding of Siglec-11 expressing cells to VAP-1 expressing cells. The mouse equivalent of Siglec-10 is Siglec-G with 4 essential changes in the CE loop sequence (see Table 6). These seemingly minor alterations in the sequence rendered the Siglec-G-transfectants unable to bind to VAP-1-transfectants.

The importance of arginines 284 and 290 in Siglec-9 for VAP-1 binding was demonstrated in surface plasmon resonance assays. Compared to the wild type Siglec-9 peptide (see Table 2 in Methods), mutated peptides with both or one arginines at the time mutated to alanines bound significantly less to VAP-1. Apparently the Arg284 is even more critical to the interaction as the binding was reduced 66%, $P=0.04$, whereas Arg290 mutation decreased the binding by 42%,

P=0.05. Finally, cells expressing Siglec-E, the mouse equivalent of Siglec-9, were unable to bind VAP-1 transfectants, presumably because the missing arginines in relevant locations.

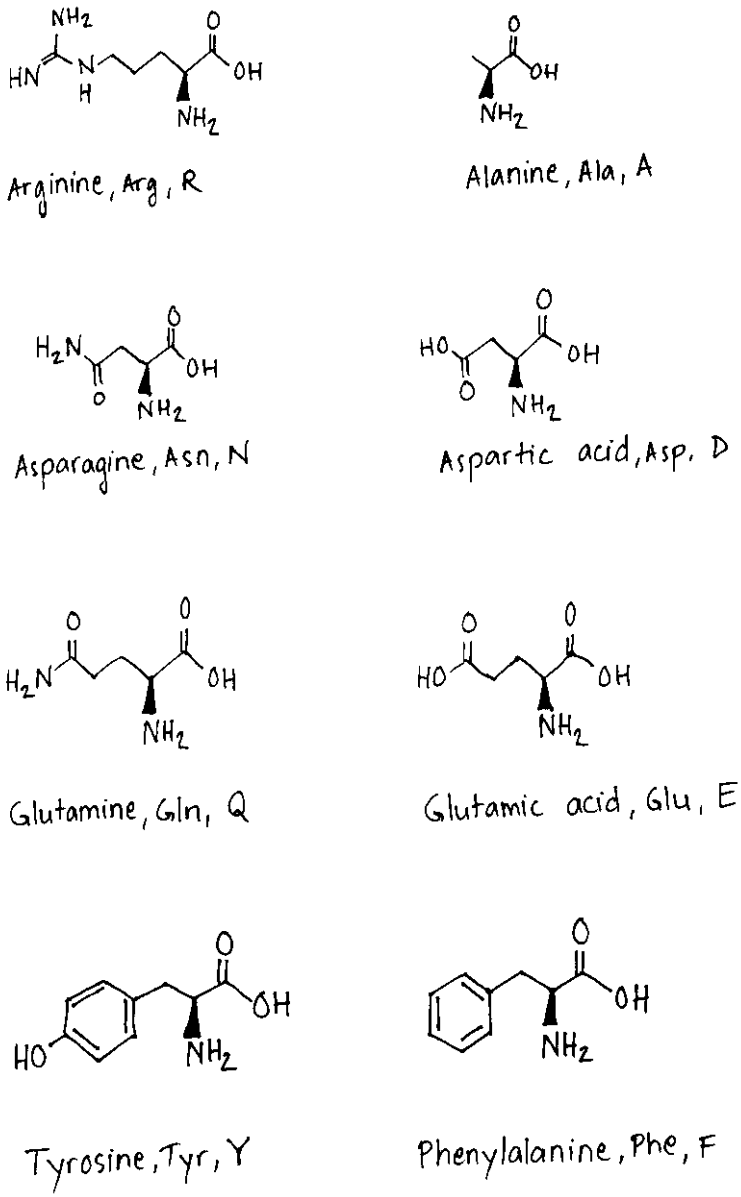

Figure 16. The structures of the relevant amino acids in the interactions of VAP-1 and its ligands Siglec-10 and Siglec-9.

These results together suggest that B cells use Siglec-10 and granulocytes use Siglec-9 when adhering to VAP-1 on endothelial cells, and that the interaction is dependent on arginines interacting with TPQ in enzyme activity-dependent and independent mechanisms.

5.2 The SSAO-activity assay was successfully miniaturized and validated for population studies (III)

The old protocol for measuring the SSAO-activities of sVAP-1 molecules in the blood samples was inadequate for large population studies. To develop the fluorometric in-house enzyme activity assay measuring the hydrogen peroxide produced by the sVAP-1 molecule in the samples, a few modifications for the old protocol were made. To increase the throughput of the assay the new protocol was designed for 384-well microplates instead of 96-well microplates. In order to reduce the background, the assay buffer was changed from Krebs-Ringer bicarbonate buffer to 0.1 M sodium phosphate buffer (SPB) as was used in the Amplex Red Hydrogen Peroxide / Peroxidase Assay Kit from Invitrogen (catalog number A22188). The dilutions of the substrate (4 mM benzylamine) and the inhibitor (100 µM hydroxylamine) were prepared freshly every day instead of storing them at +4°C for 5 days. The sample dilution of 1/100 was chosen, as the SSAO-activities measured in serum dilutions from 1/200 to 1/20 all gave the same result with the assay. To further decrease the background of the assay, the concentration of Amplex Red in the wells was reduced from 80 µM to 8 µM according to (Votyakova and Reynolds 2004). To make the measurement more convenient, instead of measuring the plate manually every 15 minutes with a microplate reader and storing the plate in +37°C incubator in between, the microplate reader was programmed to measure the plate every 5 minutes and incubate the plate at +37°C in the reader's incubator for the time between.

Since the SSAO-activity assay was fluorometric and the enzyme's activity was dependent on cations, we hypothesized that the sample format (serum vs plasma) might affect the measurements. To study this, we collected plasma and serum samples from 7 individuals. For collecting the plasma samples the blood samples were taken to heparin, ethylenediaminetetraacetic acid (EDTA), and citrate containing tubes. The tubes were kept turning for 30-60 minutes in RT and centrifuged at 2200 x g for 10 minutes to separate the cells from the plasma. For collecting the serum samples the same 7 persons donated blood to tubes without anticoagulants, but with silica to promote the clotting. The samples were let stand for 30-60 minutes and centrifuged thereafter (2200 x g, 10 min). The results showed that the chelating agents EDTA and citrate affected the enzymatic function of VAP-1 by chelating the Cu^{2+} ions, whereas heparin and serum gave similar sVAP-1 activities. These results affirmed that serum is the best matrix for the assay. Next, we wanted to confirm the specificity of the assay. To make sure that the SSAO-activity in the serum measured by the assay actually originates from sVAP-1-molecules, the sVAP-1 molecules were removed from the sera of two individuals with cyanogen bromide beads coated with VAP-1-specific antibodies recognizing different epitopes of VAP-1. The SSAO-activity was

abolished in the sVAP-1-depleted sera, and moreover, by adding different amounts of recombinant VAP-1 to the depleted sera, a linear response was achieved. The result of this experiment was repeated by measuring both the SSAO-activities as well as the sVAP-1 concentrations of 38 patient serum samples. Again the SSAO-activities of the samples increased linearly according to the sVAP-1 concentrations in the patient samples. To further validate the assay, we studied the effect of freeze-thaw cycles to the SSAO-activity, since even the protein stability is vulnerable for the freeze-thaw cycles (Lee et al. 2015; Gislefoss et al. 2017; Huang et al. 2017). When kept at -20°C, a statistically significant decrease in the SSAO-activities came apparent after the sixth and seventh freeze-thaw cycle with a 12% and 14% drop in the SSAO-activities of the samples, respectively. For the samples stored at -70°C, a similar decrease (16%) in the SSAO-activities was evident after 7th freeze-thaw cycle. Finally, the effect of long-term storage time and temperature to SSAO-activities were studied as well, since some studies recommend taking these factors into consideration (Cray et al. 2009; Gislefoss et al. 2009). After a year, the samples stored at -20°C had on average 21% decreased SSAO-activities compared to the samples measured freshly, whereas for the samples kept at -70°C the effect was on average 5% and thus did not reach statistical significance. Taken together these results strongly imply that the samples used in the SSAO-activity assays should be sera and stored at -70°C without any previous freeze-thaw cycles.

5.3 In-house sVAP-1 ELISA for population studies (IV)

The major changes made for the original in-house ELISA for sVAP-1 (Kurkijarvi et al. 1998) concerned the low quantity of samples able to be measured per plate. This stemmed from the triplicate dilutions of each sample and their negative control wells. In order to vastly increase the precision and accuracy of the assay numerous parameters were controlled to find the biggest influencers on the inter- and intra-assay variations.

During freeze-thaw cycles, the sVAP-1 levels of the samples were decreased on average by 10% (n=3, seven freeze-thaw cycles), and thus never thawed samples should be preferred. EDTA and heparin plasma samples gave the same levels (tested with low and high controls, P>0.4 in all tests). The intra- and inter-assay variation improved from 5.6 and 7.9 to 3.7 and 7.5, respectively, when the 5 µl volumes of the samples were pipetted with a mLine 1-10 µl pipette instead of a mLine 10-100 µl pipette. The amount of washings was tested and when doing only three washes instead of the normal six, the background increased, thus decreasing the specific reactions. Different lots of the milk powder used in the

blocking reagent affected the acquired luminescence values. The stability of the biotinylated mAb TK8-14 was tested by comparing once thawed and a never thawed batch of the antibody. Interestingly, the once thawed biotinylated Ab gave statistically significantly lower levels of VAP-1 (P<0.010 in all tests). Thus, the biotinylated TK8-14 Ab should be divided to appropriate quantities for each day. The final adjustments were tested on a complex one plate assay, which simultaneously tested the dilution of the samples, biotinylated Ab, and streptavidin-HRP as demonstrated in Figure 17.

	1	2	3	4	5	6	7	8	9	10	11	12
			R 1:25	R 1:25	R 1:25	R 1:25	R 1:25	R 1:25	R 1:25	R 1:25	R 1:25	Blok
A	Oma st0	EM st0	Biot 1:50	Biot 1:100	Biot 1:200	Biot 1:50	Biot 1:100	Biot 1:200	Biot 1:50	Biot 1:100	Biot 1:200	Biot 1:50
			SAP 1:500	SAP 1:500	SAP 1:500	SAP 1:1000	SAP 1:1000	SAP 1:1000	SAP 1:2000	SAP 1:2000	SAP 1:2000	SAP 1:500
			R 1:50	R 1:50	R 1:50	R 1:50	R 1:50	R 1:50	R 1:50	R 1:50	R 1:50	Blok
B	Oma st1	EM st1	Biot 1:50	Biot 1:100	Biot 1:200	Biot 1:50	Biot 1:100	Biot 1:200	Biot 1:50	Biot 1:100	Biot 1:200	Biot 1:100
			SAP 1:500	SAP 1:500	SAP 1:500	SAP 1:1000	SAP 1:1000	SAP 1:1000	SAP 1:2000	SAP 1:2000	SAP 1:2000	SAP 1:500
			R 1:100	R 1:100	R 1:100	R 1:100	R 1:100	R 1:100	R 1:100	R 1:100	R 1:100	Blok
C	Oma st2	EM st2	Biot 1:50	Biot 1:100	Biot 1:200	Biot 1:50	Biot 1:100	Biot 1:200	Biot 1:50	Biot 1:100	Biot 1:200	Biot1:200
			SAP 1:500	SAP 1:500	SAP 1:500	SAP 1:1000	SAP 1:1000	SAP 1:1000	SAP 1:2000	SAP 1:2000	SAP 1:2000	SAP 1:500
			R 1:200	R 1:200	R 1:200	R 1:200	R 1:200	R 1:200	R 1:200	R 1:200	R 1:200	Blok
D	Oma st3	EM st3	Biot 1:50	Biot 1:100	Biot 1:200	Biot 1:50	Biot 1:100	Biot 1:200	Biot 1:50	Biot 1:100	Biot 1:200	Biot 1:50
			SAP 1:500	SAP 1:500	SAP 1:500	SAP 1:1000	SAP 1:1000	SAP 1:1000	SAP 1:2000	SAP 1:2000	SAP 1:2000	SAP 1:1000
			M 1:25	M 1:25	M 1:25	M 1:25	M 1:25	M 1:25	M 1:25	M 1:25	M 1:25	Blok
E	Oma st4	EM st4	Biot 1:50	Biot 1:100	Biot 1:200	Biot 1:50	Biot 1:100	Biot 1:200	Biot 1:50	Biot 1:100	Biot 1:200	Biot 1:100
			SAP 1:500	SAP 1:500	SAP 1:500	SAP 1:1000	SAP 1:1000	SAP 1:1000	SAP 1:2000	SAP 1:2000	SAP 1:2000	SAP 1:1000
			M 1:50	M 1:50	M 1:50	M 1:50	M 1:50	M 1:50	M 1:50	M 1:50	M 1:50	Blok
F	Oma st5	EM st5	Biot 1:50	Biot 1:100	Biot 1:200	Biot 1:50	Biot 1:100	Biot 1:200	Biot 1:50	Biot 1:100	Biot 1:200	Biot1:200
			SAP 1:500	SAP 1:500	SAP 1:500	SAP 1:1000	SAP 1:1000	SAP 1:1000	SAP 1:2000	SAP 1:2000	SAP 1:2000	SAP 1:1000
			M 1:100	M 1:100	M 1:100	M 1:100	M 1:100	M 1:100	M 1:100	M 1:100	M 1:100	Blok
G	Oma st7	EM st7	Biot 1:50	Biot 1:100	Biot 1:200	Biot 1:50	Biot 1:100	Biot 1:200	Biot 1:50	Biot 1:100	Biot 1:200	Biot 1:100
			SAP 1:500	SAP 1:500	SAP 1:500	SAP 1:1000	SAP 1:1000	SAP 1:1000	SAP 1:2000	SAP 1:2000	SAP 1:2000	SAP 1:2000
			M 1:200	M 1:200	M 1:200	M 1:200	M 1:200	M 1:200	M 1:200	M 1:200	M 1:200	Blok
H	depl	depl	Biot 1:50	Biot 1:100	Biot 1:200	Biot 1:50	Biot 1:100	Biot 1:200	Biot 1:50	Biot 1:100	Biot 1:200	Biot 1:200
			SAP 1:500	SAP 1:500	SAP 1:500	SAP 1:1000	SAP 1:1000	SAP 1:1000	SAP 1:2000	SAP 1:2000	SAP 1:2000	SAP 1:2000

<>	1	2	3	4	5	6	7	8	9	10	11	12
A	783849	642921	6560000	5750000	5100000	1690000	1900000	1780000	680965	763554	610211	180107
B	554333	487233	2790000	3240000	2540000	1040000	1020000	917736	420566	415142	406301	113179
C	383710	297499	1850000	1580000	1260000	507473	475317	435607	192208	189615	180435	57826
D	198725	162257	1070000	987246	742214	305258	281340	275097	111409	97961	93234	42994
E	108370	93568	2540000	2410000	2040000	778280	693205	800527	309948	300646	263888	35702
F	65739	55799	1320000	1180000	1130000	445148	404645	371676	146560	137632	129950	26107
G	47394	47948	703438	651321	502152	220204	192444	188257	72731	74389	62104	26127
H	40931	37702	426762	357870	242726	116770	113240	90973	45813	38839	29441	21661

		Biot 1:50 SAP 1:500	Biot 1:100 SAP 1:500	Biot 1:200 SAP 1:500	Biot 1:50 SAP 1:1000	Biot 1:100 SAP 1:1000	Biot 1:200 SAP 1:1000	Biot 1:50 SAP 1:2000	Biot 1:100 SAP 1:2000	Biot 1:200 SAP 1:2000
R vs M	P 1:25	2.6	2.4	2.5	2.2	2.7	2.2	2.2	2.5	2.3
	P 1:50	2.1	2.7	2.2	2.3	2.5	2.5	2.9	3.0	3.1
	P 1:100	2.6	2.4	2.5	2.3	2.5	2.3	2.6	2.5	2.9
	P 1:200	2.5	2.8	3.1	2.6	2.5	3.0	2.4	2.5	3.2
R vs B	P 1:25	36	51	88	39	53	68	26	29	28
	P 1:50	15	29	44	24	29	35	16	16	19
	P 1:100	10	14	22	12	13	17	7	7	8
	P 1:200	6	9	13	7	8	11	4	4	4
M vs B	P 1:25	14	21	35	18	19	31	12	12	12
	P 1:50	7	10	20	10	11	14	6	5	6
	P 1:100	4	6	9	5	5	7	3	3	3
	P 1:200	2	3	4	3	3	3	2	1	1

Figure 17. A test plate to choose optimal ELISA reagent amounts. From the top: the outline for the plate wells, the luminescence values obtained, and the proportions of the luminescence values of high (R) and low (M) controls to the blank (B) in each combination of different dilutions of biotinylated detection antibody (Biot), plasma samples (P) and streptavidin-horseradish peroxidase (SAP).

In the example shown in Figure 17, the conditions of 1:100 plasma dilution, 1:100 dilution of biotinylated Ab, and 1:1000 dilution of streptavidin-HRP were chosen because of the suitable ratios between high (R) and low (M) controls and blank (B) including 1:100 dilution of VAP-1-depleted plasma in blocking

reagent. In addition, with these dilutions the luminescence values obtained were on an ideal middle area of the standard curve.

5.4 Soluble VAP-1 level is associated with cardiovascular risk factors, early signs of atherosclerosis, and major adverse cardiovascular events in the general population (III, IV)

CVD risk factors are male sex, high age, prevalent type 2 DM, smoking, high systolic blood pressure, and dyslipidemia. We measured the serum SSAO activities or the plasma sVAP-1 levels in subjects belonging to two Finnish population studies, and studied the association of VAP-1 to the aforementioned risk factors. The participants of Young Finns study (YFS) were 30-45 years old, whereas the subjects in FINRISK02 were over 51 years old. The associations of sVAP-1 to CVD risk factors are presented in Table 7.

Table 7. The association of sVAP-1 levels to CVD risk factors in two Finnish populations of varying ages. This table summarizes the main findings in short; the more detailed results can be found in III and IV.

Study population	**YFS (III)**		**FR02 (IV)**	
Characteristic	**SSAO-activity nmol/ml/h**	***P***	**sVAP-1 levels ng/ml**	***P***
Male sex (men, women)	13.8 vs 13.5	*0.024*	820 vs 840	*0.084*
Smoking (no, yes)	13.6 vs 13.5	*0.63*	820 vs 874	*<0.001*
Type 2 DM (no, yes)	13.6 vs 16.4	*0.028*	824 vs 910	*<0.001*
	Correlation coefficient	***P***	**Correlation coefficient**	***P***
Age (years)	0.047	*0.030*	0.086	*<0.001*
Systolic blood pressure	0.024	*0.26*	-0.0075	*0.71*
Total cholesterol	0.024	*0.26*	0.09	*<0.001*
HDL cholesterol	-0.012	*0.56*	0.034	*0.084*

Since the YFS cohort did not have any CVD events, we used IMT and plaques (n=54) as a surrogate markers for sub-clinical atherosclerosis. When accounting for various variables, including the traditional CVD risk factors, the SSAO activity was an independent determinant of carotid IMT and plaques in women, and the SSAO activity correlated positively with CVD risk scores in the whole population. In the FR02 cohort there were 265 incident MACE cases, and sVAP-1 levels were higher in participants with MACE than without (P<0.001), and the number of MACE cases increased with the quartiles of sVAP-1 (P=0.0017).

Furthermore, in a Cox proportional hazard model for CVD the sVAP-1 levels resulted in 20% increase in the hazard of incident MACE (standardized HR 1.20 [95% Cl 1.06-1.36], *P*=0.0046) thus confirming the ability of sVAP-1 to predict incident CVD events. Together these results verify the association of sVAP-1 to CVD risk factors and more importantly the association of sVAP-1 to the early manifestations of atherosclerosis, as well as to the MACE outcome.

5.5 Incorporation of soluble VAP-1 level to risk prediction model of incident major adverse cardiovascular event improves the reclassification of the persons in the clinically relevant intermediary risk category (IV)

Risk prediction of future CVD event can be viewed on different levels. In a recent review, Elosua et al. discuss the prevention approaches focused on either the whole population or on individuals at high risk (Elosua 2014). The general population approach uses governmental policies to affect the whole population, e.g. banning smoking in public places. The latter approach instead focuses on the individual's risk for a future event by using mathematical equations called risk functions. These risk functions estimate the individual's probability for an event in the future by using the information about the levels of traditional risk factors of an individual. We used the second approach as we first categorized the individuals into low (0-5%), intermediate (5-20%), and high (>20%) risk categories according to the traditional risk factors, and then tested the sVAP-1's ability to reclassify these individuals correctly.

In our study cohort, 56% of subjects with an incident MACE had 0-2 risk factors of the possible 6. This is in concordance with the earlier results published in other cohorts (Elosua 2014). Even with a rigorous 10-fold cross-validation in attempt to assess the performance of the predictive model in practice, incorporation of sVAP-1 levels to Framingham risk model improved the IDI (*P*=0.042), and the clinical NRI (focusing on the intermediate risk group, *P*=0.0019). Especially the model specificity was improved, since adding the sVAP-1 levels to the model improved the reclassification of the non-events in both clinical NRI and in category-free NRI (*P*<0.001 in both tests after 10-fold cross-validation). The sensitivity of the prediction model, i.e. the reclassification of the events, was borderline statistically significant when sVAP-1 levels were included in the model (*P*=0.069 in clinical NRI and *P*=0.086 in category-free NRI after 10-fold cross-validation). Nevertheless, the clinical NRI for all movements was 0.090 (CI 0.033 to 0.147) with a statistically significant *P*=0.0019.

6 DISCUSSION

6.1 First counterparts of VAP-1 discovered on leukocytes (I,II)

VAP-1 is known to facilitate leukocyte adhesion and transmigration by enzyme-activity-dependent and enzyme-activity-independent way (Salmi et al. 2001; Koskinen et al. 2004). Our experiments with the novel leukocyte ligands for VAP-1, Siglec-10 and Siglec-9, support these earlier studies, as the interactions of VAP-1 with Siglec-10 and -9 were both enzyme activity-dependent and independent. An earlier notion of small amounts of H_2O_2 forming in VAP-1 dependent lymphocyte adhesion (Koskinen et al. 2004) was now verified by Siglec-10 expressing cells in the presence of purified VAP-1. In addition, this means that the mystery of endogenous substrates for SSAO, and the physiological purpose of SSAO activity were clarified.

Siglec-10 was cloned by three different groups (Li et al. 2001; Munday et al. 2001; Whitney et al. 2001), who reported Siglec-10 expression on the surface of eosinophils, neutrophils, monocytes, and B cells. Similarly, Siglec-9 cloning was reported by three different groups (Angata and Varki 2000; Foussias et al. 2000; Zhang et al. 2000), who reported Siglec-9 to be expressed on the surface of monocytes, neutrophils, B cells, NK cells, and $CD8^+$ T and $CD4^+$ T cells. Thus, as VAP-1 is known to mediate the adhesion of neutrophils (Foot et al. 2013), monocytes (Merinen et al. 2005), NK cells and $CD8^+$ T cells (Salmi et al. 1997), $CD4^+$ T cells (Bonder et al. 2005), and peripheral blood lymphocytes (Arvilommi et al. 1996), the leukocyte ligands for these interactions might be Siglec-10 and -9. Furthermore, both Siglecs bind to glycoconjugates with sialic acids in α2,3 and α2,6 linkages, and indeed, the sialic acids on the surface of VAP-1 are α2,3 and α2,6 linked (Salmi and Jalkanen 1996).

Surprisingly, mutation in the TPQ precursor Tyr471 in the active site of VAP-1 was not enough to prevent the binding of Siglec-9, and furthermore Siglec-9 expressing cells failed to produce H_2O_2 in the presence of VAP-1 (data not shown). Recently, this interaction has been studied in docking studies, which revealed that the Siglec-9 peptide fits into the active site of VAP-1, but does not interact covalently with the TPQ (Lopes de Carvalho et al. 2018) confirming our results. Instead, two of the 6 glycans on the surface of VAP-1 are relevant for the interaction, as the Arg290 of Siglec-9 forms hydrogen bonds with the N-acetylglucosamine of one of the glycans (Lopes de Carvalho et al. 2018).

6.2 The development of high-throughput assays for sVAP-1 measurements (III, IV)

The soluble form of VAP-1 in human blood was discovered in 1998 (Kurkijarvi et al. 1998). Circulating VAP-1 molecules display the SSAO-activity and most of the serum monoamine oxidase activity is originated from sVAP-1 (Kurkijarvi et al. 2000). In our laboratory, the SSAO-activity has been measured radiochemically (Kurkijarvi et al. 2000), or with a fluorometric method, but these assays have been suitable for only 8 to 12 samples at a time. Several sources of pre-analytical variations were investigated for the SSAO-activity assay. According to these studies, the SSAO-activity was inhibited by the cation chelating anticoagulants EDTA and citrate. This was anticipated, since both are known to chelate Cu^{2+} cations (Ding et al. 2011; Liu and Lin 2013) which are vital for the TPQ reaction. The SSAO-activity remained stable through 4 to 5 freeze-thaw cycles when stored at -20 or -70 degrees. In addition, the level of SSAO-activity did not change during a one year storing at -70 degrees.

The assay was validated for numerous variables. The assay was suitable for different sample volumes, and it measured specifically the hydrogen peroxide produced by VAP-1, as the sample devoid of VAP-1 gave no signal. In addition, the assay was calibrated by adding increasing amounts of recombinant VAP-1 protein to sample matrices and measuring the SSAO-activities. The two methods were also calibrated by measuring the SSAO-activities of human samples with wide range of sVAP-1 levels.

The assay development of sVAP-1 ELISA was successful as well, and the test plate for testing the appropriate dilutions of samples, biotinylated Ab, and streptavidin-HRP is widely used in our laboratory each time a batch of any reagent is changed, making the ELISA reliable even between the series of measurements. The intra- and inter-assay coefficients of variation were 8 and 15 %, respectively, for the SSAO-activity assay on 384-well plate format, and 5 and 10 %, respectively for the sVAP-1 ELISA.

6.3 The feasibility of sVAP-1 as a biomarker (III, IV)

By demonstrating the associations of sVAP-1 levels in the blood to subclinical atherosclerosis and to incident CVD outcomes, the ability of sVAP-1 to function as a biomarker for CVD has been established. But in order to truly show the clinical utility of sVAP-1, it has to add incremental value to the clinicians by facilitating the decision making (Wang 2011; Folsom 2013). The Kaplan-Meier curves in work IV indicate possible cut-off values (829 ng/ml, or even more

stringent 975 ng/ml) for sVAP-1 levels to specify the persons at greater risk for MACE. However, these estimates accounted for only the sVAP-1 levels and not for the traditional CVD risk factors, and thus the use of more sophisticated reclassification measures were warranted. The interest for reclassifying the individuals in the intermediate risk range has increased (Khot et al. 2003; Wang et al. 2012; Folsom 2013). In a cohort study, 80% of the participants were classified to low or intermediate risk for coronary artery disease, though 60% of the events were accounted for these individuals (Marrugat et al. 2011; Elosua et al. 2013; Elosua 2014).

As cited in the review of literature, there are at least five criteria to consider when introducing a novel biomarker, all of which are met by sVAP-1. 1) The soluble form of VAP-1 present in circulation (Kurkijarvi et al. 2000) makes it easily quantifiable from blood and the new high throughput assays developed in this thesis work makes sVAP-1 measurement suitable for large population studies. 2) The costs for one individual SSAO-activity test is only 1.2 euros, and for one individual ELISA test 8.9 euros (the recombinant protein in the ELISA standard costing 6.5 euros, so any simultaneously measured samples would increase the costs by only 0.3 euros).

In addition to meeting the technical criteria, sVAP-1 meets the criterion of a novel biomarker to add incremental value for the prediction models (Wang 2011; Elosua 2014). 3) sVAP-1 was proven to have an association with the outcome already in the early phase of atherosclerosis in women, as well as to the more severe endpoint of a MACE in both sexes. 4) Even when sVAP-1 was added to the Framingham risk prediction model, it remained as a statistically significant predictor with a standardized HR of 1.20 (95% Cl 1.06-1.36). Interestingly, when both high sensitivity CRP and sVAP-1 were added to the Framingham risk prediction model to predict 9-year risk of a MACE, the HRs were similar for both of them (1.23 and 1.22 HR for standardized high sensitivity CRP and sVAP-1, respectively). Furthermore, when predicting fatal MACEs, only sVAP-1 had a significant association to the outcome. 5) Finally, a novel biomarker has to prove its usefulness in clinical setting by improving the reclassification of the individuals. The sVAP-1 was able to improve the IDI, the category-free NRI, and clinical NRI focusing on the individuals in the intermediate risk for MACE. Since these performance metrics of sVAP-1 were done in the discovery population, a rigorous 10-fold cross-validation of the results was used in order to avoid overfitting of the model (Jia 2017).

The suitability of using the Framingham risk score (Anderson et al. 1991) in a Finnish population can be discussed. The FINRISK02 study population used in the IV represented an elderly population of Finns. Noticeably, the subjects with

an incident MACE had all the traditional risk factors except one risk factor; the participants with and without MACE, had the same levels of total cholesterol, which probably reflects the use of statins in the individuals with high risk for CVD. But all the other variables included in the Framingham risk prediction model differed among the two groups, as the subjects who had MACE during the follow-up were older, more commonly men, had higher BP, lower HDL cholesterol, and higher prevalence of diabetes, were more often current smokers, and had higher use of antihypertensive treatment. Thus, the use of Framingham risk score in a Caucasian population of Finns seems legit.

To scale the results obtained from sVAP-1's ability to reclassify persons in the intermediate risk group, an extensive study including 246,699 participants investigated the value of adding CRP or fibrinogen to the risk prediction model with traditional risk factors (age, sex, smoking status, blood pressure, total and HDL cholesterol, and history of diabetes) and concluded that addition of the levels of CRP or fibrinogen would help to prevent approximately one additional event over a period of 10 years for every 400 to 500 people screened (Kaptoge et al. 2012). The sVAP-1 improved the reclassification of 9% of individuals in the intermediate risk category, although most of the correct reclassification came from the downward movements of the non-events (P<0.001), whereas the 5% of correct movements in events was borderline statistically significant (P=0.069). Nevertheless, these results with sVAP-1 are encouraging.

6.4 VAP-1 and its SSAO-activity in atherosclerosis (III, IV)

In our studies, the associations of sVAP-1 to CVD risk factors were more prominent in the older cohort (FR02), as shown in Table 7 in Results. There are several possible explanations for this. First of all, the overall health of Finns has improved tremendously during the last decades (Borodulin et al. 2015), and it is thus reasonable to say that the participants in the YFS representing Finns born between 1962-1977 are much healthier than the population represented by the FR02 with subjects born in 1927-1951. In YFS, men had higher SSAO-activities, whereas in FR02 women have higher levels of sVAP-1 even though it is not statistically significant. This could be explained by the effect of sex hormones, as the women in FR02 were mostly post-menopausal, whereas in YFS, 16% of women used oral contraceptives with a lowering effect on SSAO activities (13.6 vs 12.4 P=<0.0001). In both cohorts the number of smokers was the same (~20%), but a clear increase in sVAP-1 levels were only seen in FR02, suggesting that the years of smoking might play a role. Interestingly, the increase in SSAO activity in diabetic people was seen in YFS although the absolute

number of patients was only 17 (0.7%). In FR02 the increase was clear and the number of subjects with diabetes was 7%. The absence of associations of continuous sVAP-1 levels to systolic blood pressure, or cholesterols in YFS might reflect the healthiness of the population, since these subjects did not have any CVD events and only a few cases of type 2 DM; this said, it is intriguing that despite the lack of associations to other risk factors, SSAO activity did associate with the surrogate endpoint of IMT and plaques in multivariable models, especially in women. In FR02, sVAP-1 levels correlated with total cholesterol, but not with systolic BP or HDL cholesterol which probably reflects the usage of antihypertensive treatment and statins.

The neovessels originated from the adventitial vasa vasorum are responsible for the recruitment of lymphocytes, monocytes, and macrophages to the inflamed vessel wall in humans (Moreno et al. 2006). Interestingly, in human coronary plaques the neovessels express even 3-fold higher levels of adhesion molecules, such as VCAM-1, ICAM-1, and E-selectin than the arterial luminal endothelium (Moreno et al. 2006). Thus, the finding of VAP-1 expression on the human carotid intra-plaque neovessels is not surprising (Silvola et al. 2016). Our findings of two leukocyte ligands for VAP-1, Siglec-10 and Siglec-9, give VAP-1 the means to assists both lymphocytes and monocytes to the inflamed arterial wall through the neovessels. In addition, the amount of neovessels and thus the increased amount of inflammatory cells in a plaque are often found in vulnerable plaques, and thus are associated with adverse cardiovascular events (Chistiakov et al. 2017). By inhibiting the SSAO-activity with semicarbazide, Peng et al. were able to show a decrease in the infiltration of monocytes to and macrophages in established lesions, as well as a phenotypic switch of the SMCs from contractile phenotype to synthetic phenotype with enhanced migratory and proliferative abilities (Peng et al. 2016). This decrease in the phenotypic switch of SMCs from contractile phenotype to synthetic phenotype is atheroprotective (Zhang et al. 2016), and may be related to the functions of VAP-1 in a normal artery SMCs. However, these notions were done in mice and the fact that mice are highly resistant to atherosclerosis (Breslow 1996) has hindered the *in vivo* experimentation of atherosclerosis in mice. The only choice has been to use genetically modified animals either deficient in some protein or reciprocally overexpressing another protein (Breslow 1996). This of course leads to the fundamental question whether these animals can serve as a model for humans (Lee-Rueckert et al. 2016). “The laboratory literature and experimental community sometimes assume that the results obtained in cultured cells or animals closely correspond to humans” (Libby et al. 2011). For example, the mouse model for human atherosclerosis is $LDLR^{-/-}$ mice which, unlike in humans, express VAP-1 on the luminal side of the ECs on the plaques (Silvola et al. 2016).

6.5 The dual role of VAP-1 in leukocyte circulation in homeostasis and in atherosclerosis (I, II, III, IV)

The molecule studied in this thesis work was VAP-1, an adhesion molecule and an enzyme with countless known functions in human body. Yet, the ligands on the leukocyte surface, to which VAP-1 binds to when assisting leukocytes to adhere to the endothelium have remained a mystery until now. On top of that, the meaning of SSAO activity has puzzled the scientific community since the 1950s. It was assumed, that the amine oxidase function is needed to metabolize the potentially cytotoxic amines. However, it was discovered, that the products of VAP-1's SSAO activity are itself often more cytotoxic than the endogenous substrates (Dunkel et al. 2008). By finding the leukocyte ligands for VAP-1 we were able to shed light on a new physiological function of the SSAO activity as well. The transient covalent binding between Siglec-10 and TPQ in VAP-1's active site makes the rolling and firm adhesion steps of leukocyte adhesion cascade possible.

VAP-1 is involved in the homeostatic lymphocyte homing, as demonstrated in Figure 18. The VAP-1 molecule is one of the glycoproteins among the ESL of the cobblestone like HEVs in the peripheral LNs. Naive B cells come to the LN via blood circulation, and when reaching a HEV, the B cell makes initial contacts with the endothelium. When the B cell rolls on the endothelium, the Siglec-10 molecule expressed on its surface adheres to the sialic acids capping the N-linked glycans on the surface of VAP-1 molecule. As the B cell continues to roll, another Siglec-10 molecule on the B cell makes contacts with the active site channel of VAP-1, where Arg293 of the Siglec-10 covalently binds to the TPQ of VAP-1. This transient adhesion slows down the rolling B cell for a firmer attachment, and for the transmigration.

VAP-1 is also involved in leukocyte trafficking to inflamed and infected areas. In these situations, VAP-1 molecules are rapidly translocated from the intracellular vesicles to the surface of ECs (Salmi et al. 1993; Weston et al. 2013) where they assist the transmigration of neutrophils, monocytes, and T cells for example. In this regard, VAP-1 is found on the surfaces of the ECs in the new capillaries formed in the atherosclerotic vessel walls (Silvola et al. 2016) through neovascularization (Moreno et al. 2006). Here VAP-1 can recruit more Siglec-9^+ monocytes and T cells to the inflamed lesion site, as illustrated in Figure 19. In addition, the VAP-1 molecules on the SMCs of the artery's media layer are capable of exacerbating the atheroma progression by producing H_2O_2, aldehydes and ammonia through SSAO-activity.

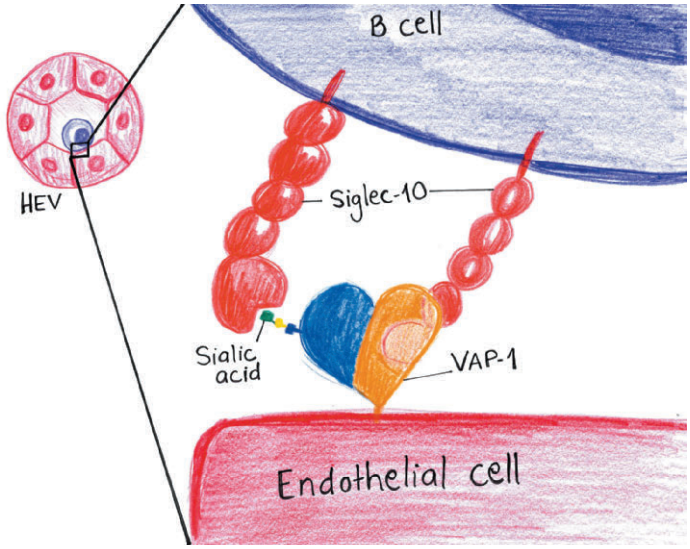

Figure 18. Role of VAP-1 and Siglec-10 in homeostatic B cell homing. A cross section of a high endothelial venule (HEV) in a lymph node (LN) is shown in the left upper corner. A close up on the interaction of B cell with the vascular endothelial cell is illustrated on the right side. The Siglec-10 on the surface of B cell is interacting first with the sialic acid on the end of the N-linked glycan. In the next phase, the arginine 293 from another Siglec-10 molecule binds to the TPQ in the active site of VAP-1. In the catalytic reaction hydrogen peroxide and ammonia are released, and the B cell can transmigrate through the endothelium to the LN.

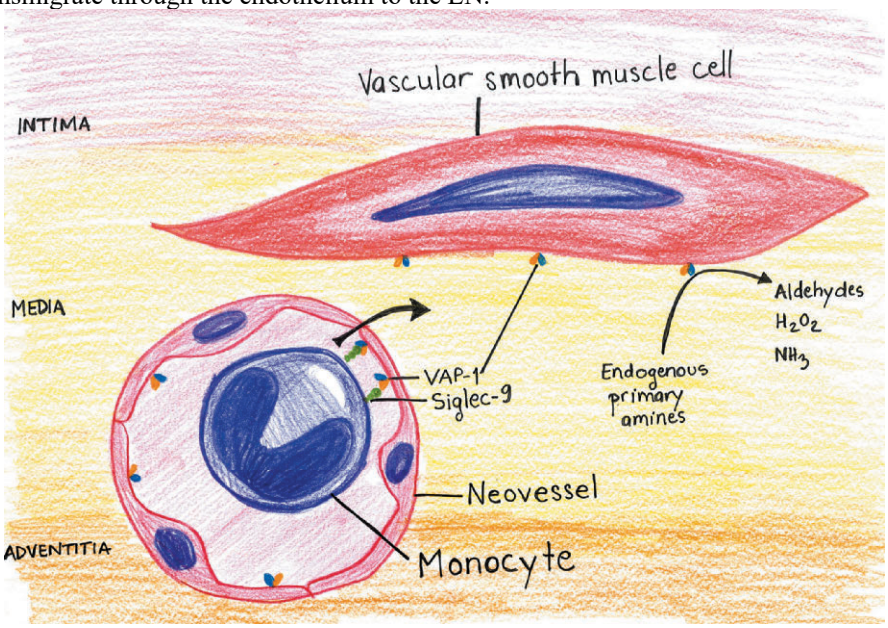

Figure 19. Role of VAP-1 and Siglec-9 in atherosclerosis progression. The VAP-1 molecules on the surface of the vascular endothelial cells in the intra plaque neovessel adhere to their monocyte ligand, Siglec-9, thus assisting monocytes to enter the inflamed atherosclerotic arterial wall. In addition, the VAP-1 molecules on the surface of the smooth muscle cells are capable of producing aldehydes, hydrogen peroxide, and ammonia through their SSAO activity, aggravating the atherosclerosis progression.

7 CONCLUSIONS

The human body is an entity. Powerful forces impact the vast organizations of cardiovascular and lymphatic systems. But in the end, it all comes down to smaller things, to the microenvironments governing the surfaces of cells.

The exteriors of all cells are covered with an endothelial surface layer (ESL). On the ESL of endothelial cells, an adhesion molecule called VAP-1 is found, with sialic acid decorations on the top of the molecule. Correspondingly, on the ESL of leukocytes, sialic acid binding molecules, called Siglecs are present. The interactions of these molecules are so specific, that it all depends on a single amino acid. The arginine in Siglec-10 ensuring the attachment to endothelial VAP-1 can also act as a substrate leading to SSAO-activity, and thus to harmful substances and inappropriate leukocyte trafficking. In the case of atherosclerosis, with all the other circumstances being in critical balance, the actions of one enzyme may tip the scale in favor of an infarction.

According to the data presented, one can conclude that the overall role of VAP-1 in atherosclerosis has been elucidated. The molecular counterparts for endothelial VAP-1 on the surface of leukocytes were identified, and the interactions were verified in numerous experiments. These specific interactions underline the elegance of the adhesion cascade; how time- and site-dependently the immune system is regulated to serve the body in changing circumstances.

Two different high-throughput methods were developed and validated to measure the sVAP-1 levels or the SSAO-activity of sVAP-1 on blood samples. The validated assays were used to measure the sVAP-1 levels or activities in large national cohorts. The hypothesis of sVAP-1 to associate with CVD risk factors and early manifestations of atherosclerosis was confirmed. The ability of sVAP-1 present in the blood to function as a biomarker was proven by the sVAP-1's ability to predict cardiovascular events in a normal Finnish population.

To conclude, VAP-1 assists leukocyte trafficking through its counterparts Siglec-9 and Siglec-10, and the actions of VAP-1 may contribute to the disease progression of atherosclerosis, and at least, it can serve as a biomarker for early atherosclerosis as well as for cardiovascular events later on.

ACKNOWLEDGEMENTS

It's said, that "It takes a village to raise a child". I would say it takes an inspiring research community, a lot of infrastructure, and a lot of money to do science. The work behind this dissertation was done in the inspirational research community of MediCity Research Laboratory as part of the Department of Medical Microbiology and Immunology at the University of Turku. The head of MediCity Research Laboratory, Professor Sirpa Jalkanen is warmly thanked and acknowledged for providing the facilities with excellent infrastructure. I would like to acknowledge and thank the National Doctoral Programme in Nanoscience and the Turku Doctoral Programme of Molecular Medicine with their directors Professor Matti Manninen and Adjunct professor Kati Elima, MD, PhD, respectively, for the funding of this work as well for travel grants, courses, and events. This study was financially supported in the form of travel grants and grants by Emil Aaltonen foundation, Emil and Blida Maunula foundation, Siiri Suominen foundation, Ida Montin foundation, Turku University foundation, Orion, and Scandinavian Society for Immunology.

I am most grateful for my supervisors Academician, Professor Sirpa Jalkanen and Professor Marko Salmi for countless things. First of all, I am thankful for the opportunity to carry out this PhD work under their supervision. I respect them both for their immense knowledge of immunology and their unique ways of thinking scientifically. Sirpa's excited and innovative thinking elicited an equally enthusiastic response in me, whereas Marko's more critical way of thinking really brought out the analytical, regulation loving side of me. Besides all the human capital provided, Sirpa and Marko are also acknowledged for arranging the financial support for these studies.

I warmly thank Professor Petri Kovanen and Professor Olli Vainio for reviewing this dissertation and for the valuable comments.

I want to thank Mikael Maksimow, PhD, for deepening my understanding of microplate based assays, and functional Excel files. Mikael's passion for sailing and wines gave pleasant changes in the topics during the hectic pace of assay validation and optimization processes.

The work behind this PhD project was done by several great researchers, the co-authors of these four articles, and I want to sincerely thank them all for their contributions. I want to especially acknowledge Elina Kiss, PhD, and Kati Elima, MD, PhD, docent, for the excellent work they did in order to find the counterparts of VAP-1; Anu Autio, PhD, and Professor Anne Roivainen for introducing me to PET-experiments; Aki Havulinna, PhD, for the data handling

and statistical analysis support, and Professors Olli Raitakari and Veikko Salomaa for the enormous help and support regarding the national population studies The Cardiovascular Risk in Young Finns and FINRISK, respectively.

In addition to the fore-mentioned co-authors, especially Teija Kanasuo and Etta Väänänen, but also Riikka Sjöroos, Mari Parsama, Sari Mäki, and Maritta Pohjansalo have enabled this work by their excellent technical help in the laboratory. All the present and former members of our research group are warmly thanked for the lively discussions in the Friday mornings, and for the friendly and scientific work ambiance. Particularly I want to thank my former roomies Sam, Annika, Norma, Anu, and Emmi for taking my mind (and my eyes) off the computer every once in a while, and Marika for the peer support as a new mom. Anne Sovikoski-Georgieva and Elina Wiik are acknowledged for their secretarial assistance, and all the technical personnel at MediCity for their help.

During the past nearly 10 years, I have had the fortune to have Kati and Kaisa as my lunch companions, but you of course are so much more to me (little doctor, style goddesses, inspirations for all culture and TV related, therapists during the small and big crises). I am so grateful for having you two as friends and I want to thank you for all the support you've given me.

Friends from the way back (Kirsi, Aino), friends from the student days (Henna, Maria, Jonna), Tynni, and the rest of my dear friends, are particularly thanked for the unforgettable moments and for being the constants in the changes of life. I want to thank Raija and Mikko for all the support and help, and for bringing up my dear husband. I wouldn't be here without my parents (*sic*) Merja and Rauli. Their unconditional love for all of us three daughters, and their eye for our unique talents gave us a remarkable growth milieu. Ann-Marie and Susanne, the best sisters in the world, because of you, my childhood was full of laughter and happiness. Thank you Perhe Aalto! Our daughter Elisabeth, the light of my life is thanked for…well, just for being, and for taking my mind of the work stuff as soon as I see her. Lastly, but no means least, I want to express my greatest gratitude to the love of my life, Ville, for always being there for me, and for all the care and love you show to me and to our beloved daughter, Effi.

Turku, August 2018

Kristiina Sautelainti

REFERENCES

Abbas, A. K., A. H. Lichtman, et al. (2016). Basic immunology : functions and disorders of the immune system.

Abbas, A. K., Lichtman, Andrew H., Pillai, Shiv (2018). Cellular and molecular immunology, Elsevier.

Abella, A., S. Garcia-Vicente, et al. (2004). "Adipocytes release a soluble form of VAP-1/SSAO by a metalloprotease-dependent process and in a regulated manner." Diabetologia **47**(3): 429-438.

Ager, A. and M. J. May (2015). "Understanding high endothelial venules: Lessons for cancer immunology." Oncoimmunology **4**(6): e1008791.

Airas, L., P. J. Lindsberg, et al. (2008). "Vascular adhesion protein-1 in human ischaemic stroke." Neuropathol Appl Neurobiol **34**(4): 394-402.

Aird, W. C. (2007). "Phenotypic heterogeneity of the endothelium: I. Structure, function, and mechanisms." Circ Res **100**(2): 158-173.

Airenne, T. T., Y. Nymalm, et al. (2005). "Crystal structure of the human vascular adhesion protein-1: unique structural features with functional implications." Protein Sci **14**(8): 1964-1974.

Akhavanpoor, M., C. A. Gleissner, et al. (2018). "Adventitial tertiary lymphoid organ classification in human atherosclerosis." Cardiovasc Pathol **32**: 8-14.

Altug Cakmak, H., S. Aslan, et al. (2015). "Assessment of the Relationship Between Serum Vascular Adhesion Protein-1 (VAP-1) and Severity of Calcific Aortic Valve Stenosis." J Heart Valve Dis **24**(6): 699-706.

Anderson, K. M., P. M. Odell, et al. (1991). "Cardiovascular disease risk profiles." Am Heart J **121**(1 Pt 2): 293-298.

Angata, T., S. C. Kerr, et al. (2002). "Cloning and characterization of human Siglec-11. A recently evolved signaling molecule that can interact with SHP-1 and SHP-2 and is expressed by tissue macrophages, including brain microglia." J Biol Chem **277**(27): 24466-24474.

Angata, T. and A. Varki (2000). "Cloning, characterization, and phylogenetic analysis of siglec-9, a new member of the CD33-related group of siglecs. Evidence for co-evolution with sialic acid synthesis pathways." J Biol Chem **275**(29): 22127-22135.

Anger, T., F. K. Pohle, et al. (2007). "VAP-1, Eotaxin3 and MIG as potential atherosclerotic triggers of severe calcified and stenotic human aortic valves: effects of statins." Exp Mol Pathol **83**(3): 435-442.

Arvilommi, A. M., M. Salmi, et al. (1997). "Organ-selective regulation of vascular adhesion protein-1 expression in man." Eur J Immunol **27**(7): 1794-1800.

Arvilommi, A. M., M. Salmi, et al. (1996). "Lymphocyte binding to vascular endothelium in inflamed skin revisited: a central role for vascular adhesion protein-1 (VAP-1)." Eur J Immunol **26**(4): 825-833.

Ashina, K., Y. Tsubosaka, et al. (2015). "Histamine Induces Vascular Hyperpermeability by Increasing Blood Flow and Endothelial Barrier Disruption In Vivo." PLoS One **10**(7): e0132367.

Aspelund, A., S. Antila, et al. (2015). "A dural lymphatic vascular system that drains brain interstitial fluid and macromolecules." J Exp Med **212**(7): 991-999.

Aspelund, A., M. R. Robciuc, et al. (2016). "Lymphatic System in Cardiovascular Medicine." Circ Res **118**(3): 515-530.

Aspelund, A., T. Tammela, et al. (2014). "The Schlemm's canal is a VEGF-C/VEGFR-3-responsive lymphatic-like vessel." J Clin Invest **124**(9): 3975-3986.

Atkinson, A. J., W. A. Colburn, et al. (2001). "Biomarkers and surrogate endpoints: Preferred definitions and conceptual framework." Clinical Pharmacology & Therapeutics **69**(3): 89-95.

Auffray, C., D. Fogg, et al. (2007). "Monitoring of blood vessels and tissues by a population of monocytes with patrolling behavior." Science **317**(5838): 666-670.

Augustin, H. G. and G. Y. Koh (2017). "Organotypic vasculature: From descriptive heterogeneity to functional pathophysiology." Science **357**(6353).

Baluk, P., J. Fuxe, et al. (2007). "Functionally specialized junctions between endothelial cells of lymphatic vessels." J Exp Med **204**(10): 2349-2362.

Barreiro, O., M. Yanez-Mo, et al. (2002). "Dynamic interaction of VCAM-1 and ICAM-1 with moesin and ezrin in a novel endothelial docking structure for adherent leukocytes." J Cell Biol **157**(7): 1233-1245.

Becchi, S., A. Buson, et al. (2017). "Inhibition of semicarbazide-sensitive amine oxidase/vascular adhesion protein-1 reduces lipopolysaccharide-induced neuroinflammation." Br J Pharmacol **174**(14): 2302-2317.

Becker, B. F., D. Chappell, et al. (2010). "Endothelial glycocalyx and coronary vascular permeability: the fringe benefit." Basic Res Cardiol **105**(6): 687-701.

Bergeret, B., H. Blaschko, et al. (1957). "Occurrence of an amine oxidase in horse serum." Nature **180**(4595): 1127-1128.

Bernier-Latmani, J. and T. V. Petrova (2017). "Intestinal lymphatic vasculature: structure, mechanisms and functions." Nat Rev Gastroenterol Hepatol **14**(9): 510-526.

Bhatnagar, A. (2017). "Environmental Determinants of Cardiovascular Disease." Circ Res **121**(2): 162-180.

Blum, K. S., S. Karaman, et al. (2014). "Chronic high-fat diet impairs collecting lymphatic vessel function in mice." PLoS One **9**(4): e94713.

Bonder, C. S., M. U. Norman, et al. (2005). "Rules of recruitment for Th1 and Th2 lymphocytes in inflamed liver: A role for alpha-4 integrin and vascular adhesion protein-1." Immunity **23**(2): 153-163.

Bono, P., S. Jalkanen, et al. (1999). "Mouse vascular adhesion protein 1 is a sialoglycoprotein with enzymatic activity and is induced in diabetic insulitis." Am J Pathol **155**(5): 1613-1624.

Boomsma, F., F. H. Derkx, et al. (1995). "Plasma semicarbazide-sensitive amine oxidase activity is elevated in diabetes mellitus and correlates with glycosylated haemoglobin." Clin Sci (Lond) **88**(6): 675-679.

Boomsma, F., H. Hut, et al. (2005). "Semicarbazide-sensitive amine oxidase (SSAO): from cell to circulation." Med Sci Monit **11**(4): RA122-126.

Boomsma, F., D. J. van Veldhuisen, et al. (1997). "Plasma semicarbazide-sensitive amine oxidase is elevated in patients with congestive heart failure." Cardiovasc Res **33**(2): 387-391.

Borodulin, K., E. Vartiainen, et al. (2015). "Forty-year trends in cardiovascular risk factors in Finland." Eur J Public Health **25**(3): 539-546.

Boulanger, C. M., X. Loyer, et al. (2017). "Extracellular vesicles in coronary artery disease." Nat Rev Cardiol **14**(5): 259-272.

Bour, S., S. Caspar-Bauguil, et al. (2009). "Semicarbazide-sensitive amine oxidase/vascular adhesion protein-1 deficiency reduces leukocyte infiltration into adipose tissue and favors fat deposition." Am J Pathol **174**(3): 1075-1083.

Bour, S., D. Prevot, et al. (2007). "Semicarbazide-sensitive amine oxidase substrates fail to induce insulin-like effects in fat cells from AOC3 knockout mice." J Neural Transm (Vienna) **114**(6): 829-833.

Breslow, J. L. (1996). "Mouse models of atherosclerosis." Science **272**(5262): 685-688.

Butcher, E. C. and L. J. Picker (1996). "Lymphocyte homing and homeostasis." Science **272**(5258): 60-66.

Cahill, L. E., M. L. Bertoia, et al. (2015). "New and emerging biomarkers in cardiovascular disease." Curr Diab Rep **15**(11): 88.

Cahill, P. A. and E. M. Redmond (2016). "Vascular endothelium - Gatekeeper of vessel health." Atherosclerosis **248**: 97-109.

Card, C. M., S. S. Yu, et al. (2014). "Emerging roles of lymphatic endothelium in regulating adaptive immunity." J Clin Invest **124**(3): 943-952.

Carlin, L. M., E. G. Stamatiades, et al. (2013). "Nr4a1-dependent Ly6C(low) monocytes monitor endothelial cells and orchestrate their disposal." Cell **153**(2): 362-375.

Chelazzi, C., G. Villa, et al. (2015). "Glycocalyx and sepsis-induced alterations in vascular permeability." Crit Care **19**: 26.

Chistiakov, D. A., A. A. Melnichenko, et al. (2017). "Role of lipids and intraplaque hypoxia in the formation of neovascularization in atherosclerosis." Ann Med **49**(8): 661-677.

Choi, I., S. Lee, et al. (2012). "The new era of the lymphatic system: no longer secondary to the blood vascular system." Cold Spring Harb Perspect Med **2**(4): a006445.

Clement, C. C., D. Aphkhazava, et al. (2013). "Protein expression profiles of human lymph and plasma mapped by 2D-DIGE and 1D SDS-PAGE coupled with nanoLC-ESI-MS/MS bottom-up proteomics." J Proteomics **78**: 172-187.

Clement, C. C., O. Rotzschke, et al. (2011). "The lymph as a pool of self-antigens." Trends Immunol **32**(1): 6-11.

Colafella, K. M. M. and K. M. Denton (2018). "Sex-specific differences in hypertension and associated cardiovascular disease." Nat Rev Nephrol.

Cook, N. R. and P. M. Ridker (2009). "Advances in measuring the effect of individual predictors of cardiovascular risk: the role of reclassification measures." Ann Intern Med **150**(11): 795-802.

Cosselman, K. E., A. Navas-Acien, et al. (2015). "Environmental factors in cardiovascular disease." Nat Rev Cardiol **12**(11): 627-642.

Cray, C., M. Rodriguez, et al. (2009). "Effects of storage temperature and time on clinical biochemical parameters from rat serum." J Am Assoc Lab Anim Sci **48**(2): 202-204.

Csordas, A. and D. Bernhard (2013). "The biology behind the atherothrombotic effects of cigarette smoke." Nat Rev Cardiol **10**(4): 219-230.

Curry, F. R. and T. Noll (2010). "Spotlight on microvascular permeability." Cardiovasc Res **87**(2): 195-197.

Cybulsky, M. I., C. Cheong, et al. (2016). "Macrophages and Dendritic Cells: Partners in Atherogenesis." Circ Res **118**(4): 637-652.

D'Agostino, R. B., Sr., R. S. Vasan, et al. (2008). "General cardiovascular risk profile for use in primary care: the Framingham Heart Study." Circulation **117**(6): 743-753.

De Rosa, S., B. Arcidiacono, et al. (2018). "Type 2 Diabetes Mellitus and Cardiovascular Disease: Genetic and Epigenetic Links." Front Endocrinol (Lausanne) **9**: 2.

Di Pietro, N., G. Formoso, et al. (2016). "Physiology and pathophysiology of oxLDL uptake by vascular wall cells in atherosclerosis." Vascul Pharmacol **84**: 1-7.

Ding, X., H. Xie, et al. (2011). "The significance of copper chelators in clinical and experimental application." J Nutr Biochem **22**(4): 301-310.

Dixon, J. B. (2010). "Lymphatic lipid transport: sewer or subway?" Trends Endocrinol Metab **21**(8): 480-487.

Dorland, Y. L. and S. Huveneers (2017). "Cell-cell junctional mechanotransduction in endothelial remodeling." Cell Mol Life Sci **74**(2): 279-292.

Doughty, K. N., N. X. Del Pilar, et al. (2017). "Lifestyle Medicine and the Management of Cardiovascular Disease." Curr Cardiol Rep **19**(11): 116.

Drozdz, K., D. Janczak, et al. (2008). "Adventitial lymphatics of internal carotid artery in healthy and atherosclerotic vessels." Folia Histochem Cytobiol **46**(4): 433-436.

Dunkel, P., A. Gelain, et al. (2008). "Semicarbazide-sensitive amine oxidase/vascular adhesion protein 1: recent developments concerning substrates and inhibitors of a promising therapeutic target." Curr Med Chem **15**(18): 1827-1839.

Elosua, R. (2014). "Cardiovascular risk functions: usefulness and limitations." Rev Esp Cardiol (Engl Ed) **67**(2): 77-79.

Elosua, R., G. Lucas, et al. (2013). "Genetics and Cardiovascular Risk Prediction: A Step Toward Personalized Medicine?" Current Cardiovascular Risk Reports **7**(1): 33-45.

Enrique-Tarancon, G., L. Marti, et al. (1998). "Role of semicarbazide-sensitive amine oxidase on glucose transport and GLUT4 recruitment to the cell surface in adipose cells." J Biol Chem **273**(14): 8025-8032.

Escobedo, N. and G. Oliver (2017). "The Lymphatic Vasculature: Its Role in Adipose Metabolism and Obesity." Cell Metab.

Evans, R., I. Patzak, et al. (2009). "Integrins in immunity." J Cell Sci **122**(Pt 2): 215-225.

Finney, J., H. J. Moon, et al. (2014). "Human copper-dependent amine oxidases." Arch Biochem Biophys **546**: 19-32.

Flaherty, J. T., J. E. Pierce, et al. (1972). "Endothelial nuclear patterns in the canine arterial tree with particular reference to hemodynamic events." Circ Res **30**(1): 23-33.

Folsom, A. R. (2013). "Classical and novel biomarkers for cardiovascular risk prediction in the United States." J Epidemiol **23**(3): 158-162.

Foot, J. S., T. T. Yow, et al. (2013). "PXS-4681A, a potent and selective mechanism-based inhibitor of SSAO/VAP-1 with anti-inflammatory effects in vivo." J Pharmacol Exp Ther **347**(2): 365-374.

Foussias, G., G. M. Yousef, et al. (2000). "Identification and molecular characterization of a novel member of the siglec family (SIGLEC9)." Genomics **67**(2): 171-178.

Galkina, E. and K. Ley (2009). "Immune and inflammatory mechanisms of atherosclerosis (*)." Annu Rev Immunol **27**: 165-197.

Garcia Nores, G. D., D. A. Cuzzone, et al. (2016). "Obesity but not high-fat diet impairs lymphatic function." Int J Obes (Lond) **40**(10): 1582-1590.

GeneCards. (2018). "AOC3 Gene." Retrieved 24.5.2018, 2018, from https://www.genecards.org/cgi-bin/carddisp.pl?gene=AOC3.

Geyer, P. E., L. M. Holdt, et al. (2017). "Revisiting biomarker discovery by plasma proteomics." Mol Syst Biol **13**(9): 942.

Gislefoss, R. E., T. K. Grimsrud, et al. (2009). "Stability of selected serum proteins after long-term storage in the Janus Serum Bank." Clin Chem Lab Med **47**(5): 596-603.

Gislefoss, R. E., M. Lauritzen, et al. (2017). "Effect of multiple freeze-thaw cycles on selected biochemical serum components." Clin Chem Lab Med **55**(7): 967-973.

Grabner, R., K. Lotzer, et al. (2009). "Lymphotoxin beta receptor signaling promotes tertiary lymphoid organogenesis in the aorta adventitia of aged ApoE-/- mice." J Exp Med **206**(1): 233-248.

Grund, B. and C. Sabin (2010). "Analysis of biomarker data: logs, odds ratios, and receiver operating characteristic curves." Curr Opin HIV AIDS **5**(6): 473-479.

Grundy, S. M., I. J. Benjamin, et al. (1999). "Diabetes and cardiovascular disease: a statement for healthcare professionals from the American Heart Association." Circulation **100**(10): 1134-1146.

Hadi, H. A., C. S. Carr, et al. (2005). "Endothelial dysfunction: cardiovascular risk factors, therapy, and outcome." Vasc Health Risk Manag **1**(3): 183-198.

Hahn, C. and M. A. Schwartz (2009). "Mechanotransduction in vascular physiology and atherogenesis." Nat Rev Mol Cell Biol **10**(1): 53-62.

Hansen, K. C., A. D'Alessandro, et al. (2015). "Lymph formation, composition and circulation: a proteomics perspective." Int Immunol **27**(5): 219-227.

Hansson, G. K. and A. Hermansson (2011). "The immune system in atherosclerosis." Nat Immunol **12**(3): 204-212.

He, Y., V. Kothari, et al. (2018). "High-Density Lipoprotein Function in Cardiovascular Disease and Diabetes Mellitus." Arterioscler Thromb Vasc Biol **38**(2): e10-e16.

Head, T., S. Daunert, et al. (2017). "The Aging Risk and Atherosclerosis: A Fresh Look at Arterial Homeostasis." Front Genet **8**: 216.

Henri, O., C. Pouehe, et al. (2016). "Selective Stimulation of Cardiac Lymphangiogenesis Reduces Myocardial Edema and Fibrosis Leading to Improved Cardiac Function Following Myocardial Infarction." Circulation **133**(15): 1484-1497.

Henry, C. B. and B. R. Duling (2000). "TNF-alpha increases entry of macromolecules into luminal endothelial cell glycocalyx." Am J Physiol Heart Circ Physiol **279**(6): H2815-2823.

Herrington, W., B. Lacey, et al. (2016). "Epidemiology of Atherosclerosis and the Potential to Reduce the Global Burden of Atherothrombotic Disease." Circ Res **118**(4): 535-546.

Heuts, D. P., J. O. Gummadova, et al. (2011). "Reaction of vascular adhesion protein-1 (VAP-1) with primary amines: mechanistic insights from isotope effects and quantitative structure-activity relationships." J Biol Chem **286**(34): 29584-29593.

Hoffmann, A., S. Kerr, et al. (2007). "Siglec-G is a B1 cell-inhibitory receptor that controls expansion and calcium signaling of the B1 cell population." Nat Immunol **8**(7): 695-704.

Hogg, N., I. Patzak, et al. (2011). "The insider's guide to leukocyte integrin signalling and function." Nat Rev Immunol **11**(6): 416-426.

Huang, L. H., A. Elvington, et al. (2015). "The role of the lymphatic system in cholesterol transport." Front Pharmacol **6**: 182.

Huang, W. Y., T. J. Kemp, et al. (2017). "Impact of freeze-thaw cycles on circulating inflammation marker measurements." Cytokine **95**: 113-117.

Huxley, V. H. and J. Scallan (2011). "Lymphatic fluid: exchange mechanisms and regulation." J Physiol **589**(Pt 12): 2935-2943.

Irjala, H., M. Salmi, et al. (2001). "Vascular adhesion protein 1 mediates binding of immunotherapeutic effector cells to tumor endothelium." J Immunol **166**(11): 6937-6943.

Jaakkola, K., S. Jalkanen, et al. (2000). "Vascular adhesion protein-1, intercellular adhesion molecule-1 and P-selectin mediate leukocyte binding to ischemic heart in humans." J Am Coll Cardiol **36**(1): 122-129.

Jaakkola, K., K. Kaunismaki, et al. (1999). "Human vascular adhesion protein-1 in smooth muscle cells." Am J Pathol **155**(6): 1953-1965.

Jaakkola, K., T. Nikula, et al. (2000). "In vivo detection of vascular adhesion protein-1 in experimental inflammation." Am J Pathol **157**(2): 463-471.

Jakobsson, E., J. Nilsson, et al. (2005). "Structure of human semicarbazide-sensitive amine oxidase/vascular adhesion protein-1." Acta Crystallogr D Biol Crystallogr **61**(Pt 11): 1550-1562.

Jalkanen, S., M. Karikoski, et al. (2007). "The oxidase activity of vascular adhesion protein-1 (VAP-1) induces endothelial E- and P-selectins and leukocyte binding." Blood **110**(6): 1864-1870.

Jalkanen, S. and M. Salmi (1993). "Vascular adhesion protein-1 (VAP-1)--a new adhesion molecule recruiting lymphocytes to sites of inflammation." Res Immunol **144**(9): 746-749; discussion 754-762.

Jalkanen, S. T., R. F. Bargatze, et al. (1986). "A lymphoid cell surface glycoprotein involved in endothelial cell recognition and lymphocyte homing in man." Eur J Immunol **16**(10): 1195-1202.

Janes, H., M. S. Pepe, et al. (2008). "Assessing the value of risk predictions by using risk stratification tables." Ann Intern Med **149**(10): 751-760.

Jia, Z. (2017). "Controlling the Overfitting of Heritability in Genomic Selection through Cross Validation." Sci Rep **7**(1): 13678.

Jousilahti, P., T. Laatikainen, et al. (2016). "40-Year CHD Mortality Trends and the Role of Risk Factors in Mortality Decline: The North Karelia Project Experience." Glob Heart **11**(2): 207-212.

Juonala, M., J. S. Viikari, et al. (2013). "Main findings from the prospective Cardiovascular Risk in Young Finns Study." Curr Opin Lipidol **24**(1): 57-64.

Kaitaniemi, S., H. Elovaara, et al. (2009). "The unique substrate specificity of human AOC2, a semicarbazide-sensitive amine oxidase." Cell Mol Life Sci **66**(16): 2743-2757.

Kannel, W. B., T. R. Dawber, et al. (1961). "Factors of risk in the development of coronary heart disease--six year follow-up experience. The Framingham Study." Ann Intern Med **55**: 33-50.

Kaptoge, S., E. Di Angelantonio, et al. (2012). "C-reactive protein, fibrinogen, and cardiovascular disease prediction." N Engl J Med **367**(14): 1310-1320.

Karadi, I., Z. Meszaros, et al. (2002). "Serum semicarbazide-sensitive amine oxidase (SSAO) activity is an independent marker of carotid atherosclerosis." Clin Chim Acta **323**(1-2): 139-146.

Ketelhuth, D. F. and G. K. Hansson (2016). "Adaptive Response of T and B Cells in Atherosclerosis." Circ Res **118**(4): 668-678.

Kholova, I., G. Dragneva, et al. (2011). "Lymphatic vasculature is increased in heart valves, ischaemic and inflamed hearts and in cholesterol-rich and calcified atherosclerotic lesions." Eur J Clin Invest **41**(5): 487-497.

Khot, U. N., M. B. Khot, et al. (2003). "Prevalence of conventional risk factors in patients with coronary heart disease." JAMA **290**(7): 898-904.

Kim, Y. H., P. Nijst, et al. (2017). "Endothelial Glycocalyx as Biomarker for Cardiovascular Diseases: Mechanistic and Clinical Implications." Curr Heart Fail Rep **14**(2): 117-126.

Kohchi, K., S. Takebayashi, et al. (1985). "Significance of adventitial inflammation of the coronary artery in patients with unstable angina: results at autopsy." Circulation **71**(4): 709-716.

Komarova, Y. A., K. Kruse, et al. (2017). "Protein Interactions at Endothelial Junctions and Signaling Mechanisms Regulating Endothelial Permeability." Circ Res **120**(1): 179-206.

Koskinen, K., P. J. Vainio, et al. (2004). "Granulocyte transmigration through the endothelium is regulated by the oxidase activity of vascular adhesion protein-1 (VAP-1)." Blood **103**(9): 3388-3395.

Kurkijarvi, R., D. H. Adams, et al. (1998). "Circulating form of human vascular adhesion protein-1 (VAP-1): increased serum levels in inflammatory liver diseases." J Immunol **161**(3): 1549-1557.

Kurkijarvi, R., S. Jalkanen, et al. (2001). "Vascular adhesion protein-1 (VAP-1) mediates lymphocyte-endothelial interactions in chronic kidney rejection." Eur J Immunol **31**(10): 2876-2884.

Kurkijarvi, R., G. G. Yegutkin, et al. (2000). "Circulating soluble vascular adhesion protein 1 accounts for the increased serum monoamine oxidase activity in chronic liver disease." Gastroenterology **119**(4): 1096-1103.

Kutkut, I., M. J. Meens, et al. (2015). "Lymphatic vessels: an emerging actor in atherosclerotic plaque development." Eur J Clin Invest **45**(1): 100-108.

Lalor, P. F., S. Edwards, et al. (2002). "Vascular adhesion protein-1 mediates adhesion and transmigration of lymphocytes on human hepatic endothelial cells." J Immunol **169**(2): 983-992.

Lee-Rueckert, M., J. C. Escola-Gil, et al. (2016). "HDL functionality in reverse cholesterol transport--Challenges in translating data emerging from mouse models to human disease." Biochim Biophys Acta **1861**(7): 566-583.

Lee, J. E., S. Y. Kim, et al. (2015). "Effect of Repeated Freezing and Thawing on Biomarker Stability in Plasma and Serum Samples." Osong Public Health Res Perspect **6**(6): 357-362.

Leening, M. J., E. W. Steyerberg, et al. (2014). "Net reclassification improvement and integrated discrimination improvement require calibrated models: relevance from a marker and model perspective." Stat Med **33**(19): 3415-3418.

Leening, M. J., M. M. Vedder, et al. (2014). "Net reclassification improvement: computation, interpretation, and controversies: a literature review and clinician's guide." Ann Intern Med **160**(2): 122-131.

Lehto, H. R., S. Lehto, et al. (2014). "Does the clinical spectrum of incident cardiovascular disease differ between men and women?" Eur J Prev Cardiol **21**(8): 964-971.

Leibowitz, A. and E. L. Schiffrin (2011). "Immune mechanisms in hypertension." Curr Hypertens Rep **13**(6): 465-472.

Levick, J. R. and C. C. Michel (2010). "Microvascular fluid exchange and the revised Starling principle." Cardiovasc Res **87**(2): 198-210.

Ley, K., C. Laudanna, et al. (2007). "Getting to the site of inflammation: the leukocyte adhesion cascade updated." Nat Rev Immunol **7**(9): 678-689.

Li, H. Y., Y. D. Jiang, et al. (2011). "Serum vascular adhesion protein-1 predicts 10-year cardiovascular and cancer mortality in individuals with type 2 diabetes." Diabetes **60**(3): 993-999.

Li, N., W. P. Zhang, et al. (2001). "Cloning and characterization of Siglec-10, a novel sialic acid binding member of the Ig superfamily, from human dendritic cells." Journal of Biological Chemistry **276**(30): 28106-28112.

Liao, S. and P. Y. von der Weid (2015). "Lymphatic system: an active pathway for immune protection." Semin Cell Dev Biol **38**: 83-89.

Liaskou, E., M. Karikoski, et al. (2011). "Regulation of mucosal addressin cell adhesion molecule 1 expression in human and mice by vascular adhesion protein 1 amine oxidase activity." Hepatology **53**(2): 661-672.

Libby, P. (2013). "Mechanisms of acute coronary syndromes." N Engl J Med **369**(9): 883-884.

Libby, P. and K. King (2015). "Biomarkers: A Challenging Conundrum in Cardiovascular Disease." Arterioscler Thromb Vasc Biol **35**(12): 2491-2495.

Libby, P., A. H. Lichtman, et al. (2013). "Immune effector mechanisms implicated in atherosclerosis: from mice to humans." Immunity **38**(6): 1092-1104.

Libby, P., P. M. Ridker, et al. (2011). "Progress and challenges in translating the biology of atherosclerosis." Nature **473**(7347): 317-325.

Lim, H. Y., C. H. Thiam, et al. (2013). "Lymphatic vessels are essential for the removal of cholesterol from peripheral tissues by SR-BI-mediated transport of HDL." Cell Metab **17**(5): 671-684.

Liu, C. C. and Y. C. Lin (2013). "Reclamation of copper-contaminated soil using EDTA or citric acid coupled with dissolved organic matter solution extracted from distillery sludge." Environ Pollut **178**: 97-101.

Lopes de Carvalho, L., H. Elovaara, et al. (2018). "Mapping the interaction site and effect of the Siglec-9 inflammatory biomarker on human primary amine oxidase." Sci Rep **8**(1): 2086.

Louveau, A., I. Smirnov, et al. (2015). "Structural and functional features of central nervous system lymphatic vessels." Nature **523**(7560): 337-341.

Lupu, C., A. D. Westmuckett, et al. (2005). "Tissue factor-dependent coagulation is preferentially up-regulated within arterial branching areas in a baboon model of Escherichia coli sepsis." Am J Pathol **167**(4): 1161-1172.

Lyles, G. A. and I. Singh (1985). "Vascular smooth muscle cells: a major source of the semicarbazide-sensitive amine oxidase of the rat aorta." J Pharm Pharmacol **37**(9): 637-643.

Macauley, M. S., P. R. Crocker, et al. (2014). "Siglec-mediated regulation of immune cell function in disease." Nat Rev Immunol **14**(10): 653-666.

Magyar, K., Z. Meszaros, et al. (2001). "Semicarbazide-sensitive amine oxidase. Its physiological significance." Pure and Applied Chemistry **73**(9): 1393-1400.

Marki, A., J. D. Esko, et al. (2015). "Role of the endothelial surface layer in neutrophil recruitment." J Leukoc Biol **98**(4): 503-515.

Marrugat, J., J. Vila, et al. (2011). "[Relative validity of the 10-year cardiovascular risk estimate in a population cohort of the REGICOR study]." Rev Esp Cardiol **64**(5): 385-394.

Martel, C., W. Li, et al. (2013). "Lymphatic vasculature mediates macrophage reverse cholesterol transport in mice." J Clin Invest **123**(4): 1571-1579.

Martel, C. and G. J. Randolph (2013). "Atherosclerosis and transit of HDL through the lymphatic vasculature." Curr Atheroscler Rep **15**(9): 354.

Marttila-Ichihara, F., K. Auvinen, et al. (2009). "Vascular adhesion protein-1 enhances tumor growth by supporting recruitment of Gr-1+CD11b+ myeloid cells into tumors." Cancer Res **69**(19): 7875-7883.

Marttila-Ichihara, F., K. Castermans, et al. (2010). "Small-molecule inhibitors of vascular adhesion protein-1 reduce the accumulation of myeloid cells into tumors and attenuate tumor growth in mice." J Immunol **184**(6): 3164-3173.

Matsuda, T., K. Noda, et al. (2017). "Vascular Adhesion Protein-1 Blockade Suppresses Ocular Inflammation After Retinal Laser Photocoagulation in Mice." Invest Ophthalmol Vis Sci **58**(7): 3254-3261.

Matsuura, E., K. Kobayashi, et al. (2006). "Oxidative modification of low-density lipoprotein and immune regulation of atherosclerosis." Prog Lipid Res **45**(6): 466-486.

Maula, S. M., T. Salminen, et al. (2005). "Carbohydrates located on the top of the "cap" contribute to the adhesive and enzymatic functions of vascular adhesion protein-1." Eur J Immunol **35**(9): 2718-2727.

McEwen, C. M., Jr. and D. C. Harrison (1965). "Abnormalities of Serum Monoamine Oxidase in Chronic Congestive Heart Failure." J Lab Clin Med **65**: 546-559.

McNab, G., J. L. Reeves, et al. (1996). "Vascular adhesion protein 1 mediates binding of T cells to human hepatic endothelium." Gastroenterology **110**(2): 522-528.

Medzhitov, R. (2008). "Origin and physiological roles of inflammation." Nature **454**(7203): 428-435.

Mercier, N., M. Osborne-Pellegrin, et al. (2006). "Carotid arterial stiffness, elastic fibre network and vasoreactivity in semicarbazide-sensitive amine-oxidase null mouse." Cardiovasc Res **72**(2): 349-357.

Merinen, M., H. Irjala, et al. (2005). "Vascular adhesion protein-1 is involved in both acute and chronic inflammation in the mouse." Am J Pathol **166**(3): 793-800.

Messner, B. and D. Bernhard (2014). "Smoking and cardiovascular disease: mechanisms of endothelial dysfunction and early atherogenesis." Arterioscler Thromb Vasc Biol **34**(3): 509-515.

Milasan, A., J. Ledoux, et al. (2015). "Lymphatic network in atherosclerosis: the underestimated path." Future Sci OA **1**(4): FSO61.

Moreno, P. R., K. R. Purushothaman, et al. (2006). "Neovascularization in human atherosclerosis." Circulation **113**(18): 2245-2252.

Morrow, D. A. and J. A. de Lemos (2007). "Benchmarks for the assessment of novel cardiovascular biomarkers." Circulation **115**(8): 949-952.

Mulivor, A. W. and H. H. Lipowsky (2004). "Inflammation- and ischemia-induced shedding of venular glycocalyx." Am J Physiol Heart Circ Physiol **286**(5): H1672-1680.

Munday, J., S. Kerr, et al. (2001). "Identification, characterization and leucocyte expression of Siglec-10, a novel human sialic acid-binding receptor." Biochem J **355**(Pt 2): 489-497.

Murata, M., K. Noda, et al. (2012). "Soluble vascular adhesion protein-1 accumulates in proliferative diabetic retinopathy." Invest Ophthalmol Vis Sci **53**(7): 4055-4062.

Nichols M, T. N., Luengo-Fernandez R, Leal J, Gray A, Scarborough P, Rayner M (2012). European Cardiovascular Disease Statistics 2012. Brussels and Sophia Antipolis, European Heart Network AISBL and European Society of Cardiology.

Niiranen, T. J., A. Lyass, et al. (2017). "Prevalence, Correlates, and Prognosis of Healthy Vascular Aging in a Western Community-Dwelling Cohort: The Framingham Heart Study." Hypertension **70**(2): 267-274.

Nitti, M. D., G. E. Hespe, et al. (2016). "Obesity-induced lymphatic dysfunction is reversible with weight loss." J Physiol **594**(23): 7073-7087.

Noonan, T., S. Lukas, et al. (2013). "The oxidase activity of vascular adhesion protein-1 (VAP-1) is essential for function." Am J Clin Exp Immunol **2**(2): 172-185.

Nourshargh, S. and R. Alon (2014). "Leukocyte migration into inflamed tissues." Immunity **41**(5): 694-707.

Nourshargh, S., P. L. Hordijk, et al. (2010). "Breaching multiple barriers: leukocyte motility through venular walls and the interstitium." Nat Rev Mol Cell Biol **11**(5): 366-378.

Nowotny, K., T. Jung, et al. (2015). "Advanced glycation end products and oxidative stress in type 2 diabetes mellitus." Biomolecules **5**(1): 194-222.

Nunes, S. F., I. V. Figueiredo, et al. (2010). "Changes in the activities of semicarbazide-sensitive amine oxidase in inferior mesenteric artery segments and in serum of patients with type 2 diabetes." Acta Diabetol **47**(2): 179-182.

Nurmi, H., P. Saharinen, et al. (2015). "VEGF-C is required for intestinal lymphatic vessel maintenance and lipid absorption." EMBO Mol Med **7**(11): 1418-1425.

O'Neil, A., A. J. Scovelle, et al. (2018). "Gender/Sex as a Social Determinant of Cardiovascular Risk." Circulation **137**(8): 854-864.

OpenStax. (2013). "Anatomy and Physiology." Retrieved 17.3.2018, 2018, from http://cnx.org/content/col11496/latest/.

Pencina, M. J., R. B. D'Agostino, Sr., et al. (2008). "Evaluating the added predictive ability of a new marker: from area under the ROC curve to reclassification and beyond." Stat Med **27**(2): 157-172; discussion 207-112.

Pencina, M. J., R. B. D'Agostino, Sr., et al. (2011). "Extensions of net reclassification improvement calculations to measure usefulness of new biomarkers." Stat Med **30**(1): 11-21.

Peng, Y., J. Wang, et al. (2016). "Inactivation of Semicarbazide-Sensitive Amine Oxidase Stabilizes the Established Atherosclerotic Lesions via Inducing the Phenotypic Switch of Smooth Muscle Cells." PLoS One **11**(4): e0152758.

Pentikainen, M. O., K. Oorni, et al. (2000). "Modified LDL - trigger of atherosclerosis and inflammation in the arterial intima." J Intern Med **247**(3): 359-370.

Picard, R. R. and R. D. Cook (1984). "Cross-Validation of Regression-Models." Journal of the American Statistical Association **79**(387): 575-583.

Potente, M. and T. Makinen (2017). "Vascular heterogeneity and specialization in development and disease." Nat Rev Mol Cell Biol **18**(8): 477-494.

Pries, A. R., T. W. Secomb, et al. (2000). "The endothelial surface layer." Pflugers Arch **440**(5): 653-666.

Puska, P., E. Vartiainen, et al. (2016). "Background, Principles, Implementation, and General Experiences of the North Karelia Project." Glob Heart **11**(2): 173-178.

Radeva, M. Y. and J. Waschke (2017). "Mind the gap: mechanisms regulating the endothelial barrier." Acta Physiol (Oxf).

Raitakari, O. T. and D. S. Celermajer (2000). "Flow-mediated dilatation." Br J Clin Pharmacol **50**(5): 397-404.

Raitakari, O. T., M. Juonala, et al. (2008). "Cohort profile: the cardiovascular risk in Young Finns Study." Int J Epidemiol **37**(6): 1220-1226.

Rajendran, P., T. Rengarajan, et al. (2013). "The vascular endothelium and human diseases." Int J Biol Sci **9**(10): 1057-1069.

Randolph, G. J. and N. E. Miller (2014). "Lymphatic transport of high-density lipoproteins and chylomicrons." J Clin Invest **124**(3): 929-935.

Reitsma, S., D. W. Slaaf, et al. (2007). "The endothelial glycocalyx: composition, functions, and visualization." Pflugers Arch **454**(3): 345-359.

Rosenson, R. S., H. B. Brewer, Jr., et al. (2016). "Dysfunctional HDL and atherosclerotic cardiovascular disease." Nat Rev Cardiol **13**(1): 48-60.

Roth, G. A., C. Johnson, et al. (2017). "Global, Regional, and National Burden of Cardiovascular Diseases for 10 Causes, 1990 to 2015." J Am Coll Cardiol **70**(1): 1-25.

Ruddle, N. H. (2014). "Lymphatic vessels and tertiary lymphoid organs." J Clin Invest **124**(3): 953-959.

Sallisalmi, M., J. Tenhunen, et al. (2012). "Vascular adhesion protein-1 and syndecan-1 in septic shock." Acta Anaesthesiol Scand **56**(3): 316-322.

Salmi, M., J. Hellman, et al. (1998). "The role of two distinct endothelial molecules, vascular adhesion protein-1 and peripheral lymph node addressin, in the binding of lymphocyte subsets to human lymph nodes." J Immunol **160**(11): 5629-5636.

Salmi, M. and S. Jalkanen (1992). "A 90-kilodalton endothelial cell molecule mediating lymphocyte binding in humans." Science **257**(5075): 1407-1409.

Salmi, M. and S. Jalkanen (1995). "Different forms of human vascular adhesion protein-1 (VAP-1) in blood vessels in vivo and in cultured endothelial cells: implications for lymphocyte-endothelial cell adhesion models." Eur J Immunol **25**(10): 2803-2812.

Salmi, M. and S. Jalkanen (1996). "Human vascular adhesion protein 1 (VAP-1) is a unique sialoglycoprotein that mediates carbohydrate-dependent binding of lymphocytes to endothelial cells." J Exp Med **183**(2): 569-579.

Salmi, M. and S. Jalkanen (2012). "Ectoenzymes controlling leukocyte traffic." Eur J Immunol **42**(2): 284-292.

Salmi, M. and S. Jalkanen (2017). "Vascular Adhesion Protein-1: A Cell Surface Amine Oxidase in Translation." Antioxid Redox Signal.

Salmi, M., K. Kalimo, et al. (1993). "Induction and function of vascular adhesion protein-1 at sites of inflammation." J Exp Med **178**(6): 2255-2260.

Salmi, M., C. Stolen, et al. (2002). "Insulin-regulated increase of soluble vascular adhesion protein-1 in diabetes." Am J Pathol **161**(6): 2255-2262.

Salmi, M., S. Tohka, et al. (1997). "Vascular adhesion protein 1 (VAP-1) mediates lymphocyte subtype-specific, selectin-independent recognition of vascular endothelium in human lymph nodes." J Exp Med **186**(4): 589-600.

Salmi, M., S. Tohka, et al. (2000). "Human vascular adhesion protein-1 (VAP-1) plays a critical role in lymphocyte-endothelial cell adhesion cascade under shear." Circ Res **86**(12): 1245-1251.

Salmi, M., G. G. Yegutkin, et al. (2001). "A cell surface amine oxidase directly controls lymphocyte migration." Immunity **14**(3): 265-276.

Salminen, T. A., D. J. Smith, et al. (1998). "Structural model of the catalytic domain of an enzyme with cell adhesion activity: human vascular adhesion protein-1 (HVAP-1) D4 domain is an amine oxidase." Protein Eng **11**(12): 1195-1204.

Schnoor, M., F. P. Lai, et al. (2011). "Cortactin deficiency is associated with reduced neutrophil recruitment but increased vascular permeability in vivo." J Exp Med **208**(8): 1721-1735.

Schwartz, C. J. and J. R. Mitchell (1962). "Cellular infiltration of the human arterial adventitia associated with atheromatous plaques." Circulation **26**: 73-78.

Schwelberger, H. G. (2010). "Structural organization of mammalian copper-containing amine oxidase genes." Inflamm Res **59 Suppl 2**: S223-225.

Shepard, E. M. and D. M. Dooley (2015). "Inhibition and oxygen activation in copper amine oxidases." Acc Chem Res **48**(5): 1218-1226.

Silvola, J. M., H. Virtanen, et al. (2016). "Leukocyte trafficking-associated vascular adhesion protein 1 is expressed and functionally active in atherosclerotic plaques." Sci Rep **6**: 35089.

Smalley, D. M. and K. Ley (2005). "L-selectin: mechanisms and physiological significance of ectodomain cleavage." J Cell Mol Med **9**(2): 255-266.

Smith, D. J., M. Salmi, et al. (1998). "Cloning of vascular adhesion protein 1 reveals a novel multifunctional adhesion molecule." J Exp Med **188**(1): 17-27.

Sniderman, A. D., R. B. D'Agostino, Sr., et al. (2015). "The Role of Physicians in the Era of Predictive Analytics." JAMA **314**(1): 25-26.

Sole, M., M. Hernandez-Guillamon, et al. (2008). "p53 phosphorylation is involved in vascular cell death induced by the catalytic activity of membrane-bound SSAO/VAP-1." Biochim Biophys Acta **1783**(6): 1085-1094.

Steinberg, D. (2002). "Atherogenesis in perspective: hypercholesterolemia and inflammation as partners in crime." Nat Med **8**(11): 1211-1217.

Steinberg, D. (2013). "In celebration of the 100th anniversary of the lipid hypothesis of atherosclerosis." J Lipid Res **54**(11): 2946-2949.

Stern, M. P. (1995). "Diabetes and cardiovascular disease. The "common soil" hypothesis." Diabetes **44**(4): 369-374.

Stolen, C. M., R. Madanat, et al. (2004). "Semicarbazide-sensitive amine oxidase overexpression has dual consequences: insulin mimicry and diabetes-like complications." Faseb Journal **18**(2): 702-+.

Stolen, C. M., F. Marttila-Ichihara, et al. (2005). "Absence of the endothelial oxidase AOC3 leads to abnormal leukocyte traffic in vivo." Immunity **22**(1): 105-115.

Stolen, C. M., G. G. Yegutkin, et al. (2004). "Origins of serum semicarbazide-sensitive amine oxidase." Circ Res **95**(1): 50-57.

Streiner, D. L. and J. Cairney (2007). "What's under the ROC? An introduction to receiver operating characteristics curves." Can J Psychiatry **52**(2): 121-128.

Sumitran-Holgersson, S. and J. Holgersson (2010). Endothelial Cells: Immunological Aspects. Encyclopedia of Life Sciences (ELS), John Wiley & Sons.

Sun, P., M. Hernandez-Guillamon, et al. (2018). "Simvastatin blocks soluble SSAO/VAP-1 release in experimental models of cerebral ischemia: Possible benefits for stroke-induced inflammation control." Biochim Biophys Acta **1864**(2): 542-553.

Tabas, I. and A. H. Lichtman (2017). "Monocyte-Macrophages and T Cells in Atherosclerosis." Immunity **47**(4): 621-634.

Tabas, I., K. J. Williams, et al. (2007). "Subendothelial lipoprotein retention as the initiating process in atherosclerosis: update and therapeutic implications." Circulation **116**(16): 1832-1844.

Tanaka, S., T. Tanaka, et al. (2017). "Vascular adhesion protein-1 enhances neutrophil infiltration by generation of hydrogen peroxide in renal ischemia/reperfusion injury." Kidney Int **92**(1): 154-164.

Tarbell, J. M. (2010). "Shear stress and the endothelial transport barrier." Cardiovasc Res **87**(2): 320-330.

Tavora, F., R. Kutys, et al. (2010). "Adventitial lymphocytic inflammation in human coronary arteries with intimal atherosclerosis." Cardiovasc Pathol **19**(3): e61-68.

Tohka, S., M. Laukkanen, et al. (2001). "Vascular adhesion protein 1 (VAP-1) functions as a molecular brake during granulocyte rolling and mediates recruitment in vivo." FASEB J **15**(2): 373-382.

Touyz, R. M., R. Alves-Lopes, et al. (2018). "Vascular smooth muscle contraction in hypertension." Cardiovasc Res **114**(4): 529-539.

Townsend, N., M. Nichols, et al. (2015). "Cardiovascular disease in Europe--epidemiological update 2015." Eur Heart J **36**(40): 2696-2705.

Trevaskis, N. L., L. M. Kaminskas, et al. (2015). "From sewer to saviour - targeting the lymphatic system to promote drug exposure and activity." Nat Rev Drug Discov **14**(11): 781-803.

Trezl, L. and J. Pipek (1988). "Formation of Excited Formaldehyde in Model Reactions Simulating Real Biological-Systems." Theochem-Journal of Molecular Structure **47**: 213-223.

Trivedi, P. J., J. Tickle, et al. (2017). "Vascular adhesion protein-1 is elevated in primary sclerosing cholangitis, is predictive of clinical outcome and facilitates recruitment of gut-tropic lymphocytes to liver in a substrate-dependent manner." Gut.

Tzima, E., M. Irani-Tehrani, et al. (2005). "A mechanosensory complex that mediates the endothelial cell response to fluid shear stress." Nature **437**(7057): 426-431.

Wang, J., G. J. Tan, et al. (2017). "Novel biomarkers for cardiovascular risk prediction." J Geriatr Cardiol **14**(2): 135-150.

Wang, J. C. and M. Bennett (2012). "Aging and atherosclerosis: mechanisms, functional consequences, and potential therapeutics for cellular senescence." Circ Res **111**(2): 245-259.

Wang, M., L. Jiang, et al. (2014). "Proinflammation: the key to arterial aging." Trends Endocrinol Metab **25**(2): 72-79.

Wang, T. J. (2011). "Assessing the role of circulating, genetic, and imaging biomarkers in cardiovascular risk prediction." Circulation **123**(5): 551-565.

Wang, T. J., P. Gona, et al. (2006). "Multiple biomarkers for the prediction of first major cardiovascular events and death." N Engl J Med **355**(25): 2631-2639.

Wang, T. J., K. C. Wollert, et al. (2012). "Prognostic utility of novel biomarkers of cardiovascular stress: the Framingham Heart Study." Circulation **126**(13): 1596-1604.

Wang, X. and D. J. Rader (2007). "Molecular regulation of macrophage reverse cholesterol transport." Curr Opin Cardiol **22**(4): 368-372.

Varki, A. (2008). "Sialic acids in human health and disease." Trends Mol Med **14**(8): 351-360.

Vasan, R. S. (2006). "Biomarkers of cardiovascular disease: molecular basis and practical considerations." Circulation **113**(19): 2335-2362.

Wessel, F., M. Winderlich, et al. (2014). "Leukocyte extravasation and vascular permeability are each controlled in vivo by different tyrosine residues of VE-cadherin." Nat Immunol **15**(3): 223-230.

Weston, C. J., E. L. Shepherd, et al. (2013). "Cellular localization and trafficking of vascular adhesion protein-1 as revealed by an N-terminal GFP fusion protein." J Neural Transm (Vienna) **120**(6): 951-961.

Weston, C. J., E. L. Shepherd, et al. (2015). "Vascular adhesion protein-1 promotes liver inflammation and drives hepatic fibrosis." J Clin Invest **125**(2): 501-520.

Vestweber, D. (2015). "How leukocytes cross the vascular endothelium." Nat Rev Immunol **15**(11): 692-704.

Whelton, P. K., R. M. Carey, et al. (2017). "2017 ACC/AHA/AAPA/ABC/ACPM/AGS/APhA/ASH/ASPC/NMA/PCNA Guideline for the Prevention, Detection, Evaluation, and Management of High Blood Pressure in Adults: A Report of the American College of Cardiology/American Heart Association Task Force on Clinical Practice Guidelines." Hypertension.

Whitney, G., S. L. Wang, et al. (2001). "A new siglec family member, siglec-10, is expressed in cells of the immune system and has signaling properties similar to CD33." European Journal of Biochemistry **268**(23): 6083-6096.

Wibo, M., A. T. Duong, et al. (1980). "Subcellular Location of Semicarbazide-Sensitive Amine Oxidase in Rat Aorta." European Journal of Biochemistry **112**(1): 87-94.

Vidrio, H. and M. Medina (2007). "Hypotensive effect of hydroxylamine, an endogenous nitric oxide donor and SSAO inhibitor." J Neural Transm (Vienna) **114**(6): 863-865.

Vink, H., A. A. Constantinescu, et al. (2000). "Oxidized lipoproteins degrade the endothelial surface layer : implications for platelet-endothelial cell adhesion." Circulation **101**(13): 1500-1502.

von Andrian, U. H. and T. R. Mempel (2003). "Homing and cellular traffic in lymph nodes." Nat Rev Immunol **3**(11): 867-878.

von der Weid, P. Y. and D. C. Zawieja (2004). "Lymphatic smooth muscle: the motor unit of lymph drainage." Int J Biochem Cell Biol **36**(7): 1147-1153.

Votyakova, T. V. and I. J. Reynolds (2004). "Detection of hydrogen peroxide with Amplex Red: interference by NADH and reduced glutathione auto-oxidation." Arch Biochem Biophys **431**(1): 138-144.

Vuorio, T., A. Tirronen, et al. (2017). "Cardiac Lymphatics - A New Avenue for Therapeutics?" Trends Endocrinol Metab **28**(4): 285-296.

Xu, H. L., M. Garcia, et al. (2014). "Pharmacologic blockade of vascular adhesion protein-1 lessens neurologic dysfunction in rats subjected to subarachnoid hemorrhage." Brain Res **1586**: 83-89.

Yin, C., S. K. Mohanta, et al. (2016). "Artery Tertiary Lymphoid Organs: Powerhouses of Atherosclerosis Immunity." Front Immunol **7**: 387.

Yoshida, S., M. Murata, et al. (2018). "Proteolytic cleavage of vascular adhesion protein-1 induced by vascular endothelial growth factor in retinal capillary endothelial cells." Jpn J Ophthalmol **62**(2): 256-264.

Yoshikawa, N., K. Noda, et al. (2012). "Blockade of vascular adhesion protein-1 attenuates choroidal neovascularization." Mol Vis **18**: 593-600.

Yu, P. H. and Y. L. Deng (1998). "Endogenous formaldehyde as a potential factor of vulnerability of atherosclerosis: involvement of semicarbazide-sensitive amine oxidase-mediated methylamine turnover." Atherosclerosis **140**(2): 357-363.

Yu, P. H., S. Wright, et al. (2003). "Physiological and pathological implications of semicarbazide-sensitive amine oxidase." Biochim Biophys Acta **1647**(1-2): 193-199.

Yu, P. H. and D. M. Zuo (1993). "Oxidative deamination of methylamine by semicarbazide-sensitive amine oxidase leads to cytotoxic damage in endothelial cells. Possible consequences for diabetes." Diabetes **42**(4): 594-603.

Zawieja, D. C. (2009). "Contractile physiology of lymphatics." Lymphat Res Biol **7**(2): 87-96.

Zethelius, B., L. Berglund, et al. (2008). "Use of multiple biomarkers to improve the prediction of death from cardiovascular causes." N Engl J Med **358**(20): 2107-2116.

Zhang, J. Q., B. Biedermann, et al. (2004). "The murine inhibitory receptor mSiglec-E is expressed broadly on cells of the innate immune system whereas mSiglec-F is restricted to eosinophils." Eur J Immunol **34**(4): 1175-1184.

Zhang, J. Q., G. Nicoll, et al. (2000). "Siglec-9, a novel sialic acid binding member of the immunoglobulin superfamily expressed broadly on human blood leukocytes." J Biol Chem **275**(29): 22121-22126.

Zhang, M., L. Liu, et al. (2016). "Inactivation of semicarbazide-sensitive amine oxidase induces the phenotypic switch of smooth muscle cells and aggravates the development of atherosclerotic lesions." Atherosclerosis **249**: 76-82.

Zolla, V., I. T. Nizamutdinova, et al. (2015). "Aging-related anatomical and biochemical changes in lymphatic collectors impair lymph transport, fluid homeostasis, and pathogen clearance." Aging Cell **14**(4): 582-594.

Zorzano, A., A. Abella, et al. (2003). "Semicarbazide-sensitive amine oxidase activity exerts insulin-like effects on glucose metabolism and insulin-signaling pathways in adipose cells." Biochim Biophys Acta **1647**(1-2): 3-9.

Annales Universitatis Turkuensis

Turun yliopisto
University of Turku

ISBN 978-951-29-7323-1 (PRINT)
ISBN 978-951-29-7324-8 (PDF)
ISSN 0355-9483 (PRINT) | ISSN 2343-3213 (PDF)

Painosalama Oy, Turku, Finland 2018